Fuel-Flexible Gasification-Combustion Technology for Production of H_2 and Sequestration-Ready CO_2

Final Technical Report

Reporting Period:

October 1, 2000 – August 31, 2004

George Rizeq, Janice West, Raul Subia, Arnaldo Frydman, Parag Kulkarni, Jennifer Schwerman, Vladimir Zamansky, and John Reinker
(GE Global Research)
Kanchan Mondal, Lubor Stonawski, Hana Loreth, Krzysztof Piotrowski, Tomasz Szymanski, Tomasz Wiltowski, and Edwin Hippo
(Southern Illinois University at Carbondale)

November 2004

DOE Award No. DE-FC26-00FT40974

GE Global Research
(GEGR)
18 Mason
Irvine, CA 92618

DISCLAIMER

ABSTRACT

GE Global Research is developing an innovative energy technology for coal gasification with high efficiency and near-zero pollution. This Unmixed Fuel Processor (UFP) technology simultaneously converts coal, steam and air into three separate streams of hydrogen-rich gas, sequestration-ready CO_2, and high-temperature, high-pressure vitiated air to produce electricity in gas turbines. This is the draft final report for the first stage of the DOE-funded Vision 21 program. The UFP technology development program encompassed lab-, bench- and pilot-scale studies to demonstrate the UFP concept. Modeling and economic assessments were also key parts of this program. The chemical and mechanical feasibility were established via lab and bench-scale testing, and a pilot plant was designed, constructed and operated, demonstrating the major UFP features. Experimental and preliminary modeling results showed that 80% H_2 purity could be achieved, and that a UFP-based energy plant is projected to meet DOE efficiency targets. Future work will include additional pilot plant testing to optimize performance and reduce environmental, operability and combined cycle integration risks. Results obtained to date have confirmed that this technology has the potential to economically meet future efficiency and environmental performance goals.

TABLE OF CONTENTS

LIST OF TABLES

LIST OF FIGURES

EXECUTIVE SUMMARY

GE's Unmixed Fuel Processor (UFP) is an innovative technology for coal-based energy plants. This draft final report summarizes program accomplishments for the DOE-funded R&D program investigating the UFP technology. The first stage of this program included lab, bench and pilot-scale experimental studies, as well as process, kinetic and economic modeling efforts. The experimental investigations were designed to provide information on the key reactions and cycles in a controlled environment. Process and kinetic modeling efforts were used to relate experimental data to different operating conditions, scales, and energy plant integration scenarios, as well as assessing the costs of different options. The results obtained to date from this program have confirmed the promise of the technology and underscore the need for further development.

The UFP is an advanced process for the steam gasification of coal that makes use of two bed materials continuously circulating between three fluidized bed reactors (R1, R2 and R3). The first material is a sorbent for the effective capture of CO_2 (also called CO_2 absorption material, or CAM) and the second is the oxygen transfer material (OTM) that accumulates oxygen from air via formation of its oxidized form, OTM-O. The UFP system is based on an energy-efficient and near-zero pollution concept for converting coal into separate streams of hydrogen, vitiated air, and sequestration-ready CO_2. The UFP is energy efficient because a large portion of the energy in coal leaves the UFP module as hydrogen and the rest as high-temperature, high-pressure gas that can produce electricity in a gas turbine. The combination of producing hydrogen and electricity is highly effective, meets all the objectives of DOE future energy plants, and provides product flexibility. The ratio of hydrogen to electricity production can be adjusted to match changing demand such that up to approximately 50% of the coal energy could be converted to hydrogen while the balance would be used for electricity production.

Experimental investigations were initially conducted at lab and bench scales to establish the feasibility of the key reactions at realistic conditions. The mechanical issues related to continuous circulation of solids among three fluidized beds were also investigated. High-temperature and pressure testing confirmed H_2 production under simulated R1 conditions at concentrations up to 80%. The absorption and desorption of CO_2 was also tested, and showed good bed utilization and CO_2 removal performance that contributed to the high H_2 purity measured.

Initial lab-scale coal gasification tests identified the relationship between CAM:OTM ratio and key performance indicators. Heat treatment of bed materials was conducted to identify the formation of new states of CAM and OTM. Results showed that no agglomeration or phase changes took place at the conditions of interest. An investigation into improving the effectiveness of CAM materials identified preparation methods that led to improved CAM performance. Detailed TGA and fluidized bed experiments were conducted to quantify OTM reduction rates in the presence of H_2 and CO as well as H_2/CO mixtures. Kinetic analysis showed that OTM reduction by CO was best described by a first-order reaction model, while data on OTM reduction by H_2 was consistent with the Avrami-Efofe'ev phase change model.

Bench-scale testing of the oxidation and reduction of the OTM was conducted at simulated R2 and R3 conditions, and a detailed test matrix design was used to develop a response surface for OTM performance as a function of reducing gas concentration (H_2 and CO) as well as gas hourly space velocity (GHSV). Oxidation of the OTM by air occurred readily and the depletion of O_2 in the product gas was used as a measure of OTM reduction performance. Testing showed that reduction of over 20% of the OTM could be achieved at R2 conditions. If necessary, this percentage can be enhanced through use of OTM particles with higher surface area.

A cold-flow model was used to assess the feasibility of solids circulation between three fluidized bed reactors. Several configurations were tested before selecting a system that used steam as transport gas to circulate the bed solids. The key variables affecting transfer rate were identified and a response surface was generated using design-of-experiment tools. The use of the cold flow model provided visual validation of the meaning of pressure drop, bed height and other measurements. Results confirmed the ability of the selected transfer mechanism to effectively and consistently transport solids between reactors.

Bench-scale results were used to guide design efforts for the pilot-scale system through process and kinetic modeling. An ASPEN model of the pilot plant was used to identify the operating conditions such as flow rates and temperatures that were used to specify equipment. The design of the reactors was a significant challenge due to their size and high temperature and pressure operation. Heat transfer modeling led to the use of two refractory layers to insulate the metal reactors from high process temperatures.

The assembly of the pilot plant was delayed due to the fourteen-month wait for a South Coast AQMD permit to "construct and operate". Three-dimensional modeling of the entire system greatly facilitated the expedited assembly of the pilot plant once the permit was granted. Experimental issues that arose during testing included the need to retrofit the reactors with auxiliary fuel during heat-up, and the re-design of the coal injection probe due to plugging. Testing continued with validation of the solids transfer method at elevated temperatures and pressures. Specific tests included the manipulation of the transport gas and reactor pressures to measure the transport rates by altering bed heights as well as the ability of the control system to maintain a constant bed level.

Pilot plant tests were conducted for coal gasification, CO_2 absorption and OTM reduction as well as OTM oxidation and CO_2 release. H_2 concentrations measured during coal gasification were as high as 60%, although calculations that considered the H_2 consumed for OTM reduction suggest that approximately 80% H_2 was produced. The OTM oxidation test had significant O_2 consumption, consistent with reduction of over 40% of the metal oxide, which is significantly higher than OTM reduction measured at bench scale. Time and budget constraints associated with the relocation of the test facilities required the deferral of additional testing at steady state and higher pressures to the next stage of this program.

An energy plant systems analysis was conducted for a full-scale UFP-based combined cycle energy plant. The process model was refined to include realistic assumptions in keeping with DOE modeling guidelines. An IGCC-based system (with conventional CO_2 separation) developed using the same methodology was used as a benchmark for the UFP modeling results.

With the model assumptions used, this preliminary assessment showed that the UFP-based plant could achieve an efficiency that was six percentage points higher than the IGCC-based plant. Based on this process modeling study, a preliminary economic assessment showed that the UFP system has comparable capital costs and electricity costs, with the UFP having slightly lower costs in both cases. However, since the UFP technology is still at an early stage of development, the UFP cost estimates are preliminary and some operational issues that may impact costs have not yet been fully characterized. Many of these issues are of high priority in future testing efforts.

Future work planned for the UFP technology is aimed at reducing the technical risks associated with a commercial full-scale UFP-based energy plant. Although development efforts have thus far focused on the fundamental reactions and processes of the UFP, continuing development will also consider and assess issues such as combined cycle plant integration, environmental impact, and long-term control and operability; issues that directly impact the economic and commercialization potential of the UFP technology.

The first stage of the UFP technology development program has been successfully completed. The program objectives were met through extensive lab and bench-scale experimentation, successful design and assembly of a pilot-scale system, and limited pilot plant testing. Modeling efforts guided pilot plant design, and were used to assess overall plant efficiencies as well as the economic viability and commercialization potential of the UFP technology. Results have provided support for the UFP's technical and commercial potential. Although many issues arose during testing, including some that negatively impacted the program schedule, no showstoppers were identified to date. Additional experimental work is needed at the pilot scale to further characterize performance and resolve open issues such as bed effectiveness and lifetime that could impact process economics. However, the results obtained to date suggest that the UFP technology has the capability to meet the efficiency, environmental and economic goals of both the DOE and industrial customers.

1.0 INTRODUCTION

Projections of increased demands for energy worldwide, coupled with increasing environmental concerns have given rise to the need for new and innovative technologies for coal-based energy plants. Incremental improvements in existing plants will likely fall short of meeting future capacity and environmental needs economically. The objective of this research and development program was to investigate GE's novel Unmixed Fuel Processor (UFP) technology and assess the technical viability of the technology at both bench and pilot scales, as well as through engineering and modeling efforts.

The UFP technology is a new, energy-efficient, and near-zero pollution concept for converting coal into separate streams of hydrogen, vitiated air, and sequestration-ready CO_2. When commercialized, the UFP technology may become one of the cornerstone technologies to meet the DOE's future energy plant objectives of efficiently and economically producing energy and hydrogen from coal with utilization of opportunity feedstocks.

The UFP technology is energy efficient because a large portion of the energy in coal leaves the UFP module as hydrogen and the rest as high-temperature, high-pressure gas that can produce electricity in a gas turbine. The combination of producing hydrogen and electricity is highly efficient, meets all objectives of DOE future energy plants, and provides product flexibility; the ratio of hydrogen to electricity production can be adjusted to match changing demand.

GE Global Research is the primary contractor for the UFP program under a contract from U.S. DOE NETL (Contract No. DE-FC26-00FT40974). Other project team members include Southern Illinois University at Carbondale (SIU-C), the California Energy Commission (CEC), and T. R. Miles, Technical Consultants, Inc. This project integrated lab, bench and pilot-scale studies to demonstrate the UFP technology. Engineering studies and analytical modeling were also performed in conjunction with the experimental program to provide insight into process behavior as well as aid design efforts. Completion of this stage of the research program has provided evidence of the viability of the main principles of the UFP technology and justification for continued development.

1.1 Objectives

The primary objectives of the UFP program were to:

- Demonstrate and establish the chemistry of the UFP technology, measure kinetic parameters of individual process steps, and identify fundamental processes affecting process economics.
- Design and develop bench- and pilot-scale systems to test the UFP technology under dynamic conditions and estimate the overall system efficiency for the design.
- Develop kinetic and dynamic computational models of the individual process steps.
- Investigate operating conditions that maximize separation of CO_2 and pollutants from vent gas, while simultaneously maximizing coal/opportunity fuels conversion and H_2 production.
- Integrate the UFP module into Vision 21 plant design and optimize work cycle efficiency.
- Determine the extent of technical/economical viability & commercial potential of the UFP module.

Work on the UFP project tasks (Table 1-1) was initiated in October 2000. The project was originally scheduled for completion in three years, but a nine-month no-cost extension granted by the DOE extended the completion date until June 2004. This extension was necessary due to a fourteen-month wait to obtain a South Coast AQMD permit "to construct and operate" the pilot plant. The extension allowed the successful completion of this research program.

1.2 Technology Concept

The UFP technology makes use of three circulating fluidized bed reactors containing CO_2 absorbing material (CAM) and oxygen transfer material (OTM), as shown in Figure 1-1. CAM is a sorbent that absorbs CO_2 to form CAM-CO_2. OTM is a metal oxide, which can be oxidized to form OTM-O. A mixture of the bed materials and coal ash is present in each reactor, and the bed materials undergo a variety of transformations and reactions as they move from one reactor to another. Each reactor serves a different key purpose: gasification, CO_2 release, or oxidation.

The first reactor from the left (R1) is the site of initial coal gasification. Coal fed to R1 is partially gasified with steam, producing H_2, CO and CO_2. Conditions in R1 facilitate CO_2 absorption by the CAM (CAM + $CO_2 \rightarrow$ CAM-CO_2). The reduction in gas-phase CO_2 concentration shifts the equilibrium of the water-gas shift reaction to deplete CO from the gas phase (CO +$H_2O \rightarrow H_2$ + CO_2). The removal of both CO and CO_2 from R1 results in a H_2-rich product stream suitable for use in liquefaction, fuel cells, or turbines. The circulation of bed materials provides a continuous supply of fresh CAM from the middle reactor (R2) and transfers spent CAM to R2 for regeneration.

Table 1-1. Main tasks of the UFP program.

Task	Task Description
Lab-Scale Experiments – Fundamentals *Task 1*	Design & assembly Demonstration of chemical processes Sulfur chemistry
Bench-Scale Test Facility & Testing *Tasks 2 & 3*	Bench test facility design Subsystems procurement& assembly Bench test facility shakedown Reactor design testing Parametric evaluation Fuel-flexibility evaluation Pilot operation support
Engineering & Modeling Studies *Task 4*	Opportunity fuels resource assessment Preliminary economic assessment Kinetic & process modeling Integration into Vision 21 plant Pilot plant control development
Pilot Plant Design, Assembly & Demonstration *Tasks 5, 6, & 7*	Process design Subsystems specification/procurement Reactor design & review Reactors manufacture Components testing Pilot plant assembly Operational shakedown modifications Operational evaluation Fuel-flexibility evaluation Performance testing
Vision 21 Plant Systems Analysis *Task 8*	Preliminary Vision 21 module design Vision 21 plant integration Economic & market assessment
Project Management *Task 9*	Management, reporting, & technology transfer

The middle reactor is the location of CO_2 release from spent CAM (CAM-CO_2 + heat → CAM + CO_2). The CO_2 sorbent is regenerated as the hot bed material transferred from the third reactor from the left (R3) enters R2, increasing the bed temperature to the level required for CO_2 release. This CO_2 release generates a CO_2-rich product stream suitable for sequestration. In addition, char present in the bed materials transferred from R1 is completely gasified in R2. The oxidized OTM transferred from R3 is reduced as it provides the oxygen needed to oxidize CO to CO_2 and H_2 to H_2O (OTM-O + CO → 2OTM + CO_2 *or* OTM-O + H_2 → 2OTM + H_2O).

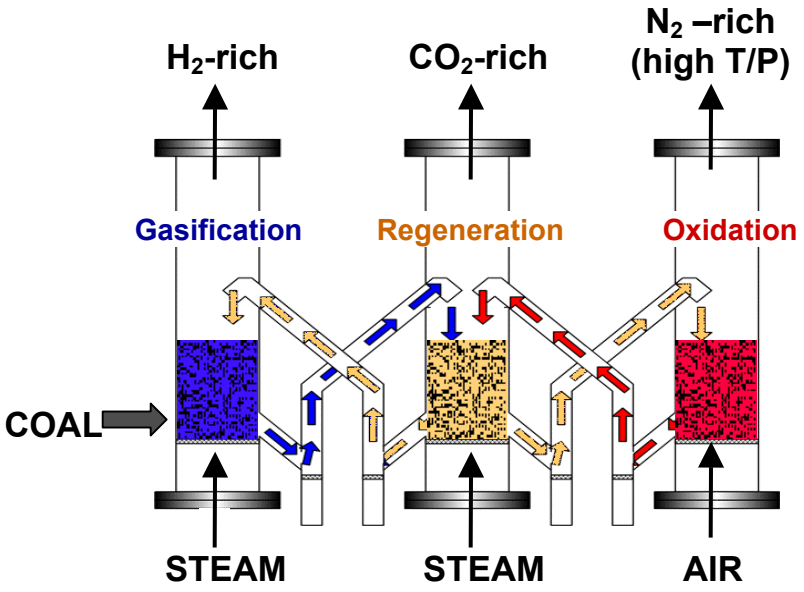

Figure 1-1. Conceptual design of the UFP technology.

The OTM is oxidized in R3 (2OTM + ½ O_2 → OTM-O + heat). Air fed to R3 re-oxidizes the OTM via a highly exothermic reaction that consumes most of the oxygen in the air fed. Thus, R3 produces high-temperature, high-pressure oxygen-depleted (vitiated) air for a gas turbine expander as well as generating heat that is transferred to R1 and R2 via solids transfer.

Reactor 2 exchanges bed materials with both R1 and R3 (there is no direct R1-R3 transfer), allowing for the regeneration and recirculation of both the CAM and the OTM. CAM absorbs CO_2 in R2 and releases it in R2. OTM is oxidized in R3 and reduced in R2. Periodically, ash and bed materials will be removed from the system and replaced with fresh bed materials to reduce the amount of ash in the system and increase the effectiveness of the bed materials.

1.3 Management and Technology Transfer

Program planning activities focused on meeting the program objectives described above. GE Global Research made use of several GE methodologies to obtain desired results and systematically conduct program design, construction, testing and modeling activities. Methodologies utilized in this program include New Technology Introduction (NTI) and Design For Six Sigma (DFSS). The NTI program is a detailed and systematic methodology used by GE to identify market drivers and continually ensure that the program will meet both current and future market needs. The NTI program is also strongly coupled with DFSS and other quality programs, providing structure to the design process and ensuring that the design meets program objectives. This was accomplished through the use of regular program reviews, detailed design reviews, market assessments, planning and decision tools, and specific quality projects aimed at identifying system features and attributes that are critical to quality (CTQ) for customers. Figure 1-2 lists documented six sigma projects by topic.

The project team met regularly to assess progress, distribute workload, and identify and remove potential roadblocks. An expanded NTI project team that included senior management and other expert personnel met monthly to gauge progress and ensure that adequate company resources were allocated and technical issues resolved to allow steady progress toward program objectives.

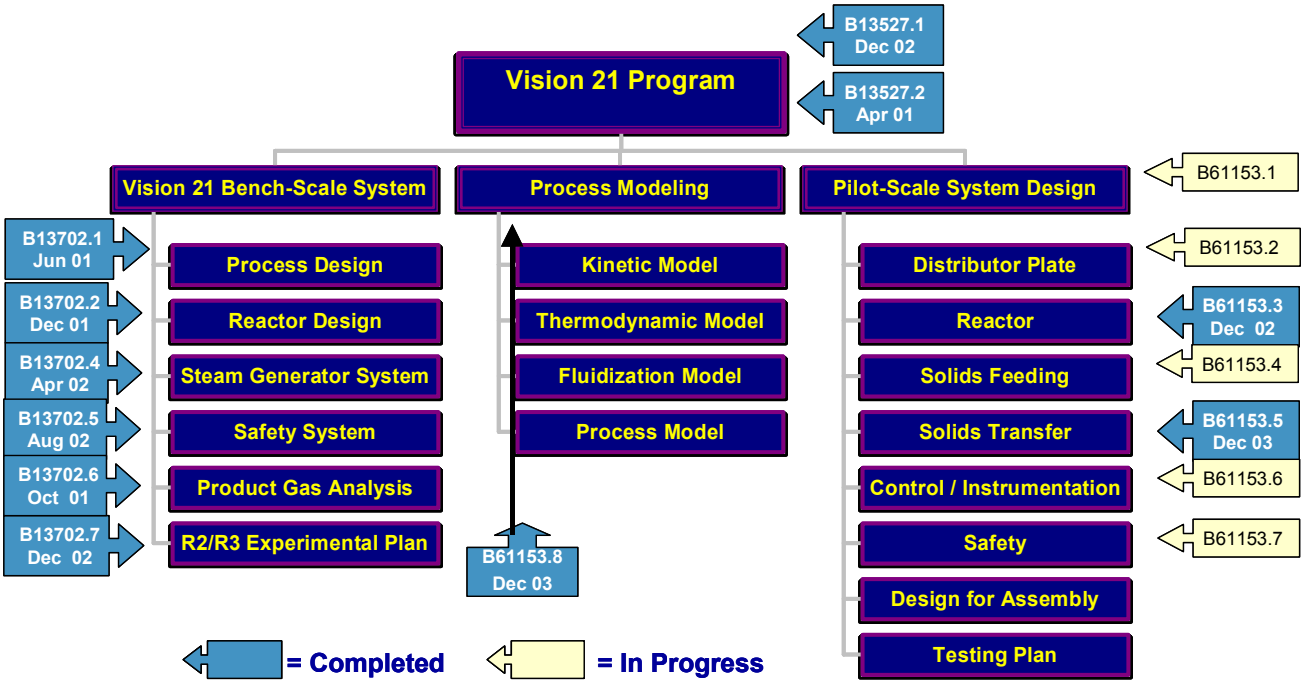

Figure 1-2. Flowchart of major program areas and structure. Documented six sigma projects listed by topic.

Program management activities also included the continuous oversight of program expenditures. This included a monthly review of actual expenditures and monthly projections of labor, equipment, contractor costs, and materials costs.

Technology transfer and networking with experts in the advanced power generation field is an important and ongoing part of project management and is required by DOE. Team members have presented progress on development of the GE patented UFP technology at over a dozen conferences during this 3+ year program. A comprehensive list of publications and presentations associated with this research program is provided in Section 7.0.

The UFP team has been actively engaged in discussions with DOE program manager Dr. Kamalendu Das, as well as decision makers leading the DOE's gasification, CO_2 sequestration, energy efficiency, fossil fuel, and Vision 21 program areas. Several meetings were held with DOE teams throughout the course of this research program, both in Irvine, CA and at DOE offices in Pennsylvania, West Virginia and Maryland. These meetings served as a source of information on the status of UFP technology development as well as an opportunity to receive feedback from the DOE on progress to date and ongoing development efforts.

GE Global Research continues to work closely with GE Energy to ensure that next generation UFP technology will meet the needs of GE Energy customers. GE Energy was particularly helpful during the Task 8 Vision 21 Plant Systems Analysis effort, providing insight into integration issues and detailed models of GE turbines. On October 30, 2003, the UFP technology concept was presented to John Rice, CEO and President of GE Energy, as one of the promising advanced technologies currently under development at GE Global Research. In addition, an overview of final project results was presented to Mark Little, Vice President of GE Energy Products. Several follow-up meetings/conference calls with GE Energy representatives were held to further discuss the market potential of this technology and evaluate technical risks and integration issues with the power island. GE Energy continues to monitor the progress of the program closely.

2.0 EXPERIMENTAL

The experimental tasks of the UFP technology development program include lab-scale, bench-scale and pilot-scale experiments. A significant effort was required to design and assemble each of the experimental facilities due to the UFP's unique requirements and high-temperature, high-pressure operating conditions. The smaller systems were operated first to establish the chemical and mechanical feasibility of key UFP processes and to provide the basis for pilot plant design efforts.

2.1 Lab-Scale Systems

2.1.1 Objectives

The primary objective of Task 1 was to perform a laboratory-scale demonstration of the fundamental chemical and physical processes involved in GE's fuel-flexible UFP technology. Specific objectives of Task 1 include:

- Support bench- and pilot-scale studies,
- Assist in process optimization and engineering analysis,
- Identify key kinetic and thermodynamic limitations of the process, and
- Verify the process parameters at laboratory scale.

These objectives were achieved through experiments conducted in plug flow, fluidized bed, and TGA experimental facilities.

2.1.2 Lab-Scale Fluidization Reactor

A fluidized bed reactor capable of withstanding temperatures up to 860°C and pressures up to 35 atmospheres was designed and constructed. The design included a four-inch double-extra-heavy gauge exterior pipe enclosing a suspended schedule 40 Inconel one-inch pipe as shown in Figure 2-1. The interior pipe was welded and sealed to a flange that was sandwiched between two four-inch, 900-pound flanges welded to the exterior pipe and outlet tube. This design kept the flange temperature below 400°C through radiation and convective cooling, thus enabling the use of graphite spiral-wound gaskets to seal the flanges at each end of the reactor.

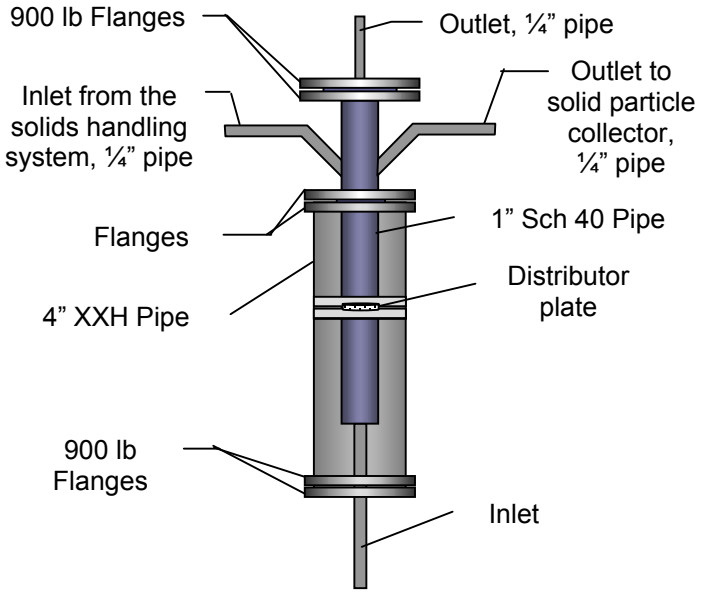

Figure 2-1. Schematic diagram of lab-scale fluidized bed reactor.

The one-inch suspended pipe contained a sintered metal frit welded between two plates to act as a distributor plate for the inlet gas. Removal of the top flange allowed easy access to the interior of the reactor, and the internal pipe was completely removable. This aided speedy analysis of the solid sorbents after cycling. Since the interior pipe experienced no differential pressure, it was constructed with thinner-walled materials without risk of failure.

The reactor was heated with a custom, high-temperature ceramic furnace and add-on pre-heater. Both were constructed of Ni-Cr 80 coiled heating elements encased in thermal ceramic refractory. The furnace, three feet in length, was mounted on two hinged arms that completely surrounded the reactor. The furnace was designed to allow the two furnace halves to swing away from the reactor to allow rapid cooling. A rigid sheet metal jacket secured the heating elements and provided a three-inch space between the exposed nickel-chromium wire and the Inconel reactor (Figure 2-2). Figure 2-3 is a photograph of the furnace in its open state, providing an unobstructed view of the reactor inside.

Figure 2-2. Furnace surrounding outer shell of lab-scale reactor.

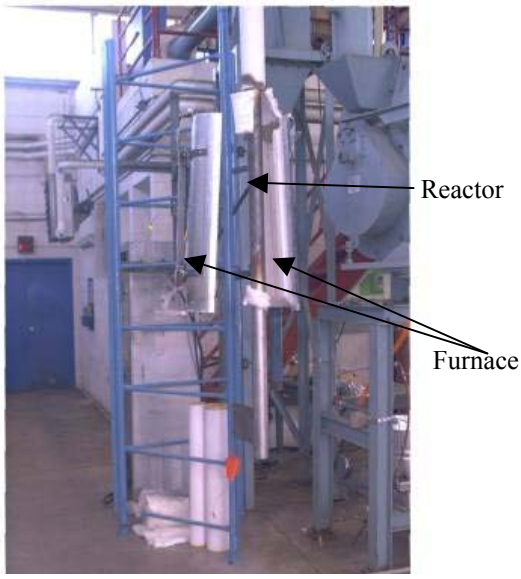

Figure 2-3. Lab-scale reactor and open furnace.

The lab-scale fluidized bed reactor system also included auxiliary equipment for feeding steam and coal, and a gas conditioning system to remove water and particulates from the product gas prior to entering any gas analyzers. It was also fully instrumented to allow control and monitoring of reactor temperatures, pressures and flow rates.

2.1.3 Coal Gasification Experiments

Experiments were conducted in SIU's lab-scale fluidized bed system to assess the impact of varying OTM:CAM ratios and coal loading on hydrogen production and hydrogen purity during the coal gasification step (R1 conditions). Bed materials were placed in the high-pressure lab-scale reactor, which was then heated to the desired temperature under flowing nitrogen at

atmospheric pressure. Steam was then introduced into the reactor and the nitrogen flow rate was adjusted to provide a flow rate equal to 15 times the minimum fluidization velocity with a composition of 85% steam and 15% nitrogen.

Coal samples were injected into the reactor using the nitrogen-driven solids delivery system. Immediately after coal injection, the outlet gas samples and the outlet volumetric flow rates were measured at one-minute intervals for 30 minutes. Gas samples were analyzed using a gas chromatograph (GOW-MAC 600). The concentration and volume of the gas produced is indicative of the effectiveness of the CAM sorbent and the extent of coal gasification. Good performance in the gasification step is characterized by production of a large amount of product gas rich in H_2, especially in tests conducted with CAM beds. The impact of OTM on coal gasification was also of interest.

2.1.4 OTM Reduction Experiments

The reduction of OTM is a key UFP process that has been tested extensively in the lab-scale system. In order to characterize and quantify the behavior of OTM, a test matrix was developed that included both TGA and fluidized bed experiments. This test matrix covered the operating range of interest for quantifying the kinetic behavior of OTM. These test runs are described in Table 2-1. The use of the same H_2/CO ratio for both the TGA and fluidized bed tests allowed more meaningful comparison of their results.

Table 2-1. Test matrix for investigation of OTM behavior.

Test #	Test type	Pressure (atm)	Bed mass (g)	Carrier gas				Temp range (°C)
				Feed gas type	H_2/CO ratio	Inert %	Total flow (SLPM)	
1	TGA	1	0.01	H_2/CO/N_2	1	90	0.0275	700-900
2	TGA	1	0.01	H_2/CO/N_2	0.75	90	0.0275	700-900
3	TGA	1	0.01	H_2/CO/N_2	0.5	90	0.0275	700-900
4	TGA	1	0.01	H_2/CO/N_2	0.25	90	0.0275	700-900
5	TGA	1	0.01	H_2/CO/N_2	CO only	90	0.2144	700-900
6	TGA	1	0.01	H_2/CO/N_2	H_2 only	90	0.2144	700-900
7	FB	20	50	H_2/CO/N_2	1	90	0.2144	700-900
8	FB	20	50	H_2/CO/N_2	0.75	90	0.2144	700-900
9	FB	20	50	H_2/CO/N_2	0.5	90	0.2144	700-900
10	FB	20	50	H_2/CO/N_2	0.25	90	0.2144	700-900
11	FB	20	50	H_2/CO/N_2	CO only	90	0.2144	700-900
12	FB	20	50	H_2/CO/N_2	H_2 only	90	0.2144	700-900
13	FB	20	50	H_2/CO/steam	1	90	0.2144	700-900
14	FB	20	50	H_2/CO/steam	0.75	90	0.2144	700-900
15	FB	20	50	H_2/CO/steam	0.5	90	0.2144	700-900
16	FB	20	50	H_2/CO/steam	0.25	90	0.2144	700-900
17	FB	20	50	H_2/CO/steam	CO only	90	0.2144	700-900
18	FB	20	50	H_2/CO/steam	H_2 only	90	0.2144	700-900
Blank	TGA	1	0.01	N_2	n/a	n/a	0.0275	700-900
Blank	FB	20	50	N_2	n/a	n/a	0.2144	700-900
Blank	FB	20	50	Steam	n/a	n/a	0.2144	700-900

The objective of the TGA experiments was to generate data for evaluation of different kinetic mechanisms and derive kinetic constants. TGA experiments were conducted using a Perkin-Elmer TGA-7 thermogravimetric analyzer with a TAC 7/DX control box upgrade driven by Pyris software. OTM samples (~12 mg) were preheated under a N_2 atmosphere (heating rate 10°C/min) to the desired temperature (700-900°C). This temperature was then maintained as a reducing gas (a mixture of CO and H_2 in N_2) was fed at a flow rate of 30 ml/min. Pressurized gas cylinders of N_2, CO and H_2 were used to feed the reducing gas mixture. The gases were dried using a molecular sieve moisture trap before being fed to the TGA.

TGA experimental results include the weight change of a sample as a function of time. This weight change can be directly related to the extent of the reaction conversion, since oxidized OTM (OTM-O) has a different molecular weight than reduced OTM (OTM-R). Reaction stoichiometry dictates that a weight loss of 10% corresponds to complete reaction from OTM-O to OTM-R. The extent of conversion [$\alpha(t)$] was calculated using the formula below:

$$\alpha(t) = \frac{m_0 - m(t)}{m_0 - m_{10\%}} \qquad \textit{(Equation 2-1)}$$

Where:

m_0 is the initial mass,
$m(t)$ is the mass at time t, and
$m_{10\%}$ is the mass corresponding to complete conversion (10% mass loss).

The Avrami-Erofe'ev method was used to compare the kinetics of the isothermal solid-state reactions taking place in the TGA. The method is based on an equation describing nucleation and growth processes:

$$\alpha = 1 - \exp(-\beta t^m) \qquad \textit{(Equation 2-2)}$$

$$\ln(-\ln(1-\alpha)) = \ln\beta + m\ln t \qquad \textit{(Equation 2-3)}$$

Where:

α is the extent of conversion at any given time, t
β is a constant, partially depended both on nucleation frequency and rate of grain growth
m is a constant associated with the geometry of the system

Plots of equation 2-3 yield lines with slope m (the linear region of such plots is generally for α values between 0.15 and 0.50). The value of m is indicative of the specific solid-state kinetic mechanism, as described in Table 2-2.

Table 2-2. Selected solid-state reaction rate equations.

$1-(1-\alpha)^{1/3} = kt$ $\alpha = 1-(1-kt)^3$	m = 1.07; Equation for phase-boundary-controlled reaction (surface reaction) for a sphere	*(Equation 2-4)* *(Equation 2-5)*
$-\ln(1-\alpha) = kt$ $\alpha = 1-\exp(-kt)$	m = 1; Equation for first-order reaction	*(Equation 2-6)* *(Equation 2-7)*
$[-\ln(1-\alpha)]^{1/2} = kt$ $\alpha = -\exp(-k^2t^2)+1$	m = 2; Avrami-Erofe'ev equation for phase change model	*(Equation 2-8)* *(Equation 2-9)*

The objective of the fluidized bed tests is to observe OTM reduction behavior in a system closer in configuration to the UFP process. Since it is not possible to directly measure the OTM mass change (as in TGA experiments), assumptions must be made in interpreting the data, particularly with regard to the involvement of reactions other than the OTM reduction reaction.

2.1.5 Heat Treatment

Preliminary heat treatment testing was conducted to characterize the behavior of CAM and OTM after exposure to high temperatures. Initial testing was conducted by heating different weight ratios of CAM and OTM in air for 45 minutes at 1200°C then cooling the sample in air. The samples were characterized for their propensity to agglomerate after heat treatment, and x-ray analyses were conducted to identify the formation of new phases.

Table 2-3. Test matrix for heat treatment of CAM and OTM.

First experimental series						
Run #	CAM (SA)	CAM-CO_2 (SA)	OTM (SA)	Flowing Gas	Temp (°C)	Time (min)
1.1	0	1	3	air	1100	45
1.2	0	3	1	air	1100	45
1.3	1	0	3	air	1100	45
1.4	3	0	1	air	1100	45

Three series of experiments were conducted; the experimental matrix for the first experimental series is detailed in Table 2-3. Tests conducted in the first test series made use of pure OTM and CAM supplied by Sigma Aldrich (SA), a chemical supplier. For the second and the third series of experiments, OTM and CAM were combined with simulated coal ash and tested with either air (second series) or steam (third series). For these tests, GE supplied OTM and CAM that had previously been used for bench-scale testing, while the simulated ash was prepared using supplies obtained from Sigma Aldrich. Simulated coal ash was prepared by mixing 49% SiO_2, 49% Al_2O_3, 1.7% Na_2CO_3 and 1.3% K_2CO_3 (taking into account the decomposition of sodium and potassium carbonate into sodium and potassium oxide at testing temperatures). Test series experimental details are provided below.

Series 1: Experiments were conducted in an open tube furnace. Mixtures of OTM and CAM of desired ratios were inserted into a preheated furnace and heated under an air atmosphere for 45 minutes at ambient pressure before being cooled in air. Samples were subjected to x-ray analysis after this heat treatment.

Series 2: Experiments were conducted in an open tube furnace. Samples of OTM, CAM and simulated ash were mixed in the desired ratios. These mixtures were then placed in a preheated furnace and heated under an air atmosphere at ambient pressure for the desired time (30 or 15 minutes). Next, the sample was cooled in air. Samples were subjected to x-ray analysis after this heat treatment.

Series 3: Experiments were conducted in a fluidized bed reactor. Samples of OTM, CAM and simulated ash were mixed in the desired ratios and placed in the reactor. These mixtures were heated under a nitrogen atmosphere to the desired temperature. Once the desired temperature was reached, a steam mixture was introduced (90% steam + 10%

nitrogen) at ambient pressure for the desired time (30 or 15 minutes). The samples were then cooled in air and subjected to x-ray analysis.

2.1.6 CAM Development

An investigation of the properties and lifetime of CAM materials was conducted. A new preparation method was developed that utilized CAM precipitation and also made use of anionic surfactants to modify the surface properties of the CAM. Three different surfactants were tested. The performance and lifetime of three CAM samples (each prepared with a different surfactant) were characterized and compared with a CAM sample prepared with no surfactants.

The CAM samples were prepared by precipitation from an aquatic solution with a concentration approximately 16 times the saturation concentration. The mixture was placed in a column reactor and CO_2 was bubbled through the solution. A glass frit was used as a diffusion plate in order to obtain a uniform CO_2 distribution. The solids were observed to start precipitating almost immediately. The pH was monitored for the duration of the precipitation reaction since as the alkaline CAM precipitated out of solution, the measured pH was dominated by the slightly acidic dissolved CO_2. Ten minutes were required for the complete precipitation of the CAM, which was indicated by a significant decrease in pH.

A Quantachrome Nova 2000 BET analyzer was used to obtain multipoint surface areas. A Microtrac S3500 was used for particle size distribution determination. Thermogravimetric analysis was employed to obtain the weight change data during CO_2 capture/release cycles.

TGA experiments were conducted isothermally at 800°C. During CO_2 capture, each CAM sample was exposed to a continuous feed of CO_2; the CO_2 absorbed by the CAM caused an increase in sample weight. Each CO_2 capture step was conducted for 15 minutes. CO_2 release was conducted under a nitrogen atmosphere, and as CO_2 was released, the sample weight decreased. Each CO_2 release step continued until no changes in weight were observed. Samples were subjected to multiple CO_2 capture/release cycles. A scanning electron microscope was used to assess CAM morphology both before and after cycling.

2.2 Bench-Scale Systems

2.2.1 Objectives

The main objectives of the bench-scale design and testing tasks were to establish the chemical and mechanical feasibility of the UFP technology and provide data for future development efforts. Two separate experimental facilities were designed, built and operated to accomplish these objectives: a bench-scale UFP system and a cold-flow model for solids transfer. The chemical feasibility of the UFP technology was investigated using the bench-scale UFP system, shown in Figure 2-4. The mechanical feasibility was established using a cold-flow solids transfer model, shown in Figure 2-5. The design and operation of these two systems are discussed below.

Figure 2-4. Bench-scale UFP system.

Figure 2-5. Cold flow model of solids transfer.

2.2.2 Bench-Scale UFP System Design

The chemical feasibility of the UFP technology is dependent on the key UFP processes/cycles that take place in the three UFP reactors: coal gasification (R1), CO_2 absorption (R1)/release (R2), and OTM oxidation (R3)/reduction (R2). In the full embodiment of the UFP concept, the three reactors continuously transfer bed materials between reactors. However, after analysis of the type of data that could be obtained with different bench-scale system configurations, a configuration was selected that allowed each reactor to be tested separately to isolate the chemical processes from the mechanical one of transferring solids between reactors. Thus, the design objective of establishing the chemical feasibility of the UFP concept was met by using a single reactor to simulate each of the three process reactors in sequence.

The bench-scale system was designed to provide the necessary feeds and analysis equipment for each of the three processes. The specifications for the reactor and other equipment were set based on a combination of requirements for the individual reactors. Thus, the bench-scale system capability included steam, coal, air, N_2 and other compressed gas feeds, and the analysis equipment provided data on H_2, CO, CO_2, total hydrocarbons (THC) and O_2 concentrations.

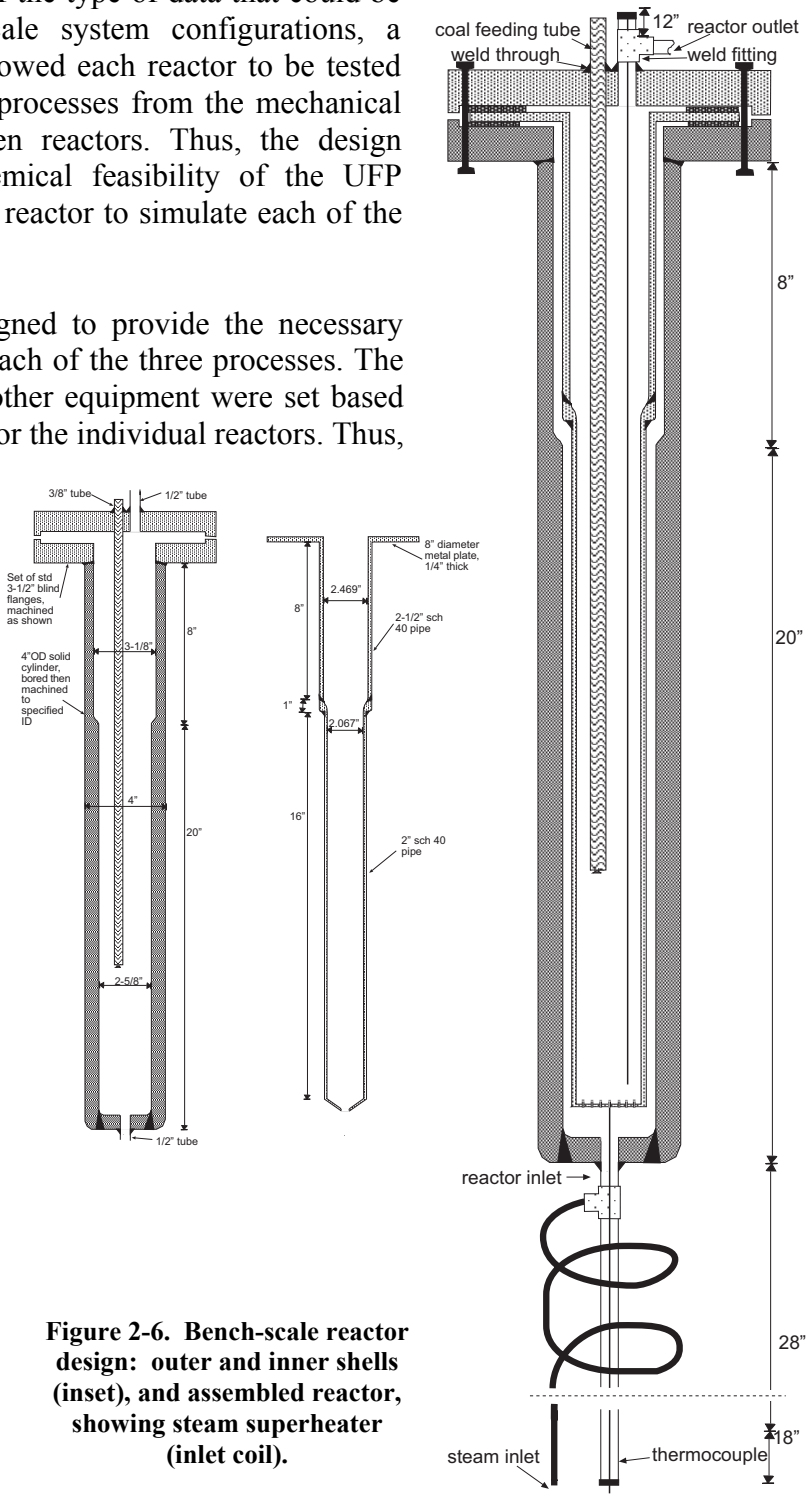

Figure 2-6. Bench-scale reactor design: outer and inner shells (inset), and assembled reactor, showing steam superheater (inlet coil).

Reactor Design

The reactor is the heart of the system, and was designed to withstand an environment of 1000°C and 300 psi. The reactor consists of a 4"OD outer shell, and a 2"ID inner shell with an expansion zone. The outer shell was welded to a flange, while the inner shell has a lip that allows it to rest between the outer shell's bottom flange and the flange lid, with two gaskets used to maintain high-pressure seals. Figure 2-6 shows the outer and inner shells separately, then in their assembled form, and with the steam superheater connected to the reactor inlet. Incoloy Alloy 800HT was used for the outer shell,

selected on the basis of its strength at high temperatures and its ability to withstand the oxidizing and reducing environments of the process. A detailed stress analysis was conducted to determine the required reactor wall thickness. The length of the reactor was specified by estimating heat lost through the reactor outer shell walls to ensure that the flange at the top of the reactor did not exceed 400°C.

The reactor was externally heated by a Lindberg Model 54579-V-s 16kW furnace with a maximum temperature of 1500°C and a 4" inside diameter. Due to the use of external reactor heating, the reactor materials were selected to withstand the full operating temperatures of the process. However, because of gasket temperature limitations, the flanges used to seal the reactor were located outside the hot zone of the furnace. The bed, containing OTM or CAM, rests on a distributor plate located at the bottom of the inner shell. During system operation, the bed expands as it is fluidized. An expansion zone (or freeboard) was provided at the top of the reactor, which features a larger diameter to decrease particle velocities and minimize entrainment and loss of particles to the outlet line.

Air/N_2 Feed System

The Air/N_2 feed system provided air during the third reactor (oxidation) step and N_2 during start-up and between tests. An air pressure booster was used to increase the pressure of shop air from 80 psi to 300 psi. A three-way valve fed either high-pressure air or high pressure N_2 to the reactor. A transmitting flow indicator measured and displayed the gas flow rate.

Steam Generator

The steam feed system included a water pump and a coil located inside an electric furnace. The system had the capability to provide continuous steam generation by bypassing steam flow to a vent when it was not needed for the reactor. This facilitated the transition between nitrogen and steam feeds to the reactor. Instrumentation was available to monitor the temperature and pressure of the steam both before and after the steam preheater coil. Shakedown testing demonstrated the successful generation of steam for water flow rates from 5 – 40 g/min and a furnace temperature of 600°C. A steam superheater was used to further increase the temperature of the inlet steam. The superheater was composed of an additional coil connected directly to the bottom of the reactor in the main reactor furnace, as shown at the bottom of Figure 2-6. The superheater ensured that the steam temperature matched the furnace temperature prior to entering the reactor.

Coal Feeding System

The coal feeding system was designed to inject measured amounts of coal into the high-pressure, high-temperature reactor with minimal plugging, deposits, and coal devolatilization in the feed tube. The coal feeding tube entered the reactor through the flange lid, and extended down into the reactor bed for enhanced coal mixing with the bed and to prevent coal entrainment (Figure 2-6). The coal was loaded into a coal reservoir and then an accumulator tank was filled with high-pressure N_2. Once the accumulator was pressurized to a predetermined pressure, the coal reservoir was slowly pressurized. Next, the valve between the coal reservoir and the reactor was opened, sending the slug of coal rapidly through the coal delivery tube and into the reactor bed. Shakedown testing of this system was first conducted at ambient temperature and pressure, with differential pressures on the order of 100 psi, then testing continued at operating pressures, and finally at high temperature and pressure. The system was modified and optimized as needed to prevent trapping of coal in the upstream portion of the system. This involved streamlining the

coal delivery line, eliminating components that led to necking in the flow path. Utilizing a heat tape, shakedown testing demonstrated the successful delivery of coal at 550°C. Coal recovery increased with increasing differential pressure, reaching 90% recovery at 100 psi.

Product Gas Analysis Equipment

The product gas exiting the reactor passed through a condenser to remove steam before it could condense in the backpressure regulator that maintained reactor pressure. A set of continuous emission monitors (CEMs) was used to measure the concentration of the dry gas. These included monitors for CO, CO_2, O_2 and hydrocarbons. A gas chromatograph (GC) was used intermittently to measure H_2 concentration.

Data Acquisition System

A Labview™ FieldPoint™ data acquisition system was programmed to collect temperature, pressure, flow rate and concentration data and record it for later analysis, as well as display the data for the benefit of system operators. The program displayed real-time data as well as a graphical history of measurements values. Data collected was formatted for compatibility with calculation templates to facilitate rapid data analysis. Figure 2-7 is the process and instrumentation diagram for the bench-scale system. The reactor is shown at the center of the diagram, with the four branches representing other major subsystems: coal feed, air/N_2 feed, steam feed, and product gas analysis and conditioning. All thermocouples, pressure transducers and flow measurement devices were connected to the data acquisition system.

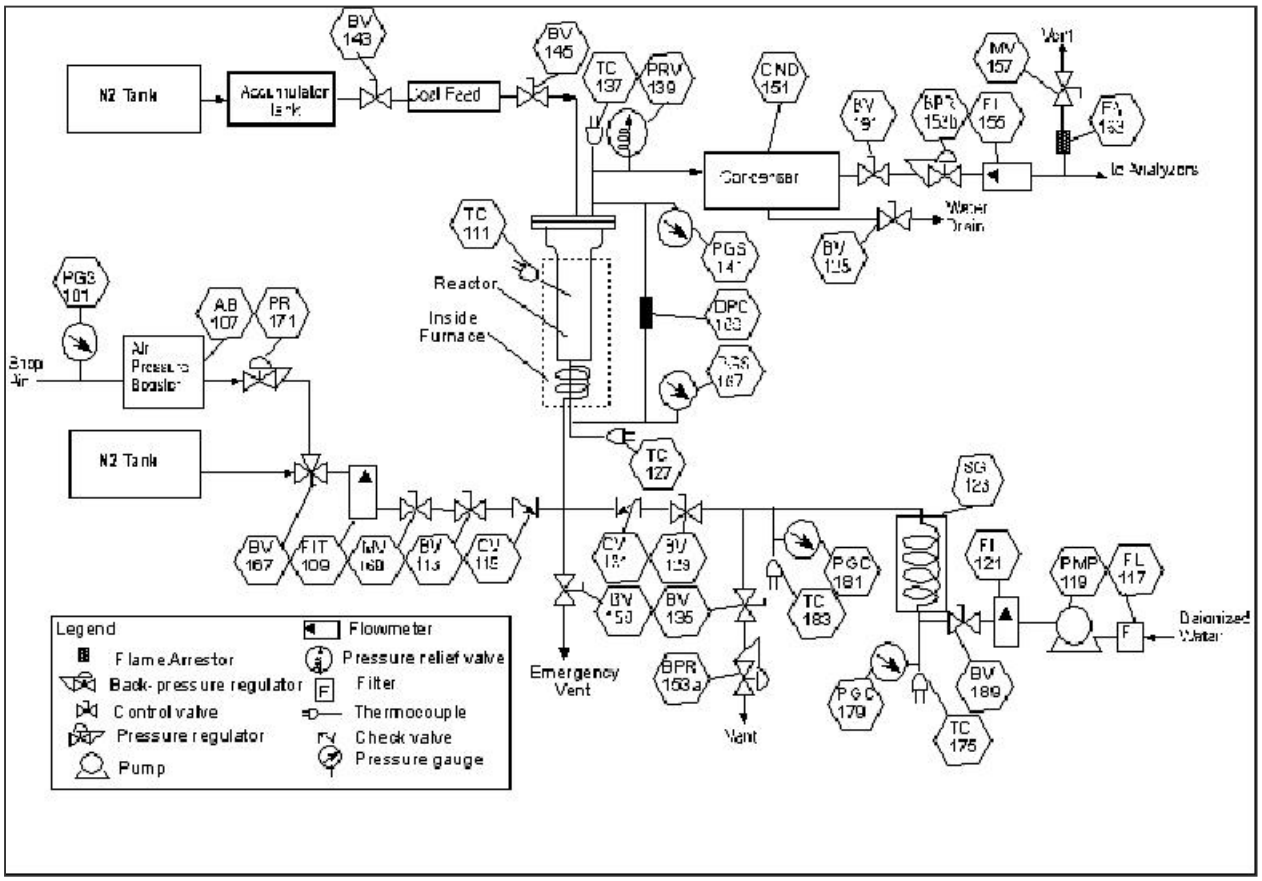

Figure 2-7. Process and instrumentation diagram for the bench-scale UFP system.

2.2.3 Bench-Scale UFP Experimental Procedure

As part of the design of each subsystem, a standard operating procedure (SOP) was developed for shakedown testing of each subsystem. These SOPs were combined and re-assessed to provide a complete system SOP. Failure mode and effects analyses (FMEAs) were conducted for each subsystem, as well as for the system as a whole. FMEAs identified the likelihood and types of system failures that may occur, and mitigation plans were developed in each instance to minimize the impact of such failures on employee safety, the environment and testing equipment. Pressure and temperature switches were installed to shut down the system in case of excessive temperature or pressure. A manual emergency shutdown button was also located on the test stand. No significant safety problems were experienced during testing.

Coal Gasification and CO_2 Absorption/Release Test Procedure

Coal gasification is coupled with CO_2 absorption, since the gasification of coal generates CO_2. The key behavior tested was the gasification of coal in the presence of CAM, which increases the purity of the product hydrogen. The release of CO_2 took place in a separate testing step. Coal gasification and CO_2 absorption/release were tested via a two-stage method. During the first testing stage, coal was injected into the fluidized bed (CAM), and the product gas concentration was measured. The second stage involved increasing the reactor temperature to the range where the CAM released CO_2 and measuring the outlet gas concentration. Results of these tests are discussed in Section 3.2.1.

OTM Oxidation/Reduction Test Procedure

OTM performance is related to the ability of the OTM to undergo the reduction reactions in R2 that in turn allow the OTM to be oxidized in R3. Experiments conducted under R3 conditions have shown that the oxidation of reduced-state OTM occurs rapidly and readily and is highly exothermic. OTM performance was most often limited by the reduction step. Initial OTM tests were conducted using coal for OTM reduction. Later tests were conducted using CO and H_2 as reducing agents to isolate OTM reduction from coal gasification. The complexity of the behavior observed led to the development of a designed experimental matrix involving the reduction of OTM with a range of concentrations of CO and/or H_2. These detailed experiments were conducted to further characterize OTM reduction behavior and establish kinetic rate constants for process modeling efforts.

Test operating conditions (independent variables) included CO and H_2 concentrations as well as the Gas Hourly Space Velocity (GHSV), while the % OTM reduction was the main response dependent variable. Thirteen tests were included in the full test matrix, and two additional optimization tests were completed after analysis of the first thirteen runs. Results of these tests are discussed in Section 3.2.2.

2.2.4 Cold-Flow Model Design

The mechanical feasibility of transferring solid bed materials between reactors is critical to the UFP technology. The heat transfer and bed material regeneration are dependent on effective bed circulation. A cold-flow model was designed to aid in solids transfer mechanism development by simulating the action of the solids transfer ducts. The first objective of the cold flow simulation was to study the parameters that influence solids transfer and prevent or minimize solids accumulation, clogging and heat loss during transport. The second objective was to minimize the

auxiliary steam flow (solids carrier gas flow) required for solids transport. The cold flow model was made with clear plexiglass to allow visual inspection of fluidization behavior that was not possible in metal reactors.

A full-scale model of the three pilot-scale reactors was built with plexiglass (Figure 2-5). Several solids transport modes/designs were identified and compared. An initial method assumed that solids should move from the top of one fluidized bed to the bottom of the next. However, early experiments demonstrated that this method was not feasible in practice; the head pressure at the intake point was lower than the head pressure at the delivery point, requiring excessive solids carrier gas flows to ensure transport. The direction of solids flow was subsequently reversed, allowing solids transfer with reasonably small flow rates of auxiliary carrier gas (25-50% of the fluidization gas flow rate). Figure 2-8 is a cross-sectional view of R2, showing the location of the two solids transfer ducts that transport bed materials from R1 and R3 into R2 and the direction of solids transfer. The ducts for transport of bed materials out of R2 can be seen in the inset picture.

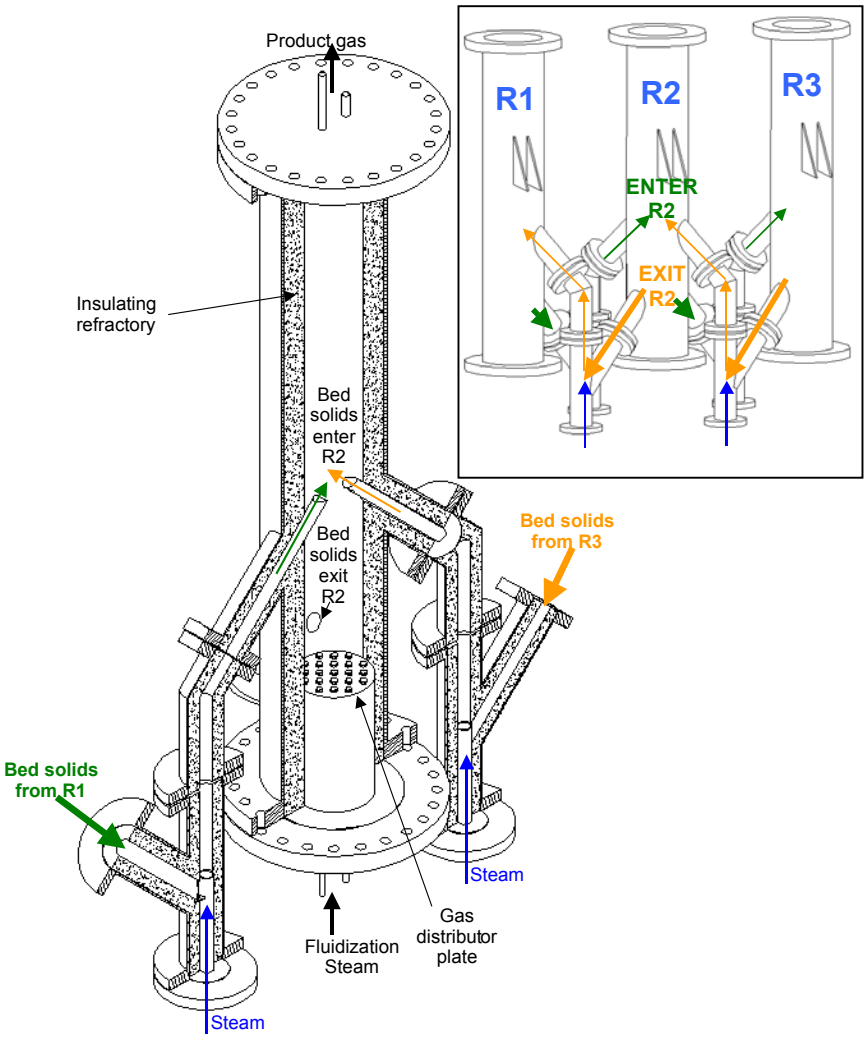

Figure 2-8. Reactor 2 cross-sectional view of two solids transfer ducts and overall view of transfer legs in all three reactors (inset).

The diameter of the intake duct is the main parameter that determines the mass flow rate of solids drawn from a reactor. This diameter was selected to ensure that the flow of solids matched the design requirements. Process modeling and equilibrium calculations were used to estimate the mass flow rate of solids required for continuous UFP operation.

2.2.5 Cold-Flow Model Experimental Procedure

Carbon dioxide at 60 psi was used as the fluidizing media, with the flow rate controlled by two rotameters of different ranges. A fine magnetic pressure gauge with a range of 0-2 in. H_2O and a manometer with a range of 0-100 in. H_2O measured pressure drop across the plexiglass tube. Low-moisture construction sand sieved to 125 μm particle diameter was used as the bed material.

Based on preliminary observations, a test matrix was developed using the following variables: fluidized bed height, intake orifice diameter, transport duct internal diameter, duct angle, and solids carrier gas flow rate. The mass flow rate of solids was measured as an indication of performance. The criteria for good solids transport include:

1) Measured mass flow rate of solids approximates (less than 25% difference) the mass flow rate of solids obtained by gravity (open hole on the side of the fluidized bed).
2) Carrier fluid flow rate is less than 50% of the fluidization flow rate.
3) No solids accumulation is visible in the transport duct.
4) The solid-fluid mixture is dilute (more than 99% porosity) in the transfer duct.

During testing, the first two criteria were quantified and measured, while the others were visually monitored via the transparent PVC ducts. A scale-up methodology was developed to allow extrapolation of cold flow model results to actual pilot-scale conditions. This was especially important in scaling flow rates (both fluidization and solids transport).

Previous tests included the discharge of bed solids onto a scale at atmospheric pressure for flow rate measurements. This procedure was modified to allow the discharge of bed solids into a water-filled vessel to better simulate operating conditions, mimicking the head pressure at the point of entry into the neighboring reactor and providing other advantages to aid in the robust design of the solids transfer system.

2.3 Pilot-Scale System

2.3.1 Objectives

Specific objectives of the pilot plant design effort included:

- Creation of a conceptual design for the UFP pilot-scale plant;
- Documentation of the process and instrumentation diagram (P&ID);
- Development of reactor designs for (1) fluidized gasification of coal/CO_2 absorption (Reactor 1), (2) CAM decomposition and OTM reduction (Reactor 2) and (3) OTM oxidation (Reactor 3); and
- Identification and specification of subsystems.

2.3.2 Design

Reactors

The harsh environment experienced by the UFP reactors required a detailed analysis of heat transfer and mechanical stress that was conducted based on ASME codes to ensure the integrity of the reactors and minimize the potential for material failure. The three reactors were designed for 300 psi pressure, and temperatures varying from 750 to 1300°C. The upper temperature limit may potentially be achieved in R3, while R1 and R2 typically operate at lower temperatures. However, all three reactors were designed to meet the same (highest temperature) specifications. Key features of the reactor design are provided below:

- Metal shell material: 304 SS, schedule 40, 18" nominal OD
- Maximum shell temperature: 1000°F (538°C)
- Insulating liners (inside metal shell)
    - Innermost layer: high strength, abrasion-resistant material
    - Outer layer: insulating, low thermal conductivity material
- Insulation (outside metal shell)
    - Minimal insulation to prevent excessive shell temperature

The insulating liners figured prominently in the reactor design. The innermost layer was composed of high strength, abrasion-resistant ceramic material. The next layer was an insulating, low thermal conductivity material capable of protecting the metal shell from exposure to elevated temperatures. The third layer was the metal shell, which was rated for the operating pressure and shell temperature. The outermost layer was an insulating blanket, which limited heat loss while also preventing excessive shell temperatures.

A detailed design review was conducted to ensure that the reactors met ASME code standards. The reactors were fabricated in the GEGR machine shop in Irvine and subjected to hydrostatic testing at 900 psi and ambient temperature. After 48 hours of exposure, minimal pressure loss was identified and inspection showed no loss of integrity in the reactor or welds. All the welded ports on all three vessels passed the test.

After verification of the integrity of the reactor shell, the three reactors were cast with two layers of refractory, as shown in Figure 2-9. First, a 2 1/8" layer of Kaolite 2300-LI was cast, followed by 1 3/8" of KaoTAB95. The solids transfer ducts were also cast with the same refractory layers. For each layer cast, forms were designed to provide the appropriate refractory thickness, and a jig was used to hold the forms in place with the reactors standing vertically. A combination of mixing and vibration was used to ensure that the refractory material was tightly packed. Each refractory layer was allowed to set for 24 hours before removal of the jig and forms. This process was then repeated for the second refractory layer. The refractory was cured when the complete system was assembled during shakedown testing.

Figure 2-9. Photo of R1 shell with two cast refractory layers.

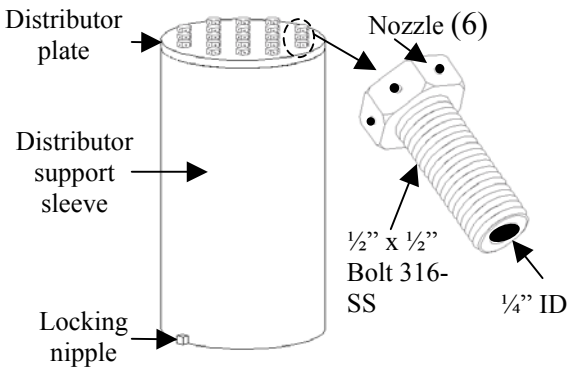

Figure 2-10. Pilot-scale distributor plate design with detail of nozzle bolts.

The distributor plates used in the pilot-scale system were designed and tested. The same distributor plate design was used for all three reactors. Working closely with the in-house machine shop, the innovative approach (illustrated in Figure 2-10) included the use of ½" hex bolts with a ¼" hole drilled from the bottom up to the bolt head, where three 1/16" nozzle holes were drilled completely through the bolt head to produce six nozzles. The orientation of the bolts allows for staggered nozzle flows to enhance fluidization. The distributor plate was designed to operate at temperatures up to 1000ºC and provide 10 psi of differential pressure. A support sleeve was used to locate the distributor plate in the correct region and prevent fluidization gas from bypassing the distributor plate. The distributor plate design shown in Figure 2-10 includes a close-up view of the bolts used as nozzles.

The three reactors were connected by a series of flanged solids transfer ducts. Reactors 1 and 3 had two solids transfer ducts, while Reactor 2 had four solids transfer ducts (Figure 2-8). The appropriate alignment of the reactors was essential to their leak-free assembly. To aid this work, fully detailed AutoCAD drawings were prepared and a stand was manufactured to provide the appropriate reactor spacing and alignment. The stand was also designed to support the weight of the filled, flanged reactors. The design of the stand required that pairs of gussets be welded to each reactor. These gussets allow the reactors to be supported from the middle of the reactors, allowing for thermal expansion while providing access to the reactors from below. The assembled reactors are shown in Figure 2-11.

Figure 2-11. Assembled pilot-scale reactors on stand.

Coal, Steam and Air Feed Systems

Systems were developed to allow coal, steam and air to be fed to the pilot-scale reactors. The coal was fed as coal-water slurry. Steam was generated in a boiler and superheater, and then

passed through a second-stage superheater to provide the needed reactor inlet temperatures. Air was conditioned and compressed for high-pressure delivery.

A Seepex progressive cavity pump (rated for 0.2 gpm at 300 psi) was selected for its ability to pump coal-water slurry into a high-pressure vessel. Shakedown testing of the pump system led to a reconfiguration of the pressure relief system to incorporate a pressure switch to shut down the pump rather than relieving pressure (which was identified as a potential hazard in the safety review.) Initial testing of the pumping system demonstrated the ability of the pump to deliver slurry into a pressure vessel maintained at 300 psi. In addition, a stirring system was used to minimize settling in the tank feeding the pump.

Hercules Boiler of Los Angeles, CA constructed a custom 900 lb/hr boiler and superheater. Due to temperature limitations of steam metering equipment, it was necessary to provide additional superheating to each steam feed line after the flow rate has been controlled to its desired set point. This was accomplished through the use of five second-stage superheaters. Each second-stage superheater consists of a 46 kW electric furnace that contains a metal coil. The length of the coil and the size of the furnace were specified based on detailed heat transfer analysis to allow the heating of a 400°C inlet stream to a temperature of 900°C, the required feed temperature for some reactors.

The air system included a low-pressure air compressor and a high-pressure booster, along with two 240-gallon receiver vessels to provide uninterrupted flow of high-pressure air to the system. A Davey 50-BAQ screw-type air compressor was used to charge the low-pressure receiver vessel with 120 psi air. This air was then fed to the Kaeser N 501-G air booster, which has a capacity of 115cfm @450 psi. The high-pressure receiver vessel was maintained at 500 psi, and allowed a steady flow of high-pressure air to the system while the booster cycled on and off. A dryer was used to remove moisture from the air after the Davey compressor.

Control, Monitoring and Analysis Systems

The control and monitoring of the pilot-scale system was conducted via using National Instruments LabVIEW software and hardware. The LabVIEW user interface was designed to allow operators direct control over all valves and control points. System monitoring was conducted with a variety of pressure, temperature, concentration and flow transmitters that interfaced with the LabVIEW program. Figure 2-12 is a process and instrumentation diagram (P&ID) for the pilot-scale system showing the location of these transmitters as well as other gauges, equipment, actuated control valves and manual valves.

The LabVIEW virtual controllers and the interactive user interface were tested and modified to provide desired operability. The user interface includes several different screens for controlling and monitoring the process. The main control screen has controls for all of the on/off and analog control valves as well as a numerical display of all the data acquired. Other screens include real-time plots of reactor temperature, CEMS gas concentrations, and bed heights. The program designer worked with system operators to provide a monitoring screen with key numerical measurements displayed to indicate their relative location on a diagram of the system, as shown in Figure 2-13. This arrangement facilitated a greater intuitive understanding of the interactions of temperature, pressure, flow rate, pressure drop and bed height for each reactor as well as for the system as a whole.

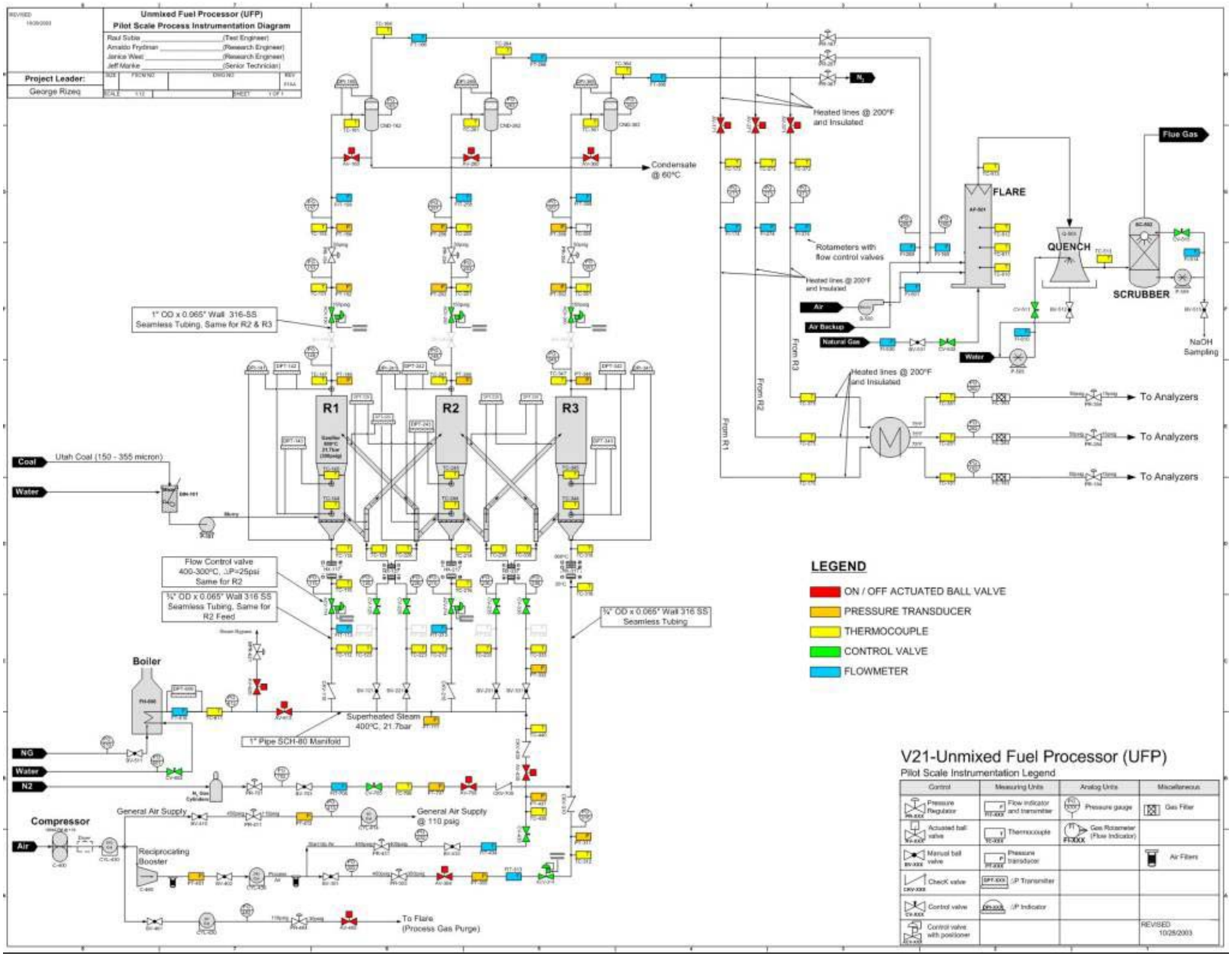

Figure 2-12. Process and instrumentation diagram for the pilot-scale system.

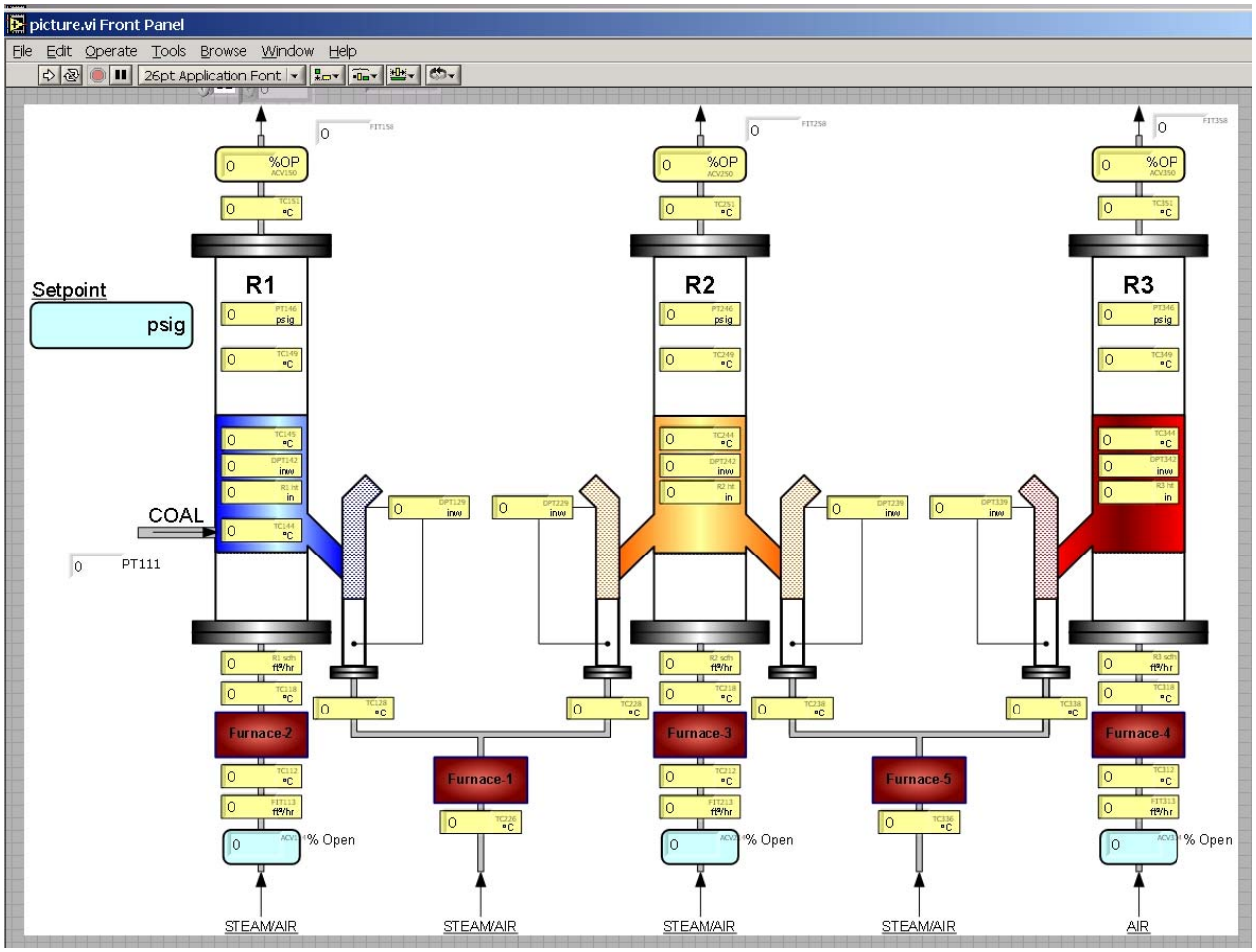

Figure 2-13. LabVIEW data acquisition screen with data measurements displayed to indicate their relative location on a diagram of the system.

Analysis of the concentrations of the product gas was conducted with both continuous emissions monitors (CEMS) and a micro gas chromatograph (GC). Dedicated CEMS were used for the product gases from each reactor, while the GC was used primarily for measurement of H_2 in Reactor 1. A new H_2 CEMS was also used for pilot-scale performance testing. The pilot-scale system was designed to allow the control of operating parameters within design limits and the monitoring and recording of key process variables and performance indicators.

During reactor heat-up and other unattended operation, a unique feature of LabVIEW was used to allow remote monitoring of the system. Operators and team members could view the real-time status of the system using a network connection. The system also has the capability for remote control operation, although this capability has not yet been implemented.

2.3.3 System Assembly

A fourteen-month delay in obtaining a South Coast AQMD permit "to construct and operate" prevented the system from being assembled as a single unit until November 2003. The planning work conducted while awaiting permit approval greatly expedited the assembly of the pilot plant, allowing most system components to be assembled in a few short weeks.

A detailed three-dimensional model of the UFP pilot plant was developed using AutoCAD to aid in system assembly. This model made use of the actual dimensions of system components, and was used to assess clearances and accessibility. Figure 2-14 is a to-scale drawing showing the layout of the pilot-scale system in relation to the control room and bench-scale system. Figure 2-15 is a photo of the completely assembled pilot-scale system.

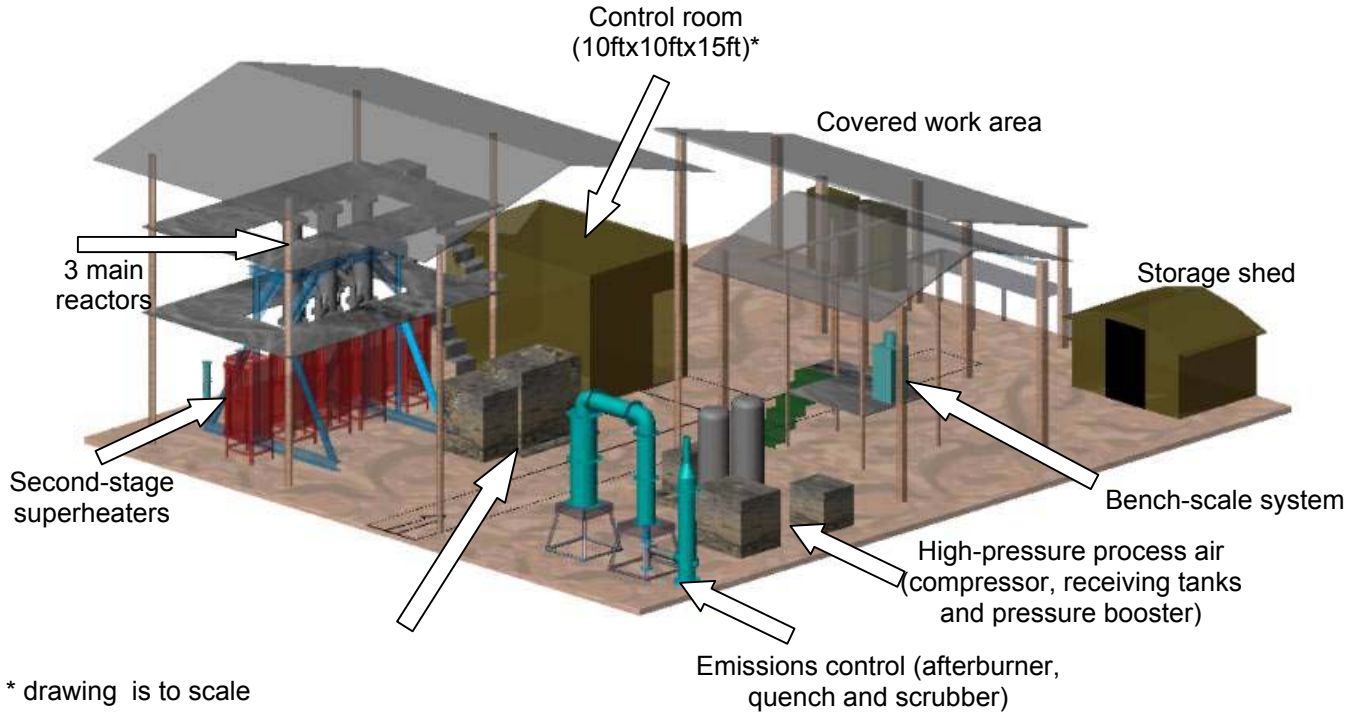

Figure 2-14. Layout of pilot-scale system.

Figure 2-15. Photo of assembled pilot plant system.

3.0 RESULTS AND DISCUSSION

3.1 Lab-Scale Testing Results

3.1.1 Coal Gasification Results

Laboratory-scale coal gasification tests were conducted in a high-temperature fluidized bed as described in Section 2.1.1. During the first 5 minutes of each test, significantly larger outlet flow rates were detected, attributable to the early release of volatile matter. Meanwhile, hydrogen production was observed to fall to negligible amounts approximately 15 minutes after the start of each experiment. After 15 minutes, the CO_2 content in the outlet gases tended to increase slightly as the CAM began to release CO_2 (caused by a shift in absorption equilibrium at low gas-phase CO_2 concentrations). Thus, the first 5 and 15 minutes of each test were chosen as evaluation periods of significance, and the results are reported accordingly. Selected lab-scale test results are provided in Table 3-1 for tests conducted with a constant bed size and different coal loadings. One of the tests was conducted with an OTM bed, while three were conducted with CAM beds.

For these batch tests with the same bed size, increasing the amount of coal places an increased performance demand on the bed materials. For CAM beds, it is possible to exceed the capacity of the CAM to absorb CO_2, as evidenced by the increasing CO_2 concentrations measured at lower CAM:coal ratios. OTM beds react with CO and H_2 to form reduced-state OTM, thus the CO and H_2 concentrations measured are lower than the raw product gas concentration for tests conducted with an OTM bed. These relationships are being analyzed to provide insight into the kinetics that will be used to quantify the relationship between bed size and bed residence time.

Selected results from coal gasification testing are provided in Table 3-1 for a series of tests conducted with injection of 2.5 grams of coal and a constant bed mass (60 g). The CAM-OTM index is a measure of the relative amounts of CAM and OTM, with an index of 1 corresponding to a pure CAM bed, and an index of –1 corresponding to a pure OTM bed. Figure 3-1 shows the volume of product gas and the volume of H_2 for each test listed in Table 3-1, with data from both 5 and 15 elapsed minutes of testing.

Since CAM absorbs CO_2, thus removing it from the product gas, it is expected that high CAM-OTM index tests will have reduced amounts of product gas, as shown in Figure 3-1. This effect is balanced to some extent by increased conversion of CO to CO_2 via the water-gas shift reaction. Also, as discussed above, OTM reacts with CO and H_2 to form reduced-state OTM, resulting in both reduced total volume and reduced volume of H_2, as illustrated in Figure 3-1.

Table 3-1. Results from lab-scale high temperature coal gasification tests.

Test #	Elapsed time	Bed contents (g)		CAM-OTM index	Gas composition (vol. fraction)				Volume (liters)	
		CAM	OTM		H_2	CO	CO_2	CH_4	H_2	Total
1	15	60	0	1	0.59	0.17	0.21	0.03	0.531	0.9
	5				0.63	0.18	0.14	0.05	0.353	0.56
2	15	60	0	1	0.59	0.15	0.23	0.03	0.472	0.8
	5				0.59	0.13	0.13	0.15	0.330	0.56
3	15	55	5	.83	0.49	0.28	0.14	0.09	0.475	0.97
	5				0.55	0.26	0.07	0.12	0.319	0.58
4	15	50	10	.67	0.46	0.23	0.17	0.14	0.529	1.15
	5				0.51	0.19	0.13	0.17	0.382	0.75
5	15	40	20	.33	0.53	0.21	0.20	0.06	0.636	1.2
	5				0.47	0.23	0.22	0.08	0.343	0.73
6	15	30	30	0	0.50	0.15	0.26	0.09	0.545	1.09
	5				0.46	0.18	0.23	0.13	0.280	0.61
7	15	0	60	-1	0.34	0.19	0.32	0.15	0.231	0.68
	5				0.38	0.19	0.27	0.16	0.182	0.48

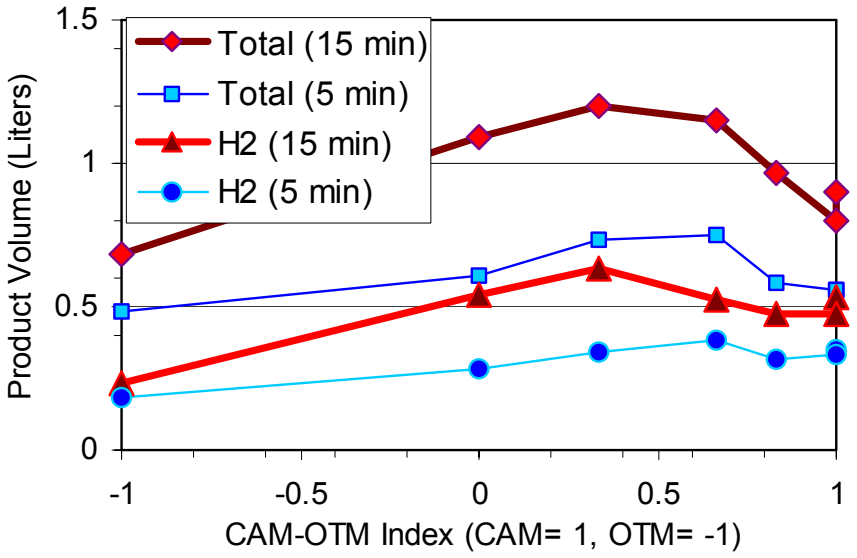

Figure 3-1. Lab-scale coal gasification results: product volume and H_2 volume at different bed compositions.

3.1.2 OTM Reduction Results

TGA experiments were conducted at a range of reducing gas compositions. In each test, 90% N_2 was fed, with the remaining 10% varying from all H_2 to all CO and various mixtures between. Selected results are provided below.

The reaction time scale varies widely (particularly for lower temperatures) for reduction by CO and by H_2, as shown in Figures 3-2 and 3-3. Note the difference in time scales, as at 700°C, complete reduction by CO is achieved after 30 minutes, while reduction by H_2 is complete after only one minute. The difference in time scale is less dramatic at higher temperatures. For example, at the expected pilot-scale operating temperature for OTM reduction (~900°C), complete reduction by CO is achieved in about three minutes, while reduction by H_2 is achieved in less than half a minute. Previous bench-scale data have shown similar behavioral trends.

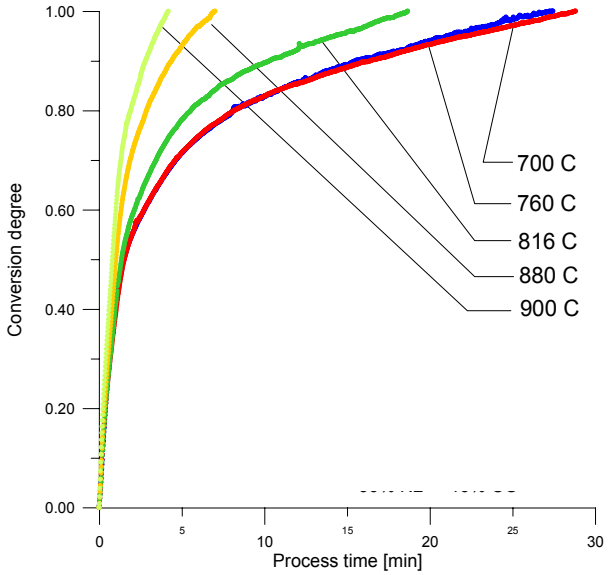

Figure 3-2. Conversion degree as a function of time for a 90% N_2, 10% CO mixture at a variety of temperatures.

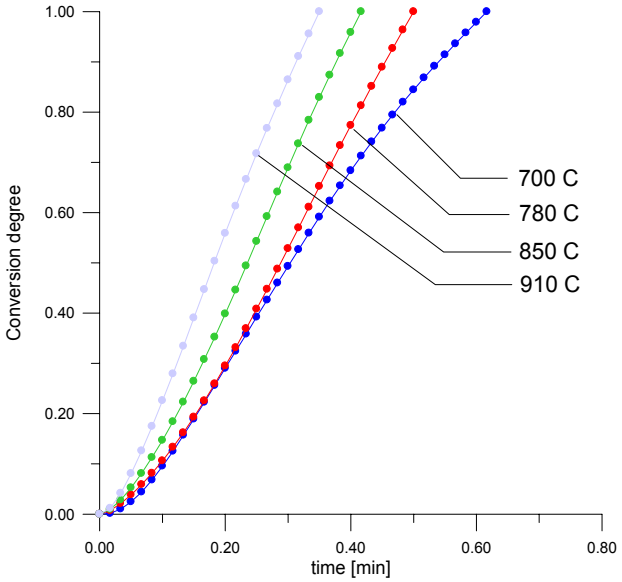

Figure 3-3. Conversion degree as a function of time for a 90% N_2, 10% H_2 mixture at a variety of temperatures.

Preliminary kinetic analysis suggests that the initial reduction by CO (up to 50% conversion) is best described by the first-order reaction model. The observed average m-value was 0.9, close to the value of 1.0 predicted by the first-order model. For initial reduction by H_2, the average m-value was 1.7, and analysis suggests that the Avrami-Erofe'ev phase change model (m = 2) best describes this data.

Mixtures of CO and H_2 were also evaluated, and the results are shown in Figures 3-4 and 3-5. Results indicate that the Figure 3-4 mixture (5.7%CO, 4.3% H_2) requires less time to achieve complete conversion (~5 minutes) than the H_2-dominant (2%CO, 8%H_2) mixture used in Figure 3-5 (~25 minutes). These results suggest that conversion time is not linear with %H_2. Similar results were reported for the bench-scale system. Kinetic analysis indicated that the initial reduction behavior of both mixtures was best described by the Avrami-Erofe'ev phase change

model. The Figure 3-4 mixture had an average m-value of 1.6, while the H_2-dominant mixture (Figure 3-5) had an average m-value of 1.15.

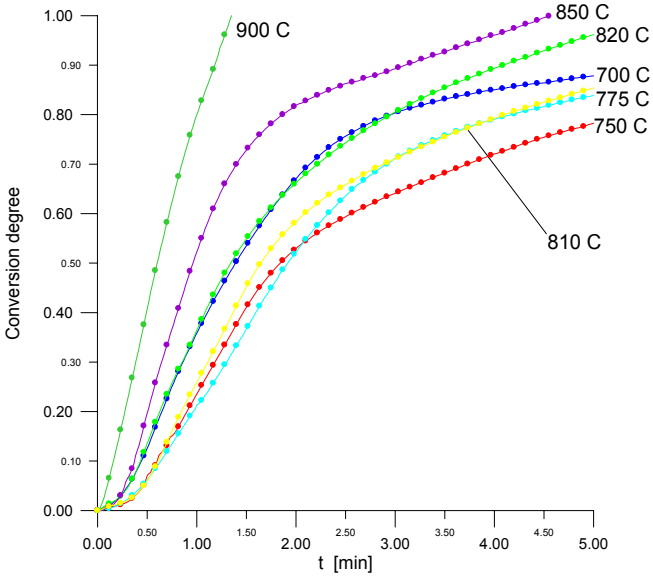

Figure 3-4. Conversion degree as a function of time for a 90% N_2, 5.7% CO, 4.3% H_2 mixture at a variety of temperatures.

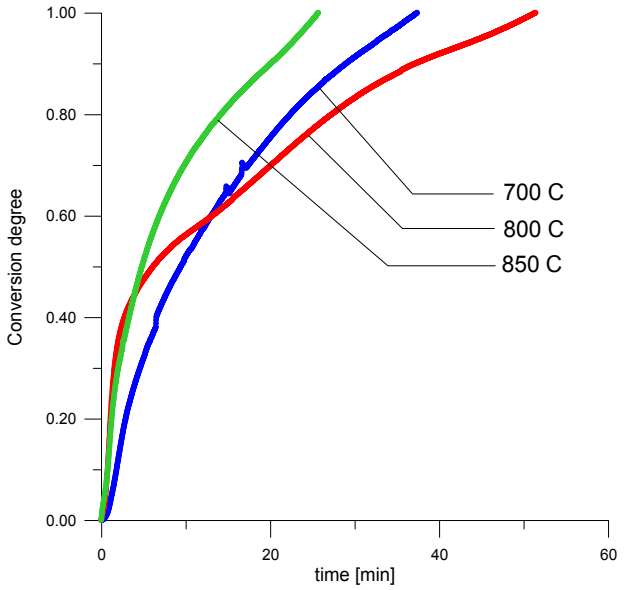

Figure 3-5. Conversion degree as a function of time for a 90% N_2, 2% CO, 8% H_2 mixture at a variety of temperatures.

Using k-values from the derived kinetic expressions, reaction data were used to derive preliminary activation energy values. Due to some perturbations associated with low temperatures (<780°C), activation energies were derived using data only from temperatures between 780-900°C, as recommended by Tokuda (1979).

TGA experiments conducted previously were used to develop a kinetic model for OTM reduction. Figure 3-6 shows the impact of temperature on the extent of OTM reduction for a range of hydrogen concentrations. At 800°C, only at hydrogen concentrations approaching 10% is the OTM reduction complete (α=1) during the five-minute time interval shown. Meanwhile, at 900°C, complete OTM reduction is achieved at all concentrations shown, with increased H_2 concentrations causing reactions to proceed to completion more quickly. These results are encouraging, since the UFP's middle reactor will be operated at temperatures greater than 900°C to ensure CAM decomposition and CO_2 separation, thus ensuring that OTM reduction occurs more readily in the middle reactor, despite potential low H_2 and CO concentrations. Maximizing OTM reduction in R2 minimizes the amount of oxidized OTM entering the gasification reactor (R1), thus minimizing the consumption of product H_2 for OTM reduction.

3.1.3 Heat Treatment Experiments

Heat treatment experiments were also conducted. Photographs of the CAM/OTM/Ash mixtures were taken both before and after testing to allow qualitative comparison of behavior. Baseline diffractograms were also obtained using x-ray analysis of pure CAM and OTM samples. These

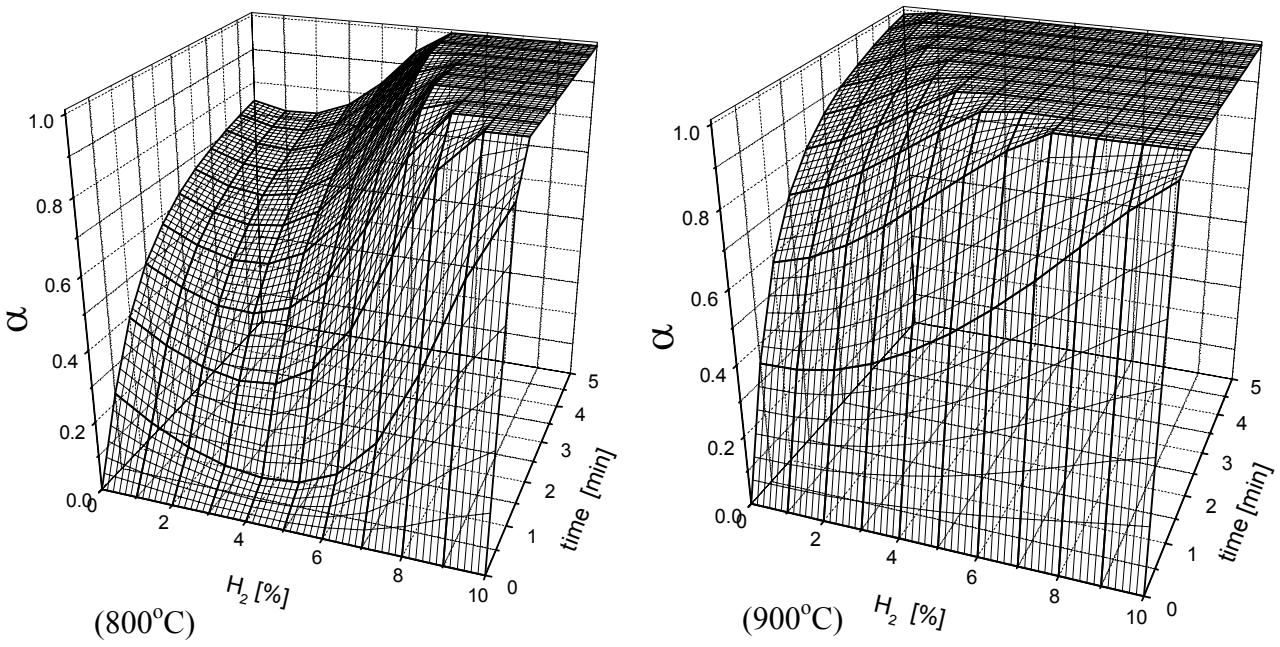

Figure 3-6. Kinetic modeling results showing the impact of temperature on conversion extent (α) over time for reduction of OTM with 0-10% H_2.

baseline diffractograms provided increased confidence in interpreting results of x-ray analysis conducted after completion of tests from the test matrix.

No significant agglomeration was observed in any of the samples after heat treatment. Only test 1.1, conducted with small particle-size pure OTM and CAM-CO_2, showed the formation of a complex CAM-OTM phase (see Figure 3-7). In all other tests, OTM and CAM present at the beginning of the test were also identifiable via diffractogram after heat treatment. Testing conducted under a steam atmosphere as part of the third experimental series led to formation of hydrated forms of CAM and OTM. No other forms of OTM or CAM were identified via x-ray diffraction.

Heat treatment at temperatures of 950°C and above typically caused thermal decomposition of CAM-CO_2 to form CAM. During tests conducted at 750°C, decomposition of CAM-CO_2 to CAM was not always complete (some CAM-CO_2 was present in the diffractogram). Tests conducted with simulated ash had detectable levels of SiO_2 and Al_2O_3, but K and Na were present at concentrations below the detection limit of the x-ray diffraction analyzer.

These heat treatment results are encouraging since testing results suggest that CAM and OTM of the type used for the pilot plant do not agglomerate or form complex solid mixtures at the representative conditions tested.

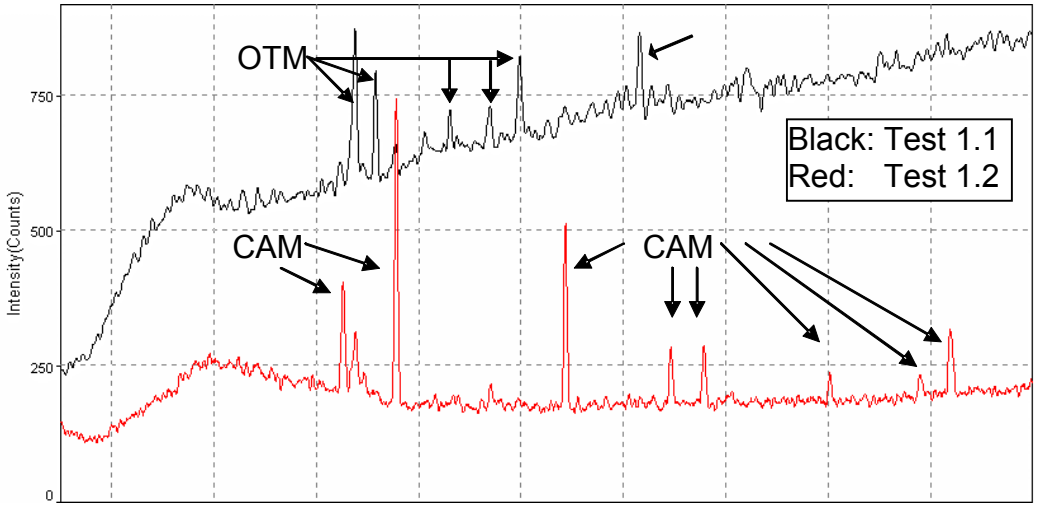

Figure 3-7. Diffractograms from experiments 1.1 and 1.2.

3.1.4 CAM Development Results

A commercially-prepared CAM sample obtained from Aldrich Chemical was tested for comparison with the CAM samples prepared by precipitation. The four precipitated CAM samples were tested to characterize specific surface area and particle size distribution. The results of BET analysis and particle size analysis are provided in Table 3-2, and show that the use of surfactants increased the specific surface area. CAM-S1 showed an increased mean particle size, while CAM-S2 and S3 had decreased particle sizes. All of the precipitated CAM samples had higher specific surface areas than the commercially-prepared Aldrich CAM. Thus, the new precipitation preparation method had a positive impact on surface area.

Table 3-2. Characteristics of the CAM sorbents prepared with different surfactants.

Sample	Specific Surface Area (m^2/g)	Mean Size (μm)	Median Size (μm)
CAM -no surfactant	588	9.24	9.99
CAM -surfactant 1	663	10.43	10.43
CA M -surfactant 2	634	6.38	6.38
CAM -surfactant 3	614	4.93	5.31
Aldrich CAM	495		

The results of TGA experiments provide insight into the CO_2 capture and release through their measurement of sample weight changes during the capture/release cycle. The weight % measured is an indicator of the state of the CAM, and the rate of change in weight is proportional to the rate of desorption. Figure 3-8 shows the TGA results starting after a preliminary 15-minute CO_2 capture step. CAM-S1 shows superior performance, as it more completely releases the CO_2 (as evidenced by a reduction in weight %) at a much faster rate than any of the other

sorbents tested. All of the precipitated sorbents showed more complete CO_2 release than the Aldrich CAM. The CO_2 release step was continued until no changes in weight were observed; thus, the subsequent CO_2 capture step began at a different time for each CAM sample. CAM-S3 demonstrated a particularly slow CO_2 release step as well as a significant performance degradation in the subsequent CO_2 capture step, as the weight increase due to CO_2 capture was significantly lower than the 100% measured prior to the first CO_2 release step.

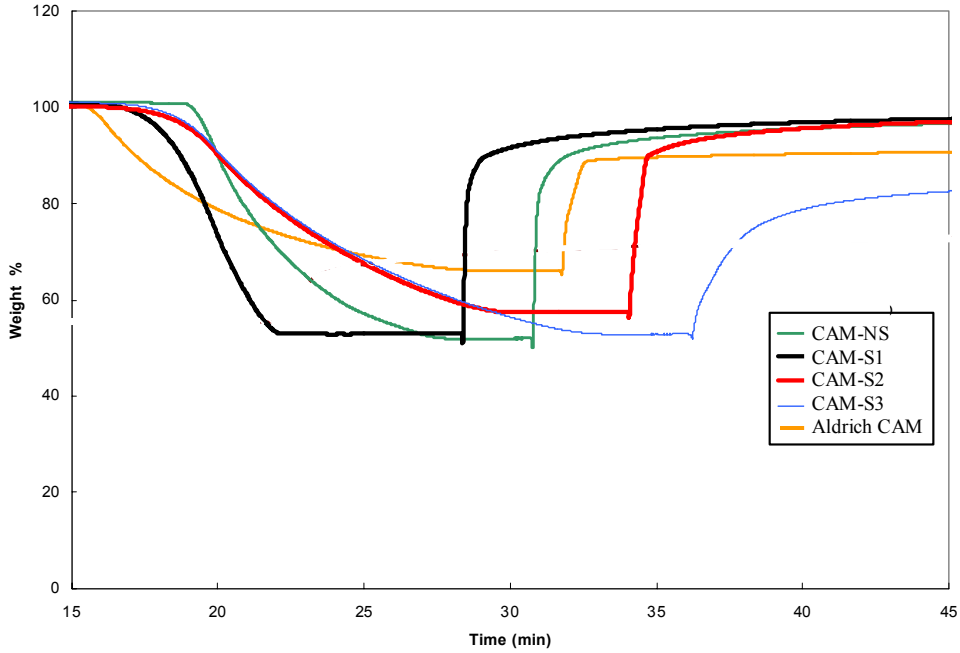

Figure 3-8. Comparison of the TGA response of a CO_2 capture/release cycle for different CAM materials.

The CO_2 capture results during TGA testing are summarized in Figure 3-9 and show the change in $\%CO_2$ uptake after multiple cycles. All of the precipitated CAM samples showed improved performance relative to the Aldrich CAM, and the use of surfactants generally improved CO_2 capture, particularly after 6 cycles. The performance of the precipitated CAM prepared without any surfactant (CAM-NS) decreased markedly after each of the first six cycles, then increased to 70% uptake after ten cycles. The performance of CAM-S1 showed a similar trend, but increased to 80% uptake after ten cycles. CAM-S2 decreased gradually with each additional cycle, while CAM-S3 exhibited a steep decline over the first two cycles, then a steady increase over the next five cycles, leveling out at approximately 70% uptake after six cycles. These results, coupled with the rate of weight change results discussed previously, suggest that CAM-S1 was the most promising of the CAM materials tested.

The changes in CAM performance after several cycles were investigated using a variety of techniques. SEM microscopy was used to characterize the morphology of CAM samples both before and after cycling. The micrographs show that a physical change in the samples had occurred, with the surface becoming less rough. This change was associated with the degradation in performance illustrated in Figure 3-8, which showed CO_2 uptake decrease from 100% to 65% after four cycles.

The results of the CAM testing showed that use of the precipitation method for CAM preparation yielded higher specific surface areas, and that surfactant 1 improved the rate of CO_2 release and CO_2 absorption, as well as the performance over time. The demonstrated ability to manipulate CAM properties and performance via preparation method suggests that CAM materials can be further optimized for high performance and long lifetime.

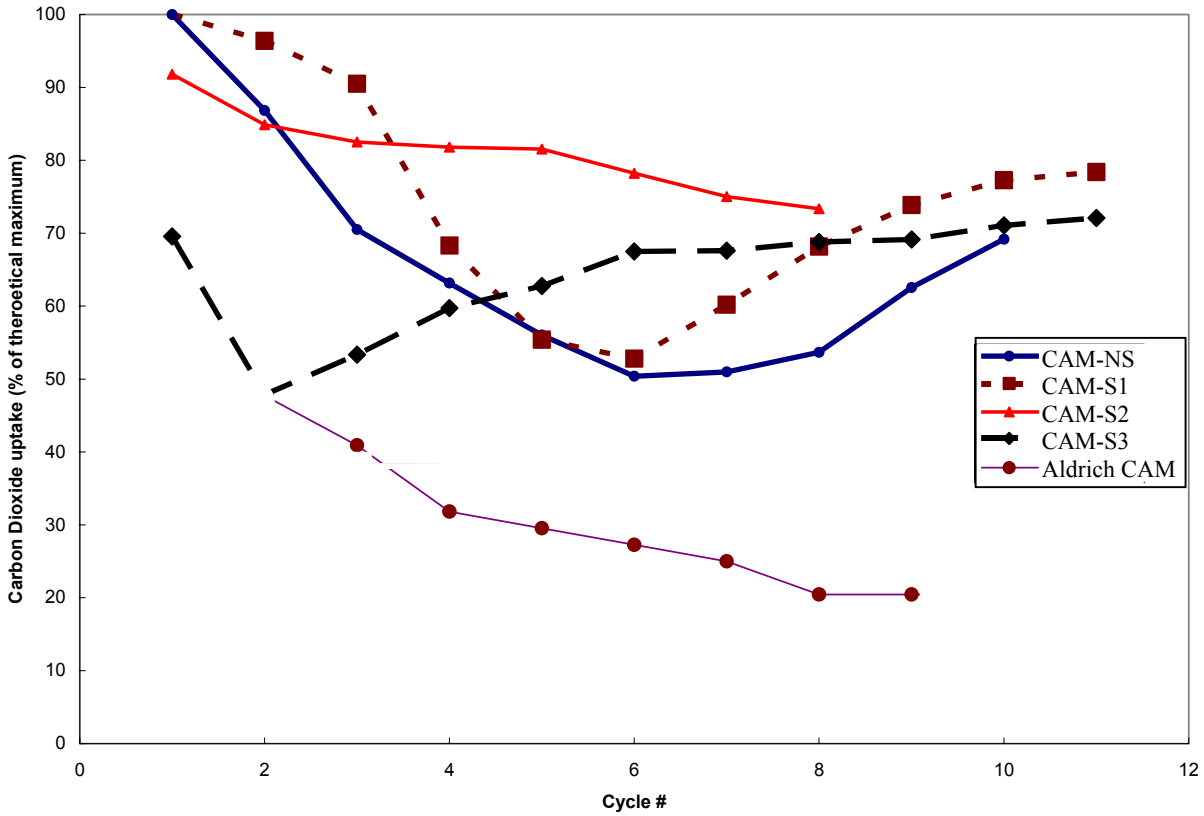

Figure 3-9. Change in CO_2 uptake after multiple CO_2 capture/release cycles for the four precipitated CAM sorbents and the commercially-prepared Aldrich CAM sorbent.

3.2 Bench-Scale Testing Results

The objectives of the bench-scale testing task were to establish the chemical and mechanical feasibility of the UFP concept. The bench-scale system also provided data on individual UFP processes to aid in pilot plant design and testing. Bench-scale testing focused on performance assessments and parametric testing of the three key UFP processes/cycles: coal gasification, CO_2 absorption/release, and OTM oxidation/reduction. Experimental results have illustrated the way key processes occur, identified key variables and ranges of operating conditions that produce desired results, and validated the overall UFP concept by demonstrating the chemical feasibility of its key reactions and processes.

3.2.1 Coal Gasification and CO_2 Absorption/Release Testing

Initial bench-scale testing focused on coal gasification and CO_2 absorption using a CAM bed. For comparison, preliminary tests were also conducted with an inert bed possessing no CO_2-

absorbing capacity. A unique feature of the UFP technology is its inherent production of high-purity H_2 due to the absorption of CO_2 by CAM. Early experiments confirmed this capability. Gasification test results showed decreased CO_2 concentrations and product gas flow rates for the CAM bed tests. The CO_2 concentration increased more rapidly and with a higher peak concentration during gasification in an inert bed. The CO concentration behaved in a similar manner, with increased concentrations during gasification in an inert bed. The reduced CO_2 concentrations were due to the absorption of CO_2 by the CAM bed. Meanwhile, the reduction in CO was caused by the participation of CO in the water-gas shift reaction ($CO + H_2O \rightarrow CO_2 + H_2$), driven by the low CO_2 concentrations in the reactor.

Further investigation was directed at quantifying H_2 production and CO_2 absorption. As discussed above, the absorption of CO_2 during coal gasification had a significant impact on product gas composition. Unfortunately, CO_2 absorption cannot be measured directly; however, since only absorbed CO_2 can be released, it can be measured indirectly via the CO_2 released during a subsequent regeneration step. The regeneration of CAM was conducted at an elevated temperature, generally 920°C. In previous tests conducted with an inert bed, all of the CO_2 generated was released during coal gasification. In contrast, using a bed composed of CAM, only a small fraction of the CO_2 was released during coal gasification; the remainder was absorbed by the CAM and released during a subsequent regeneration step. This process is depicted in Figure 3-10 for both an inert bed and a CAM bed. The CO_2 flow rate is significantly higher for the inert bed case during coal gasification, while for the CAM bed, the CO_2 flow rate reaches its peak value during the regeneration step after the CAM regeneration temperature is reached.

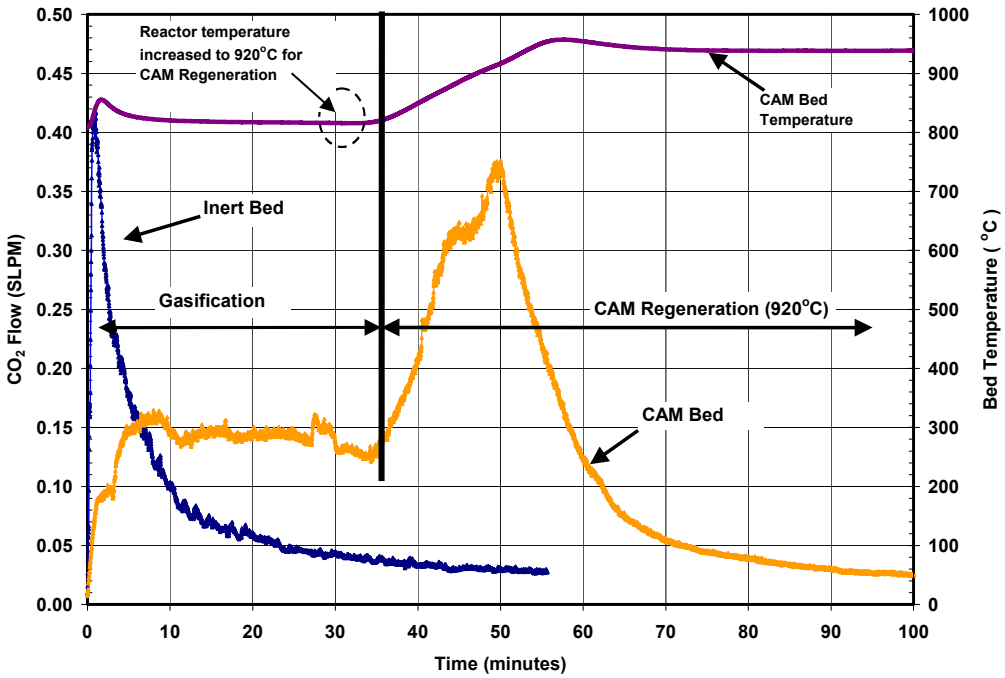

Figure 3-10. CO_2 released during coal gasification and CAM regeneration for a CAM bed, and during coal gasification for an inert bed. The temperature profile for the CAM bed case is also shown.

Parametric Testing: Impact of Gasification Temperature

Temperature is a key variable affecting CO_2 absorption and release. In order to quantify its impact, parametric coal gasification experiments were conducted at temperature of 750, 800 and 850°C, followed by CAM regeneration at 920°C. CO_2 concentrations from these tests are provided in Figure 3-11. Since the total amount of carbon present in the system was fixed, more CO_2 present during the coal gasification step leads to less CO_2 present during the CAM regeneration (CO_2 release) step. As might be expected, as the bed temperature approaches the CAM regeneration temperature, less CO_2 is absorbed. At higher temperatures, the equilibrium between CO_2 absorption and release is biased toward CO_2 release. Thus, at 850°C, the CO_2 concentration during coal gasification is significantly higher than at the lower temperatures. As a result of this reduced CO_2 absorption, less CO_2 is released during the subsequent CAM regeneration step. At both 750 and 800°C, peak CO_2 concentrations were achieved during the CAM regeneration step, indicating increased levels of CO_2 absorption during the coal gasification step.

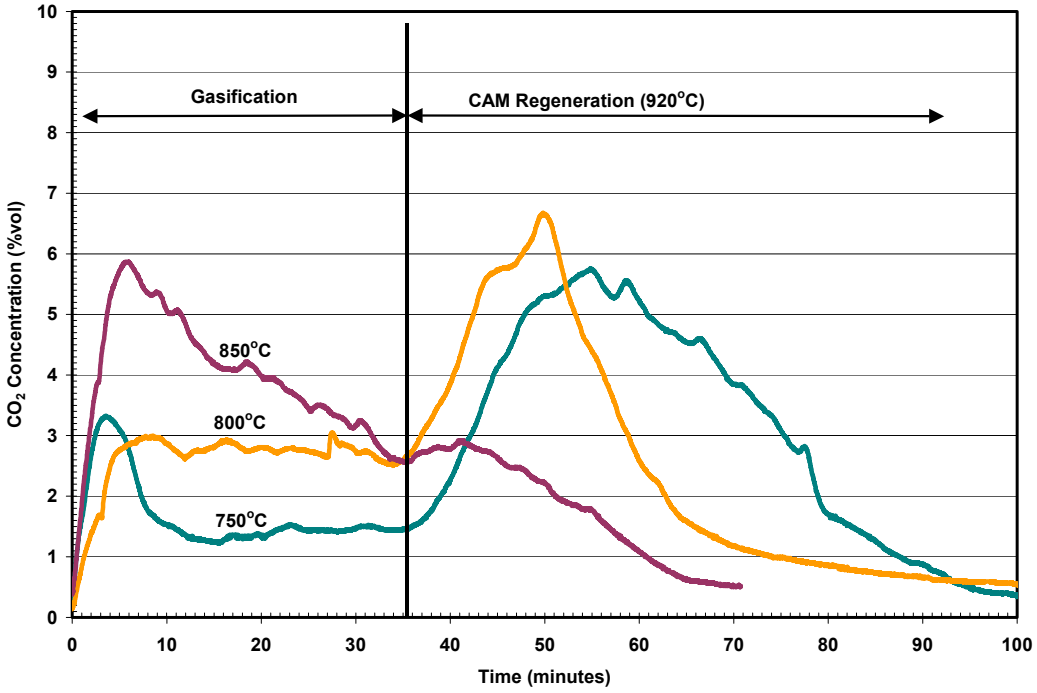

Figure 3-11. CO_2 concentrations at three different gasification temperatures, with CO_2 release at 920°C for each run.

However, CO_2 concentrations were not the only consideration; the objective of the coal gasification step was to produce high-purity hydrogen. H_2 concentrations greater than 80% were achieved at 750 and 800°C, as shown in Figure 3-12. The increased CO_2 concentration present at 850°C had the effect of decreasing the H_2 concentration, peaking at only 72%. Although H_2 concentrations were similar at 750 and 800°C, the H_2 flow rates varied. H_2 flow rates were measured for the first 15 minutes of the 30-minute gasification step, since flows were relatively constant and very small after that time. The majority of the flow occurred in the first five minutes of the step. The highest peak flow rate was achieved at 800°C, substantially higher than that

achieved at 750°C, despite the similar product H_2 concentrations at these two temperatures. The high H_2 flows at 850°C were less impressive when the low H_2 concentrations (and thus high impurity concentrations) were considered.

It is necessary to strike a balance between a bed temperature too high for CO_2 absorption to occur and a temperature so low that the coal gasification is hampered. Based on these bench-scale testing results, 800°C was selected as the optimal temperature for bench-scale coal gasification tests.

The experimental investigation of coal gasification and CO_2 absorption provided quantitative data on the impact of R1 temperature on H_2 yield and purity as well as CAM effectiveness. This data was used to identify desirable operating conditions and validate predicted behavior from process modeling efforts.

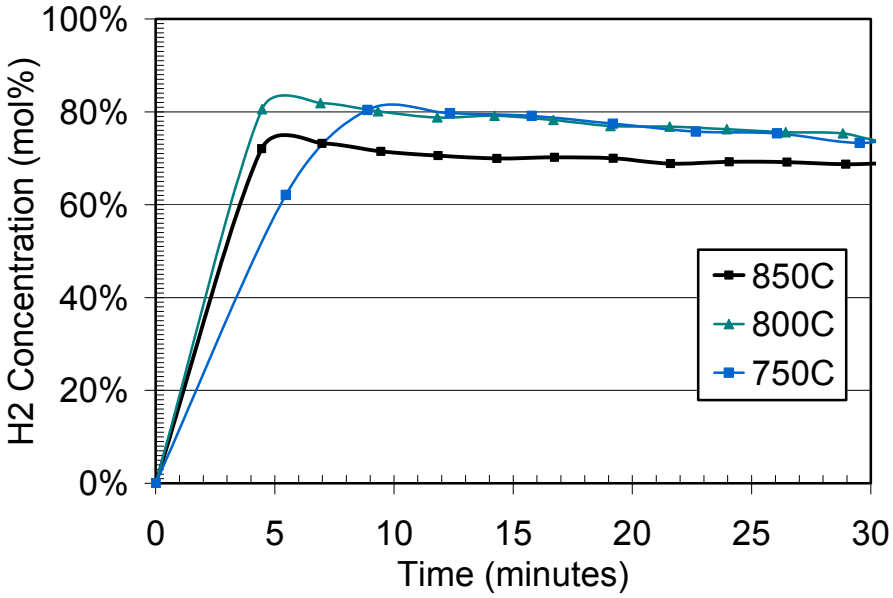

Figure 3-12. H_2 concentrations at three different bed temperatures during gasification and CAM regeneration.

3.2.2 Oxygen Transfer Material Performance

OTM Reduction with Coal

OTM/coal tests were conducted in two steps. First, an OTM bed was fluidized by steam at 920ºC, then a batch of coal was fed to the reactor. The coal gasification products (primarily CO and H_2) provided the fuel for OTM reduction. In the UFP system, the fuel for OTM reduction is char transferred from R1. However, as the objective of these initial tests was to verify that the OTM bed could undergo oxidation/reduction with gasified fuel, the use of coal in place of char had a minimal impact on the interpretation of results.

The second step of the OTM test was OTM oxidation, accomplished by first lowering the temperature of the reactor to 750ºC under flowing N_2 (to prevent overheating during OTM oxidation), then feeding air to the reactor and measuring the increase in bed temperature and the oxygen concentration of the product gas. The temperature increase during the oxidation step was rapid and significant. The magnitude of the temperature increase during the oxidation step is an indirect measure of the amount of OTM that was reduced (and thus made available for oxidation) in the reduction step. The amount of O_2 consumed may also be used as an indirect measure of the amount of OTM that was reduced during the reduction step.

The extent of OTM reduction is related to the amount of reducing fuel present. During the OTM tests, varying amounts of coal were used to provide the fuel for OTM reduction. The objective of these tests was to identify the maximum temperature increase achievable during the oxidation step. Preliminary results suggested that excess fuel might adversely impact the OTM oxidation/reduction cycle, as can insufficient fuel.

OTM Reduction with CO and H_2

After completion of test runs relative to the test matrix described in Section 2.2.3, an initial transfer function was developed and used to identify operating conditions predicted to provide peak OTM reduction. Two additional optimization tests were conducted at the conditions predicted to provide high OTM reduction. The results in Table 3-3 show that the %OTM reduction achieved in these tests exceeded the performance of all previous test runs and validated predictions of the initial transfer function. An optimized transfer function was then derived from results of all fifteen tests based on a surface fit and making use of second-order interactions. This transfer function is provided below:

$$X_{OTM} = 44.7 + 1.6[CO] - 0.93[H_2] - 0.033GHSV - 0.13[CO][H_2] + 8.8\times10^{-4}[H_2]GHSV - 0.17[CO]^2 - 0.013[H_2]^2 + 6.9\times10^{-6}GHSV^2$$

Where:

- X_{OTM} = fraction of OTM reduced (wt%)
- [CO] = concentration of CO at 900°C and 300 psi (0 – 7.4 vol. %)
- [H_2] = concentration of H_2 at 900°C and 300 psi (0 – 14.7 vol. %)
- GHSV = gas hourly space velocity, volumetric steam flow/volume of bed (1500 – 3200)

Table 3-3. OTM test conditions and results for full test matrix.

Test #	Independent Variables			Response
	Local feed concentration		GHSV	OTM Reduction
	[CO] vol. %	[H_2] vol. %	(hr^{-1})	(%)
1	3.1	12.4	1798	10.6
2	6.4	6.4	1573	9.4
3	0	7.1	1718	10.8
4	6.1	12.1	1562	6.9
5	7.4	0	1665	10.2
6	0	14.7	2144	15.4
7	0	13.2	1515	12.8
8	5.5	0	3170	11.1
9	3.1	6.2	1931	10.9
10	3.6	0	1544	12.9
11	0.0	0	2443	4.0
12	6.0	12.0	2527	11.5
13	3.3	6.6	2517	12.7
Opt-1	0	13.1	2611	19.0
Opt-2	0	14.0	2452	20.0

The 15-test transfer function was used to calculate predicted performance for the actual test conditions, and these predictions were compared to the actual experimental results, with excellent agreement. A three-dimensional plot of the effects of CO concentration and GHSV on OTM reduction at 10% H_2 concentrations is shown in Figure 3-13. The region of expected pilot-scale operation is shown, and is expected to result in reduction of up to 20% of the OTM present in the bed. This provides sufficient OTM reduction activity for the UFP system.

Use of OTM Oxidation to Gauge OTM Reduction

Analysis of OTM performance is complicated by the participation of the OTM reduction reactants and products in the water-gas shift reaction when CO is one of the reactants. The key reactions are shown below. The water-gas shift reaction is reversible and highly dependent on local concentrations. Thus, composition measurements of the product gas must be interpreted with care, as reduction products can, in turn, become water-gas shift reactants. In the UFP technology, both CO and H_2 are produced by coal gasification/char oxidation in R2, while steam is fed as the fluidizing gas. However, the complexity of these interactions provides limited data concerning the individual kinetic rates of CO and H_2 consumption by OTM reduction. The reactions of interest are shown below:

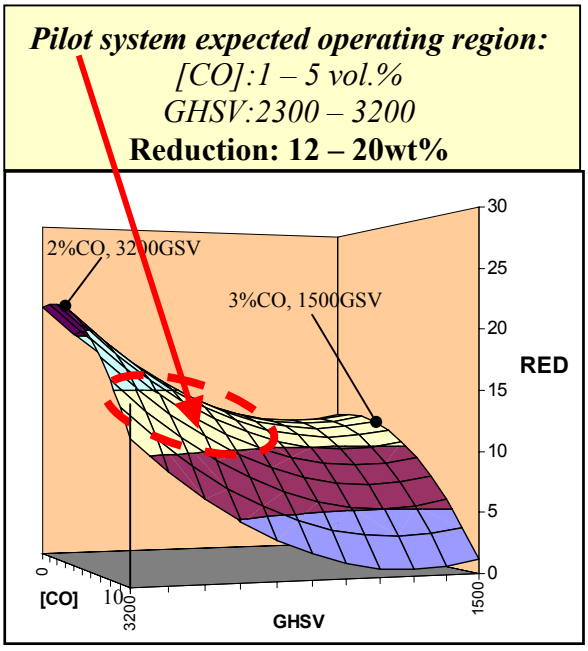

Figure 3-13. Transfer function predictions of OTM reduction as a function of CO concentration and GHSV at 10% H_2 concentration.

$OTM\text{-}O + CO \rightarrow 2OTM + CO_{2\text{-}red}$ OTM reduction with CO

$OTM\text{-}O + H_2 \rightarrow 2OTM + H_2O$ OTM reduction with H_2

$CO + H_2O \rightarrow CO_2^* + H_2$ water-gas shift

Where: OTM-O is the oxidized state of OTM .

The distinction between the OTM reduction reactions and the water-gas shift reactions is most clear in tests using CO as the reducing gas. CO_2 is a product of both the OTM reduction and the water-gas shift reactions. Since H_2 is not a product of the OTM reduction reactions, the amount of H_2 in the product gas is an indication of the extent of the water-gas shift reaction (and thus the amount of CO_2 produced via the water-gas shift reaction). Therefore $\{H_2\} = \{CO_2^*\}$, where $\{H_2\}$ is the number of moles of H_2 and $\{CO_2^*\}$ is the number of moles of CO_2 produced via the water-gas shift reaction. Using {} in the text symbolizes number of moles of the chemical constituent between the brackets.

The measured CO_2 concentration is composed of contributions from both the water-gas shift and the OTM reduction reactions; thus, for tests of reduction by CO, $\{CO_{2\text{-}tot}\} = \{CO_{2\text{-}red}\} + \{CO_2^*\}$ and $\{CO_{2\text{-}red}\} = \{CO_{2\text{-}tot}\} - \{CO_2^*\}$. The degree of OTM reduction can be determined by relating $\{CO_{2\text{-}red}\}$ to the OTM-O concentration and comparing this value to the initial amount of OTM-O in the bed $\{OTM\text{-}O_{\text{-}bed}\}$ per the OTM reduction with CO reaction above. Therefore, since the stoichiometry of the reduction reaction with CO dictates that one mole of CO_2 is produced for every mole of OTM-O [i.e., $\{CO_{2\text{-}red}\} = \{OTM\text{-}O\}$], %OTM reduction = $\{CO_{2\text{-}red}\}$ / $\{OTM\text{-}O_{\text{-}bed}\}$. This can be easily calculated since $\{CO_{2\text{-}red}\}$ can be obtained from the measured $CO_{2\text{-}red}$ concentration and the $\{OTM\text{-}O_{\text{-}bed}\}$ can be obtained from the weighted $OTM\text{-}O_{\text{-}bed}$ initial amount.

The oxidation step (simulating R3 in the UFP system) involves the reaction:

$$2\ OTM + \tfrac{1}{2}\ O_2 \rightarrow OTM\text{-}O$$

The measured amount of O_2 consumed can also be used to independently arrive at a % OTM reduction level. Since ½ mole of O_2 reacts to produce each mole of OTM-O, $\{OTM\text{-}O_{\text{-oxid}}\} = \frac{1}{2}\{O_2\}$, where $\{O_2\}$ is the number of moles of O_2 consumed. Thus, %OTM reduction = $\frac{1}{2}\{O_2\} / \{OTM\text{-}O_{\text{-bed}}\}$.

In test matrix runs #5 and #10 (from Table 3-3), CO was used as the sole reducing gas. For these tests, the %OTM reduction was calculated by the two above-described methods: CO_2 generated (based on measurements of CO_2 taken during the reduction step) and oxygen consumed (based on measurements of O_2 taken during the oxidation step). Table 3-4 shows reasonably good agreement between results calculated via the two methods; for Run #5, 10.4 vs. 9.5% OTM reduction, and for Run #10, 12.5 vs. 12.8% OTM reduction. The good agreement between these values provides support for the calculation assumptions, especially relative to the amount of CO_2^* from the water-gas shift reaction. The O_2 consumption results for several test matrix experiments are shown in Figure 3-14.

Table 3-4. Results of CO reduction experiments: %OTM reduction calculated via both reduction step and oxidation step experimental measurements.

run #	mol OTM in bed	Reduction Step				Oxidation Step		
		OTM : %CO ratio	% CO fed	mol CO_2 generated by OTM reduction	**% OTM reduction— Reduction Step**	% O_2 fed	mol O_2 consumed	**% OTM reduction— Oxidation Step**
5	1.28	0.16	8	0.13	**10.4**	4.1	0.24	**9.5**
10	1.57	0.39	4	0.20	**12.5**	7.4	0.40	**12.8**

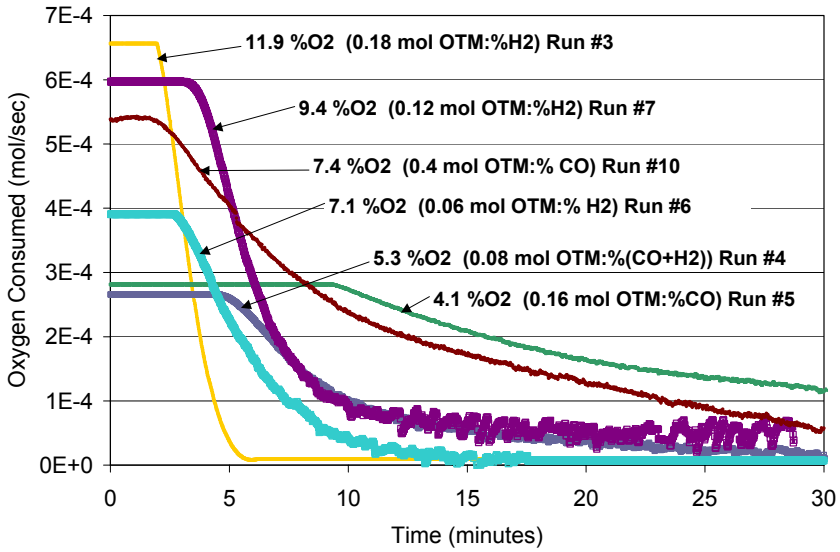

Figure 3-14. O_2 consumption during OTM air regeneration step.

3.2.3 Cold-Flow Model Results

Early experiments identified key variables affecting solids transfer flow rates, so the experimental matrix was optimized to provide meaningful data with fewer experiments. Experimental data were analyzed using the Design-Expert 6.0 tool, which was used to generate contour plots of the design space. One key experimental observation centered on the identification of an optimized flow rate of carrier gas. As carrier gas flow increased, solids flow increased with carrier flow up to the optimum carrier flow. Above this optimum carrier gas flow rate, solids flow decreases with increasing carrier gas flow, presumably due to a "vortex effect" at the induction point.

The contour plots obtained from experimental data analysis were used to identify the optimum carrier gas flow at different operating conditions, as shown in Figure 3-15. This information, in turn, was used to identify the analogous pilot-scale operating conditions to provide the required solids transfer flow. Understanding the trends in behavior was beneficial in the assessment of solids transfer performance when the three reactors were integrated and the solids transfer rate could not be measured directly.

The establishment of optimal operating conditions for the solids transfer mechanism validated the mechanical feasibility of the circulation of solids between three fluidized beds. Additional testing was conducted in the pilot-scale system that further validated these results.

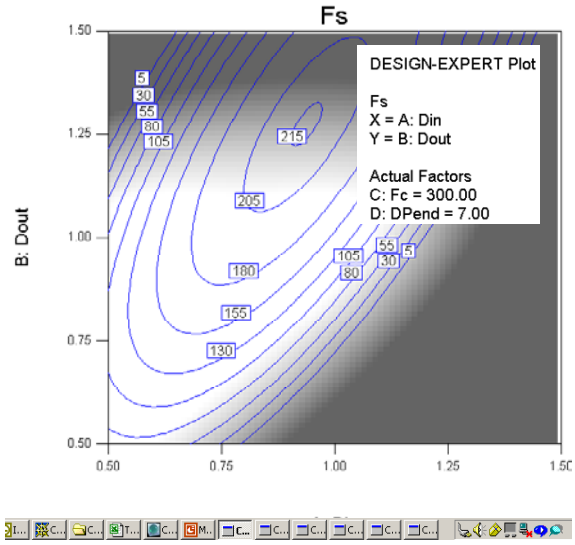

Figure 3-15. Contour plots of cold flow model data: relationship between flow rate and inlet and outlet diameters.

3.3 Pilot-Scale Testing Results

Assembly and testing of the pilot-scale system was delayed due to the fourteen-month wait for a South Coast AQMD permit "to construct and operate." After the system was assembled and shakedown testing had commenced, an unforeseen circumstance arose with the Irvine Test Site property owner (the Irvine Company) who wanted to use the land for a housing project. This required the facilities be dismantled and removed to a new location. The timeline for relocating facilities, coupled with the expected timeline for receiving new operating permits at the new site, led to the decision to complete testing for this stage of the project prior to the test site move.

This time constraint, along with several technical issues that arose during shakedown testing, required the modification of the original testing plan in order to obtain coal test data on the system prior to its disassembly and reassembly, an endeavor projected to take several months beyond the already-extended program timeframe and available budget. The emphasis on results continued to be, as throughout the program, to obtain data that support the validity of the UFP technology and its potential to meet long-term energy efficiency and environmental targets. Although the method of providing this data was modified due to the constraints above, the

experimental results obtained provide confirmation of the key UFP performance parameters and underscore the need for continued development and experimentation.

3.3.1 Shakedown Test Results

Key system components were tested individually while awaiting approval for system assembly, so shakedown testing after system assembly was focused on process-wide testing. Table 3-5 is a list of shakedown tests that were completed, with the test type, key operating conditions, and key measurements noted for each test.

Tests 1 through 3 focused on validating fluidization behavior. Baseline values for fluidization parameters were assessed by measuring the pressure drop across each distributor plate with no bed in place. The each of the three reactors, as well as each solids transfer leg has a distributor plate. Each distributor plate was characterized without a bed in place to provide baseline values. In addition, baseline values of pressure drop across a well-characterized bed were also recorded to provide a basis for monitoring changes in pressure drop during process operation.

Table 3-5. Process shakedown tests.

#	Test Type	Feed (Air or Steam)			Operating conditions		Reactor Top Flanges	Bed circula-tion	Key Measurements
		R1	R2	R3	T (°C)	P (psig)			
1	dP of leg distributor plate (no bed)	Air	Air	Air	Ambient	14.7	Open	On	dP_leg
2	dP of bed distributor plate (no bed)	Air	Air	Air	Ambient	14.7	Open	Off	dP_reactor
3	dP of bed	Air	Air	Air	Ambient	14.7	Open	Off	dP_reactor, bed height
4	Verify bed movement	Air	Air	Air	Ambient	14.7	Open	On	dP_reactor, dP_leg
5	Bed circulation rate	Air	Air	Air	Ambient	14.7	Open	Varies	dP_leg, bed height
6	Leak test	Air	Air	Air	Ambient	60	Closed	Off	System pressure
7	Pressure uniformity across reactors	Air	Air	Air	200	30	Closed	On	Reactor pressure
8	Verify bed movement	Air	Air	Air	200	30	Closed	On	dP_reactor, dP_leg
9	Solids transfer rate	Air	Air	Air	200	30	Closed	On	dP_leg, bed height
10	Reactor heat-up	Stm	Stm	Air	800	30	Closed	On	Temperature

The solids transfer mechanism was validated with the top flanges open (Tests 4 and 5) to allow visual inspection of both fluidization and solids transfer. Video clips were recorded, showing the pulsing solids flow into the reactors. Figure 3-16 shows two photos of the inside of R2, both before (left photo) and during (right photo) one of the solids transfer tests. The solids transfer inlet ports can be seen near the bottom, just above the bed. The two inlets in R2 showed pulsing behavior, with solids injection alternating between the two ports. These qualitative results were helpful in illustrating solids transfer behavior. This observed behavior was correlated with the measured pressure drops, providing insight into the meaning of the measured values that were the key source of fluidization and transfer information once the top flanges were replaced.

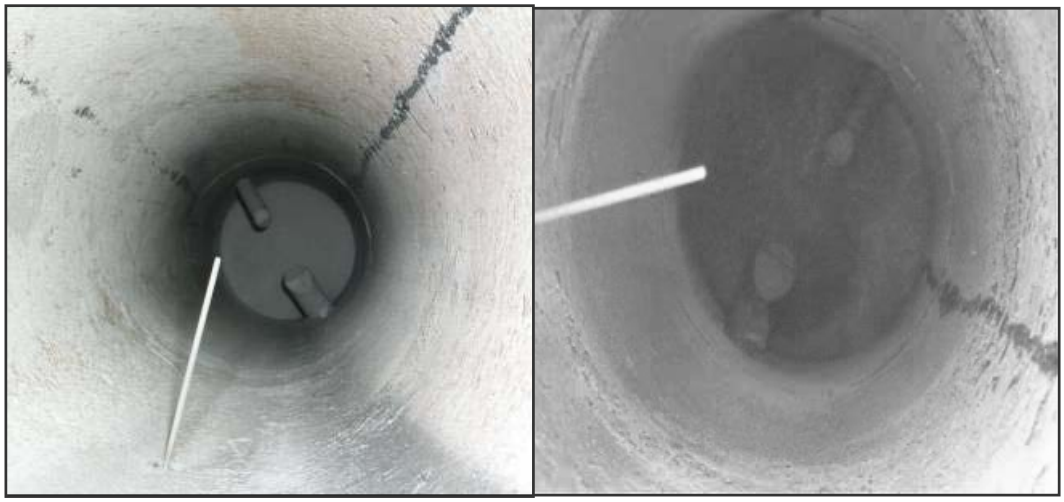

Figure 3-16. Photo showing inside of pilot-scale R2 fluidized bed, with two solids transfer inlet ports (near bottom) and one thermocouple (near top) with a static bed (left photo) and during filming of a solids transfer test (right photo).

The method for measuring bed height was also validated during these experiments. This method is shown in Figure 3-17, and makes use of two differential pressure measurements for each reactor. These measurements were used in the equation shown, which uses the heights of the differential pressure taps to estimate bed height based on density differences. Bed heights were measured directly via measurements taken with a long pole lowered into the reactors while the reactor top flanges were open. The bed height measurements compared favorably with the calculated values.

$$L_{bed} = \frac{DPT142}{DPT143} \times H_1 + H_2$$

$H_1 = 9$ in

$H_2 = 4$ in

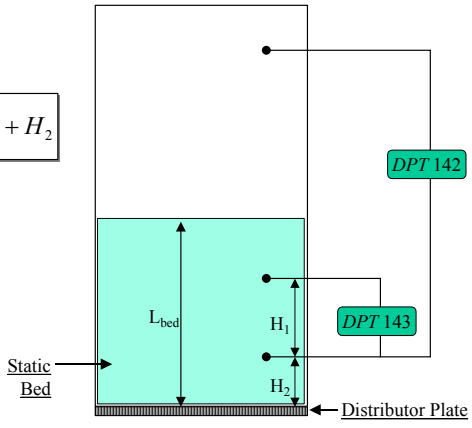

Figure 3-17. Approach for measuring fluidized bed

By selectively altering the transport steam flow, the solids transfer rates were manipulated, leading to accumulation of bed solids in selected reactors. Solids transfer rates were calculated using the change in bed height over time while the rate was being manipulated. These tests of bed movement and

solids transfer rate were repeated after the top flanges were replaced and the system was operated at slightly elevated pressures (Tests 8 and 9 of Table 3-5). Results of these tests are described in detail below.

Operation at elevated pressures first required the minimization of leaks from the system. A leak test (Test 6) was conducted to identify system leaks prior to testing at elevated pressures. The responsiveness of the valves controlling reactor pressure was evaluated using manual control of the valves, with good results (Test 7). Characterization tests were grouped to allow all atmospheric pressure testing to be completed before conducting tests with the top flanges closed. When the top flanges were closed, the piping of reactor exit lines was completed, and the instrumentation completed and tested.

The second-stage superheaters were designed to heat up reactors at stat up (Test 10) and provide auxiliary heat for the system as needed. However, reactor temperatures initially did not rise as expected due to excessive heat losses, which was related to the need for high temperatures to completely cure the reactor refractory material. After extended heat-up periods using second-stage superheaters, one reactor was retrofitted with propane to provide additional auxiliary heat to get the reactor to pre-gasification temperature. Heat-up test results are provided below.

Solids Circulation

The circulation of bed materials is a key mechanical aspect of the UFP technology. During initial testing of the solids circulation system, the bed heights remained steady. Visual monitoring of the transfer exit inside the reactor showed a pulsed transfer of bed materials into each reactor. Indirect bed height measurements were conducted during tests with bed circulation, and these tests showed that bed levels could be maintained over time. Figure 3-18 shows the bed heights calculated during 140 minutes of testing. The heights stayed relatively steady throughout the duration of the test. The figure also shows the differential pressures measured in each reactor, which are only slightly lower than the predicted differential pressure of 25.3 inches of H_2O.

During one shakedown test, the bed heights were manipulated to provide evidence of the rate of solids transfer. Figure 3-19 shows the increase in R3 bed height due to solids accumulation when transfer from R3 to R2 was temporarily halted. Since transfer from R2 to R3 continued, the increase in bed height is directly proportional to the rate of solids transfer from R2 to R3. During this period, a flow rate of 1.26ft^3/hr was estimated.

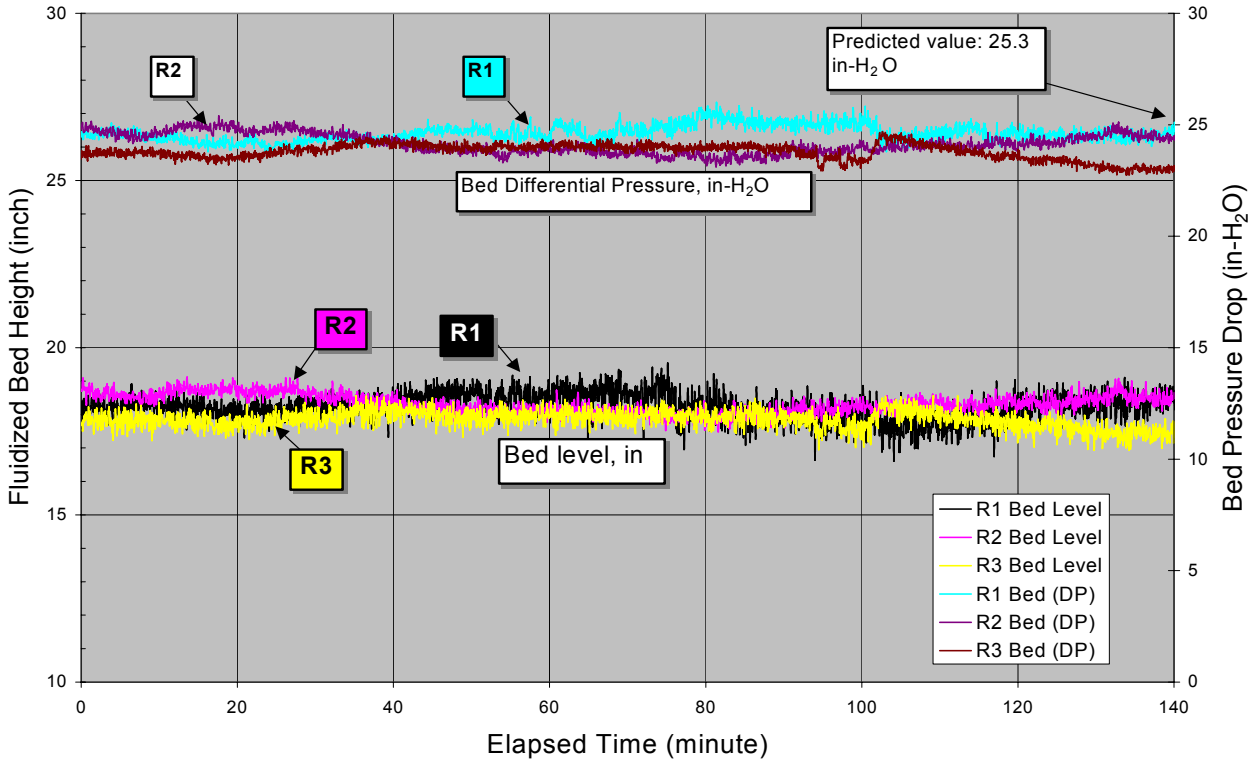

Figure 3-18. Performance curves during 140 minutes of steady solids circulation.

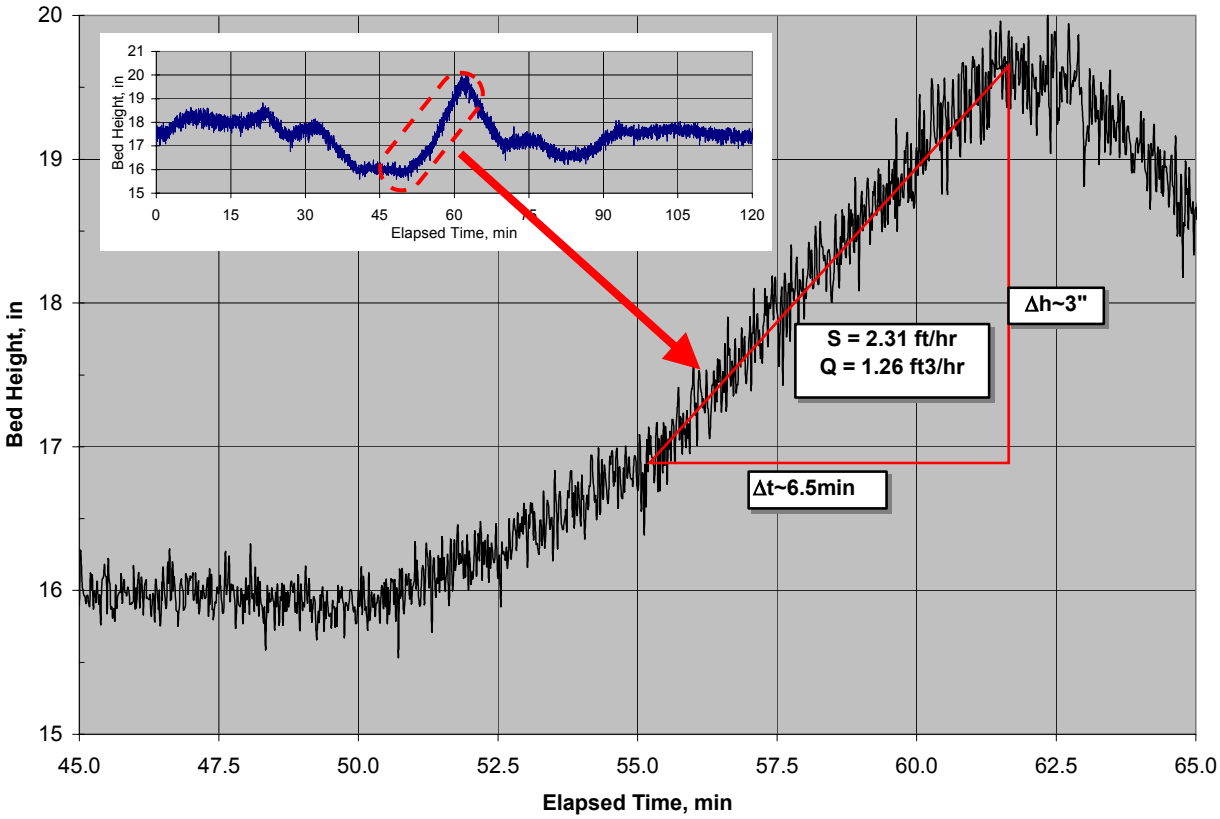

Figure 3-19. Rate of accumulation of bed materials in R3, as measured by bed height, when transfer of bed materials from R3 to R2 was temporarily halted.

Since the solids transfer takes place in a closed system, a bed height increase in one reactor should be compensated by a decrease in bed height in another reactor. During one test, a series of solids transfer system parameters were manipulated to characterize the ability of system operators to control bed heights. Figure 3-20 shows the bed heights for all three reactors while solids transfer flows were either turned on or off. The symmetric nature of bed height increases and decreases offers further validation of the bed height measurement method, as well as the consistency of the solids transfer rates. During the test shown in Figures 3-19 and 3-20, the total bed height (the sum of the three reactor bed heights) had a standard deviation of only 0.3 inches, while the individual reactor bed heights had standard deviations of 0.8. Although the bed heights were being manipulated, the sum of all bed heights remained relatively steady throughout the duration of the test, as shown in Table 3-6.

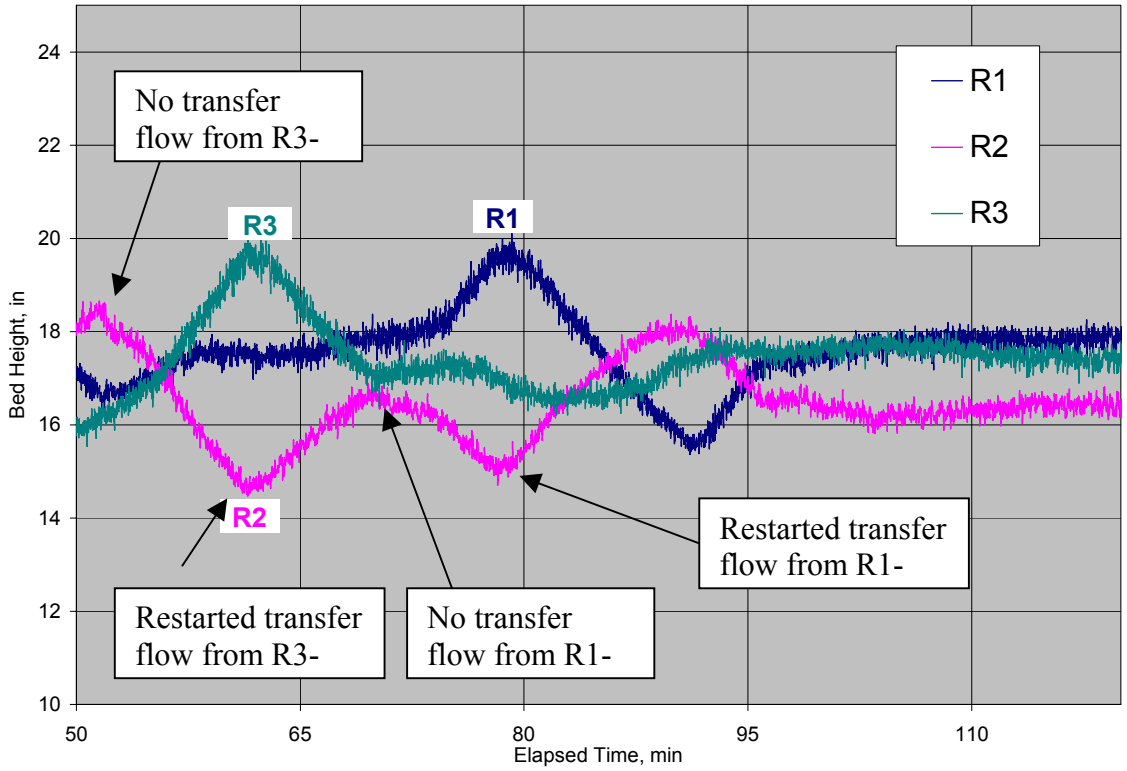

Figure 3-20. Manipulation of solids transfer flow and impact on bed height.

Reactor Heat-Up

The heat-up of the reactors was complicated by the need to cure the refractory at high temperature in air. The second-stage superheaters were limited in their ability to provide heat to the system since they were primarily designed to operate for preheating to prevent condensation after switching to steam. During refractory curing, a large

Table 3-6. Measurements of bed heights during two-hour shakedown test: Variation in data.

Bed Height	R1	R2	R3	Total
Average	17.6	16.5	17.4	51.5
Maximum	20.1	18.6	20.0	52.5
Minimum	15.4	14.5	15.5	50.0
Standard deviation	0.8	0.8	0.8	0.3

amount of water was driven off the refractory, but this occurred very slowly at the second-stage superheater's heat input rate. Thus, R1 was retrofitted with propane feed to provide auxiliary heat particularly for start up to increase the reactor temperature to pre-gasification condition. Since the retrofit did not include an ignition system, it was necessary to increase the reactor temperature (using the second-stage superheater) above the ignition temperature of propane to ensure auto ignition. This technique had previously been used for reactor heat-up in a different project, and worked well in this application as well.

CO_2 Release From Bed Material

Before coal slurry could be fed into the pilot-scale reactor for coal gasification testing, the CAM was prepared by releasing any CO_2 present from the CAM. CO_2 release takes place at high temperatures (~900°C). This was accomplished by extending the heat-up of the fluidized bed to reach temperatures above 900°C using the retrofitted propane heat-up system described above.

Figure 3-21 shows the CO_2 concentration and bed temperature during CO_2 release. Although CO_2 is expected as a propane combustion product, the CO_2 levels measured were high and somewhat transient due to the CO_2 generated during the release process. The slow increase in temperature is an indication that significant heat was required to release CO_2 from the CAM. CO_2 concentration peaks were followed by a decrease in bed temperature, which immediately reduced CO_2 release. After 210 minutes, CO_2 release from the bed was complete, as indicated by the subsequent sharp increase in bed temperature and decrease in CO_2 concentration.

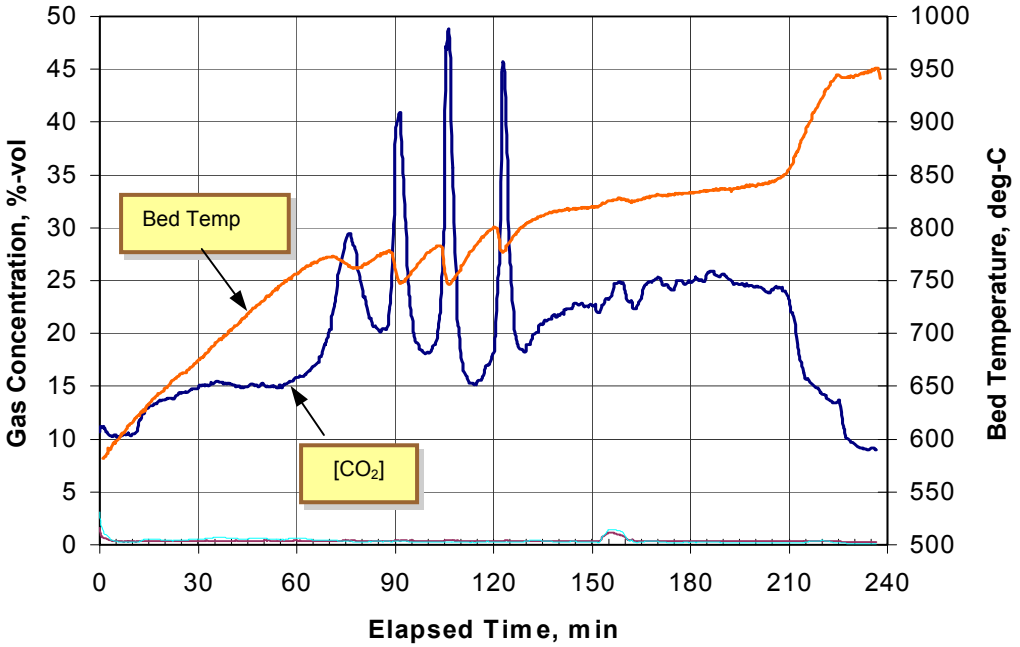

Figure 3-21. Curing refractory and releasing CO_2 from CAM during initial reactor heat-up with propane fired at 40,000 Btu/hr.

3.3.2 Coal Test Results

Testing conducted with coal, both at bench scale and pilot scale, confirmed the basic principles of the UFP technology. Although additional testing is needed to identify operating limits and

optimize performance, the data generated to date support the projections of UFP performance and did not identify any showstoppers.

Since the shakedown test data demonstrated the ability of the pilot plant to circulate solids between three reactors with reasonable control, the initial coal test was conducted in a single reactor to validate the coal-slurry feeding mechanism and the main chemical processes one step at a time. The plan was to also conduct coal tests with the three reactors circulating, but those tests were deferred to the next stage of this program due to the timing constraints associated with the May 14 deadline for vacating the Irvine Test Site and relocating the pilot plant to a new GE test site in Santa Ana, CA (12 miles north of the main GE Global Research office in Irvine.)

As discussed above, coal testing was conducted in a single reactor operated in semi-batch mode with a mixed CAM-OTM bed (1:1 by weight) and operating at approximately 20 psig. The semi-batch operation required the use of two operating modes: gasification and oxidation. During the gasification mode, the bed was fluidized with steam, and coal slurry was fed for a period of several minutes. Steam fluidization continued after the coal slurry was stopped, and gasification products were monitored. Coal gasification; CO_2 absorption by CAM; and OTM reduction by H_2 and CO are the key process that took place during the gasification stage. During the oxidation mode, the bed was fluidized with air. The consumption of O_2 by OTM and related bed temperature increase; as well as the release of CO_2 at elevated temperatures are the key processes that took place during the oxidation stage.

Coal Gasification

Figure 3-22 shows the temperature profiles in the reactor during the coal gasification stage. Superheated steam entered the reactor at ~920°C for the duration of the gasification test. The

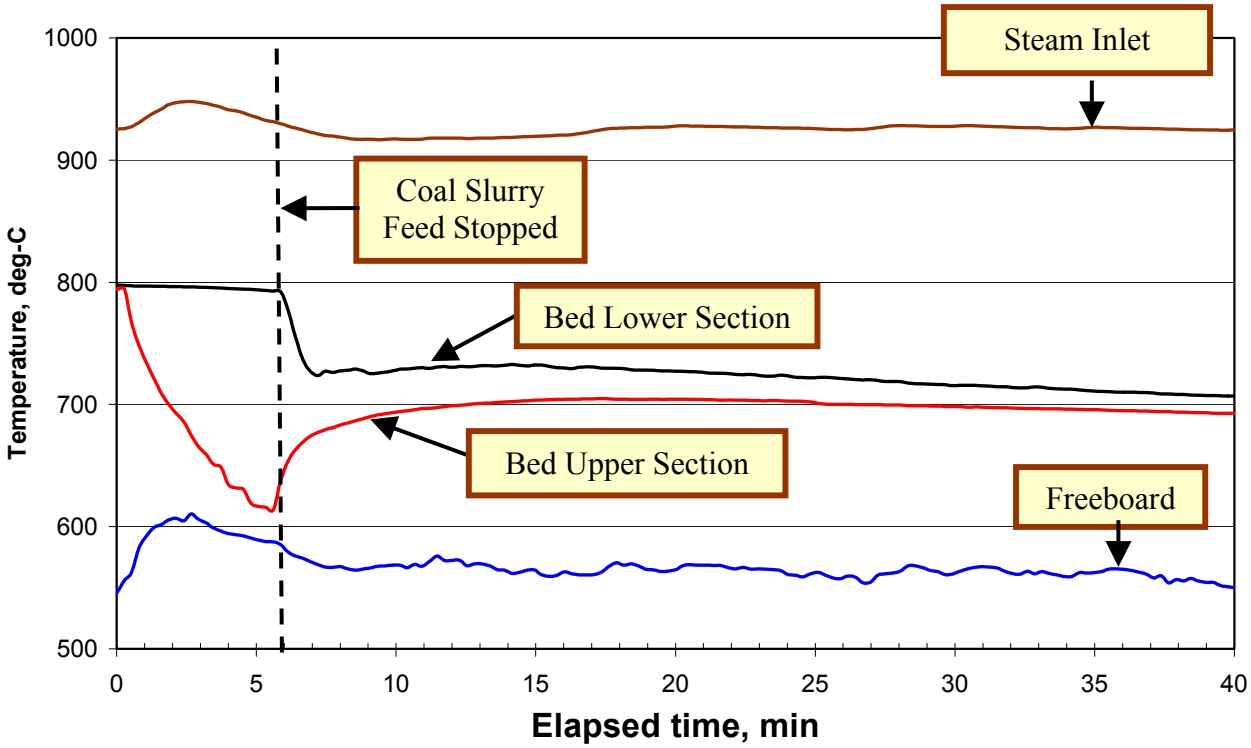

Figure 3-22. Temperature profiles during coal gasification test.

temperatures of both the lower and upper sections of the bed were initially at 800°C, while the freeboard region near the top of the reactor was at ~550°C. The coal slurry (approximately a 50/50 water/slurry mixture) was fed into the fluidized bed near the top of the bed. The water content of the slurry had a significant effect on bed temperature, as illustrated by the upper bed's steep temperature drop during the first six minutes of testing. However, the temperature in the lower section of the bed remained ~800°C due to the steam feed inlet temperature of ~ 900°C; The temporary increase in the temperature of the freeboard region suggests that the coal slurry feed may have disturbed the fluidized bed causing temporary bed agglomerates and allowing the fluidizing steam to channel through the bed to the freeboard.

During the coal gasification test, it was decided to stop feeding the coal slurry when the upper bed temperature decreased to 600°C. However, steam fluidization continued. As seen in Figure 3-22, at the time coal slurry feed stopped, both the upper and lower bed temperatures began to approach 700°C, an indication of improved bed fluidization and mixing.

The product gas concentrations during the first twenty minutes of the test are shown in Figure 3-23. Since the OTM was in its oxidized state at the start of testing, a portion of the H_2 produced during gasification reacted to reduce the OTM (H_2 + OTM-O → H_2O + 2OTM). The extent of H_2 participation in OTM reduction was calculated based on the amount of OTM that was oxidized in the subsequent test described below. This was used to calculate the actual peak H_2 concentration, which was estimated at approximately 80% during this test. Thus, the measured peak H_2 concentration (~60%) shown in Figure 3-23 is lower than the actual H_2 concentration (~80%) due to the consumption of H_2 by the OTM. The estimated peak H_2 concentration is consistent with bench-scale gasification testing results.

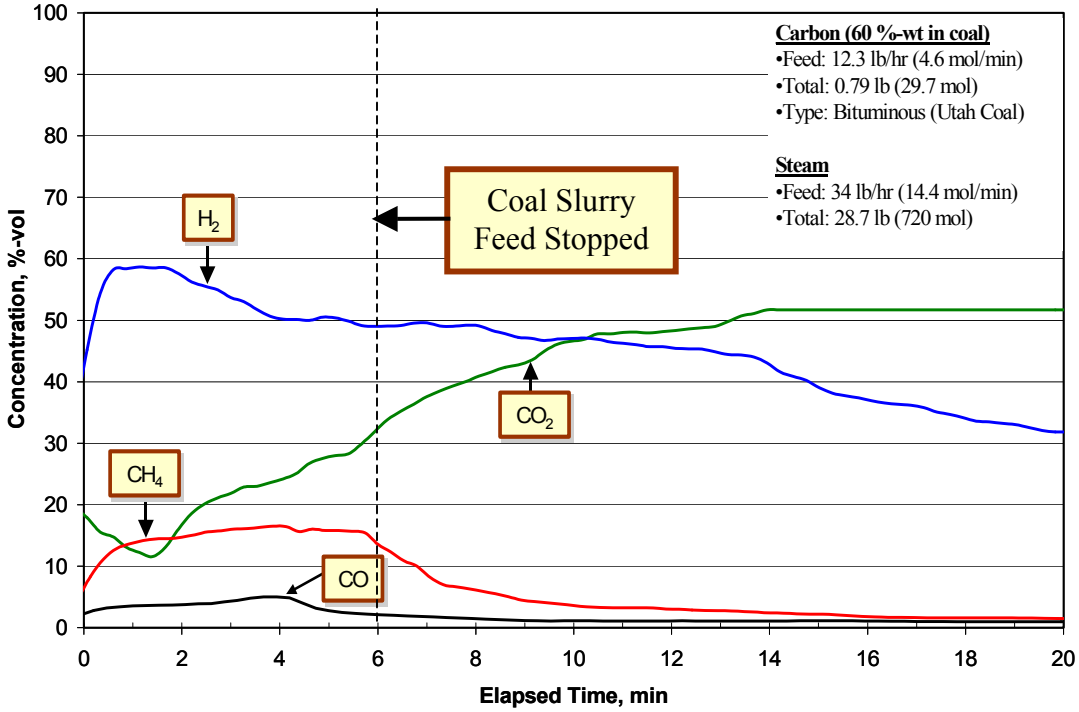

Figure 3-23. Product gas concentrations during gasification test.

The reduction of OTM and the gasification of coal are separated in the integrated UFP system (when operating the three reactors in circulating mode), occurring in R2 and R1, respectively, and would lead to measured H_2 yields closer to 80% in R1. However, the above-described gasification test provides confirmation of both processes concurrently. The measured CH_4 concentration markedly decreased after the coal slurry feed was stopped. This is because methane is a product of coal devolatilization, which takes place quickly when the coal is initially fed into the reactor.

The CO_2 concentration was low initially, then increased rather steadily. This performance is consistent with the limited amount of bed material and the fact that it was not being regenerated as the case would be when the system is operating in a circulating mode. Since the test was conducted in semi-batch mode, the product gas volume decreased as the test continued, and thus, the high concentrations of CO_2 were not necessarily present in large amounts as coal gasification was reaching equilibrium. In addition, as gasification products declined, it is possible that CO_2 absorbed by the CAM may have been stripped by the steam fluidization gas, shifting the absorption equilibrium toward desorption, even at the low gasification temperatures. In steady-state operation, a continuous supply of fresh CAM would be circulated to the gasification reactor, allowing a low CO_2 concentration to be maintained during gasification.

OTM Oxidation

Air was fed to the reactor during the oxidation stage, which immediately caused an increase in temperature from 700 to 820°C. Figure 3-24 shows the temperature profile as well as the O_2 consumed, calculated as the difference between the O_2 concentration in air and the measured O_2 concentration in the product stream. During the first ten minutes of the test, 13.3 moles of O_2

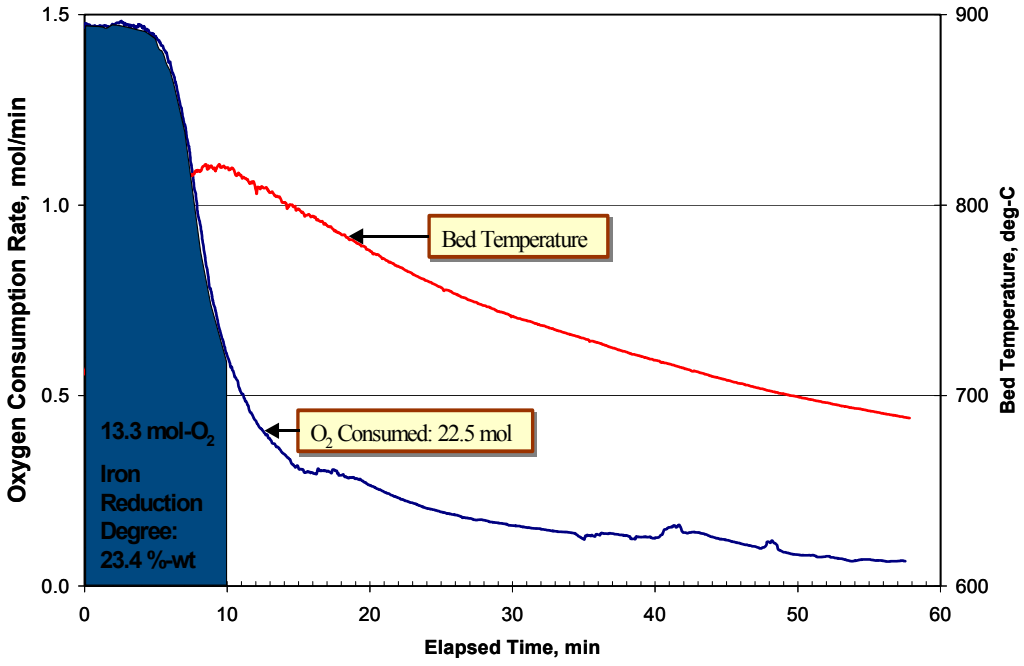

Figure 3-24. Oxygen consumption rate during pilot-scale oxidation test.

were consumed, which corresponds to reduction of 23% of the OTM. Ultimately, 22.5 moles of O_2 were consumed, corresponding to 40% OTM reduction. This OTM performance is significantly better than the 20% reduction predicted by the bench-scale studies. The higher H_2 concentrations present may have contributed to the improved performance. The reduction of OTM by coal combustion products (unmixed combustion) is one of the unique features of the UFP technology that is not as well characterized, and the good performance illustrated provides further confirmation of the viability of this technology.

The coal testing conducted on the pilot-scale system provided valuable information and encouraging support for the UFP technology. Due to time constraints described previously, additional testing with coal at higher pressures and in steady-state mode has been deferred to the next stage of this program, which will benefit from the lessons learned during this project.

3.3.3 Lessons Learned

The UFP bench and pilot-scale systems presented significant design challenges. The strategy of separating the key processes to more fully characterize them individually has been beneficial to the overall understanding of the process, as well as the generation of data in support of modeling efforts.

Experimental design reviews identified the increased significance of temperature rather than pressure in conducting preliminary tests. The combination of high temperatures and pressures severely limits the safe operating limits of many construction materials. The UFP technology is constrained by the range of coal gasification temperatures and CO_2 release temperatures. At lower temperatures, the UFP system will not perform adequately. However, the impact of pressure on performance is not as significant; CO_2 absorption/desorption is slightly improved at higher pressures, but shows reasonable performance even at lower pressures. The most significant benefits of high-pressure operation come from the integration of high-pressure product streams with gas turbine expansion, CO_2 sequestration, and high-pressure H_2 processes. Therefore, when conducting tests, it is important to adhere closely to the recommended operating temperatures, and establish the operability and safety of the system prior to adding the complication and safety concerns of high-pressure operation. Control systems are more sensitive at high pressures, so it is important to first establish a robust control scheme at low pressures. Initial pilot-scale tests focused on low-pressure operation. The operational experience gained will be beneficial in future high-pressure testing as well.

During shakedown testing, the difficulty of achieving high bed temperatures during refractory curing was a significant issue that was resolved through retrofitting the system for combustion-based heating. The capability for rapid heat-up is a desirable feature for long-term testing programs. Two approaches to the heat transfer and heat loss issues are 1) increase heat input and 2) reduce heat loss. The ideal solution is likely a combination of the two. Alternate methods for auxiliary heat-up have been investigated, including methods that could potentially be used to provide auxiliary heat during operation, particularly in the gasification reactor. In addition, the disassembled reactors have been inspected to identify any failures in the refractory lining, and alternate insulation configurations are under consideration for future tests. Any new refractory will likely be cured separately, using high-capacity burners that would not be feasible to incorporate into the system design.

The coal slurry feeding system provided several challenges. In addition to the significant heat sink provided by the slurry water, the slurry-feeding probe was prone to plugging. The results of the gasification test showed that the feed rate of coal slurry exceeded the system's ability to steadily evaporate the water and incorporate the slurry into the bed with good mixing. Lower water content in the slurry (including dry coal feeding systems), lower slurry feed rates, higher fluidizing steam temperatures, and larger, better-mixed beds are all possible approaches to facilitating steady-state gasification with continuous coal feeding. The slurry-feeding probe proved particularly problematic, as the probe would heat up, creating an environment where the water in the slurry would rapidly evaporate, leaving the solid coal behind to plug the line. These types of plugging were difficult to resolve during initial testing, and generally required the replacement of the probe or very vigorous cleaning. This issue was associated with the initial start-up of the slurry feed, since the slurry probe was not hot enough to completely evaporate the water from a flowing slurry stream. Thus, different approaches included purging the probe with N_2 prior to feeding coal slurry, feeding a slug of water ahead of the slurry, and priming the probe at low temperature. The design of the probe itself is also an area of future modification. It is worth noting though that slurry feeding is much more problematic at small scale because of line plugging. At larger scales both slurry flow rates and injection diameters are larger making slurry feeding more reliable.

4.0 MODELING AND ENGINEERING STUDIES

Modeling and engineering studies were conducted to provide guidance for experimental activities as well as to predict performance at conditions of interest. Process modeling initially focused on using bench-scale data and technical literature to model the pilot plant. After the pilot plant model was developed, the UFP system was scaled up to full size and included as a module of a fully integrated Vision 21 energy plant. Comparisons were made with existing technologies to benchmark and assess benefits of the UFP technology.

4.1 Process Modeling

4.1.1 Pilot Plant Process Modeling

An ASPEN process model was developed to assess the impact of different operating conditions on performance and thus identify reasonable ranges for pilot-scale operating variables. Key variables included the coal feed rate, coal conversion in R1 (a function of temperature and residence time), coal slurry water content, reactor operating temperatures, fluidization feed rates and solids transfer rates. Modeling results were used extensively during the design of the pilot plant, and guided the specification of valves and flowmeters as well as the overall system design. Fluidization models were used to identify the fluidization flow rates required for different bed sizes, and results were compared with cold-flow model data to gauge fluidization quality.

The ASPEN-based model developed for the UFP pilot plant included the three main reactors interconnected with solids transfer ducts. Coal and steam were fed into the first reactor, steam was fed into the second reactor, and air was fed into the third reactor. Auxiliary steam was fed into the solids transfer ducts to entrain and transport bed materials between reactors. Unit operations unique to ASPEN included a virtual coal decomposer to convert coal to components recognizable in ASPEN, separator units to separate the solids and the gases exiting each reactor, mixers to add steam to the solids being transferred between reactors, and solids splitters to divide the solids stream exiting Reactor 2 for delivery to R1 and R3. The complete process flow diagram used for the ASPEN simulation is shown in Figure 4-1.

Three key input variables were identified: coal feed rate to R1, coal conversion in R1 and initial OTM bed fraction. Additional simulations were conducted to identify the peak performance of each reactor individually. Then the response surfaces were compared to identify the set of operating conditions that resulted in the best overall performance. These conditions were used for pilot plant design and test planning.

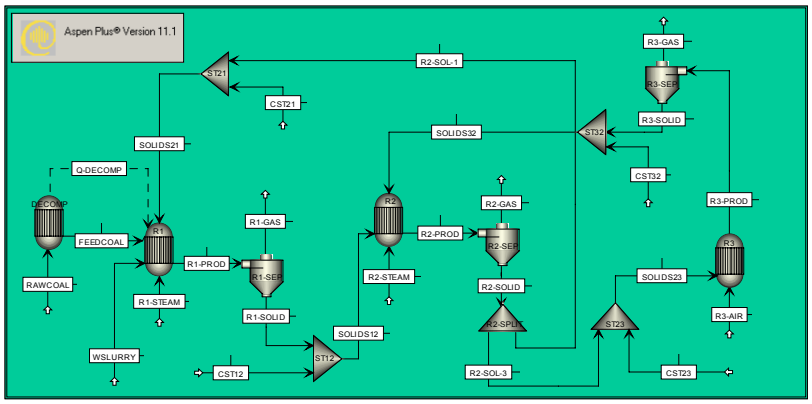

Figure 4-1. Aspen simulation used for pilot plant model.

4.1.2 Vision 21 Plant Systems Analysis

Environmental concerns are driving improvements throughout energy plants. The DOE's Vision 21 targets for future power plants include high efficiency and virtually no environmental impact. In order to assess the efficiency for an entire power plant, the UFP technology must be integrated with a combined cycle plant. This was accomplished using ASPEN and Gatecycle models to simulate the integration of the UFP with a future Vision 21 plant. An "apple-to-apple" ASPEN analysis was conducted to benchmark and compare the performance of a UFP-based combined cycle plant with a conventional Integrated Gasification Combined Cycle (IGCC) plant. With the assumptions used in the analysis, the ASPEN modeling results indicated that the efficiency of the UFP-based system was approximately six percentage points higher than the efficiency of a conventional IGCC with CO_2 separation. Additional detailed models were developed for the combined cycle plant using Gatecycle software, the standard for the GE Energy gasification team. The Gatecycle model incorporates actual maps of GE turbines and would potentially provide more representative results for the UFP-based plant than the ASPEN modeling results that use typical efficiencies of turbines.

ASPEN Modeling

Figure 4-2 is a simplified version of the ASPEN Plus process model developed for the UFP-based combined cycle. As shown in Figure 4-2 for the three-reactor UFP technology, the first reactor produces a H_2-rich fuel stream, which is cleaned and cooled before it is sent to a H_2 separation device such as a pressure swing adsorber (PSA). The second reactor produces a CO_2-rich stream, which is cooled and dried before it is sent to a CO_2 compressor for additional compression to sequestration-ready conditions. The third reactor produces vitiated air at high temperature and pressure, which is sent to a gas turbine expander and a heat recovery steam generator (HRSG) unit.

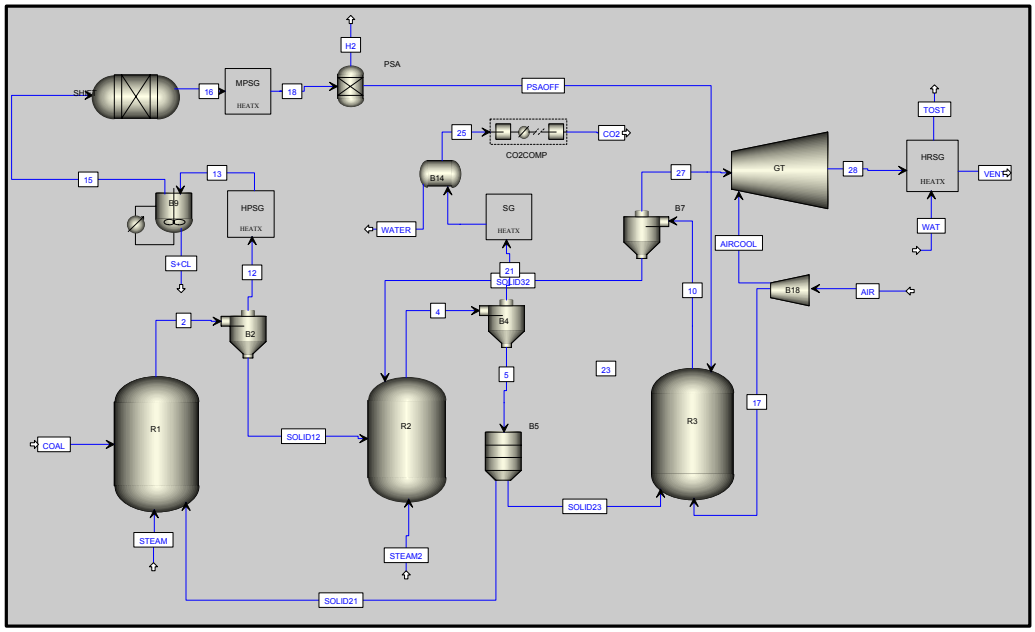

Figure 4-2. Simplified process flow diagram for UFP technology integrated with combined cycle plant for co-production of hydrogen and electricity from coal.

Figure 4-3 shows the process flow diagram for the entire steam cycle including the HRSG and steam turbines. This steam cycle includes three different pressure levels, with high, intermediate and low-pressure steam turbines. The US DOE (NETL office) provided this model to aid in developing realistic process efficiencies by eliminating the need for simplifying and generally conservative assumptions. DOE process modeling guidelines were followed throughout model development. Major modeling assumptions for this UFP-based plant are listed in Table 4-1.

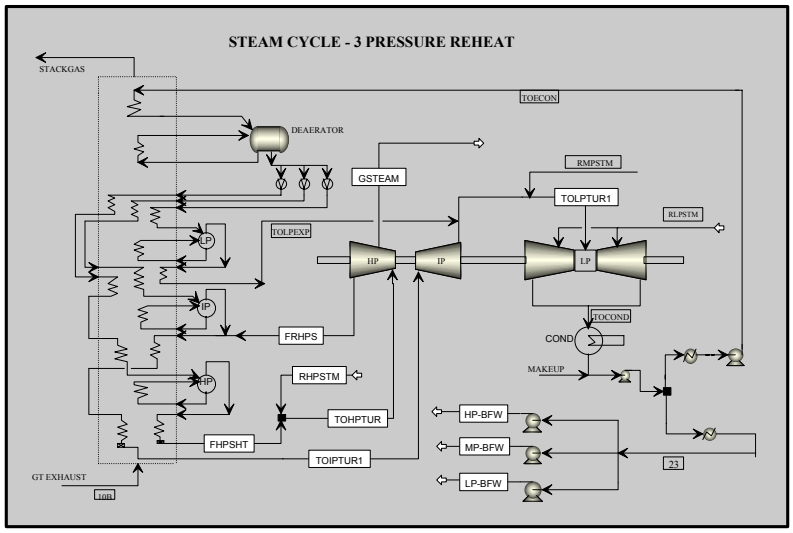

Figure 4-3. Process flow diagram for the 3-pressure reheat steam cycle.

Table 4-1. Major process modeling assumptions for the full-scale UFP integrated with combined cycle plant.

1	Three main reactors (gasifier, CO_2 separator and oxidizer) thermodynamically limited at steady state (Gibbs reactors)
2	Maximum temperature of the solids limited to 1275°C at steady state
3	Maximum heat exchanger metal temperature limited to 650°C
4	Process conducted at ~30 atm pressure
5	Simulated gas turbine: (LM 6000 SPT) with 3-stage expansion and cooling air
6	3-pressure reheat steam cycle with high, intermediate and low pressure steam turbines o Steam generated at: 1800, 500, 300, 42 and 17 psi o Internal pinch point: 15°C
7	Mechanical and auxiliary losses (in compressors, turbines, control systems etc.) o Mechanical losses in ST Generator: 1.5% o Mechanical and generator losses in GT Generator: 2.5% o Auxiliary losses: 2%
8	Stack gas temperature: 100°C
9	CO_2 stream compressed to 2100 psi (sequestration-ready pressure)
10	Coal type: Illinois #6 Old Ben #26 mine (HHV 11,666 Btu/lb)

The net process efficiency for each process configuration was estimated using this equation:

$$\text{Net Efficiency, \%} = \frac{\text{HHV of } H_2 \text{ produced (MW)} + \text{Net electricity (MW)}}{\text{HHV of coal fed (MW)}} \times 100\ \%$$

The UFP-based plant efficiency was compared to the efficiency of an IGCC process. Figure 4-4 shows the simplified process flow diagrams for (A) a typical IGCC-based system with CO_2 separation and (B) a UFP-based combined cycle system. The process model assumptions were identical for both systems to allow direct comparison of the results. The major difference between (A) and (B) is the replacement of the three UFP reactors with a gasifier, CO_2 separator and air separation unit (ASU) in the IGCC process simulation (A).

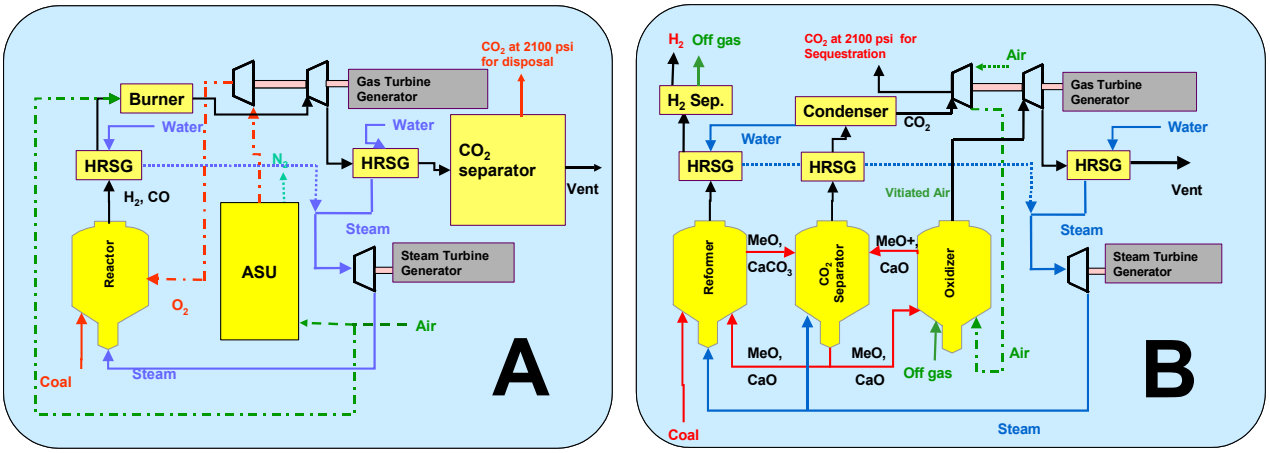

Figure 4-4. Process flow diagrams for (A) Typical IGCC process with CO_2 separation and (B) UFP system integrated with the combined cycle plant.

Table 4-2 is a comparison of UFP and IGCC-based process efficiencies. Both technologies were compared at ~85% CO_2 separation. The H_2 HHV (MW) to electricity (MW) ratio used for both processes was 0.4. With model assumptions, results show that UFP-based plant is approximately six percentage points more efficient than an IGCC plant with conventional CO_2 separation.

Table 4-2. Comparison of the efficiencies for the IGCC process and the UFP technology.

Difference in energy utilization	**Δ=UFP-IGCCw/CO_2**
Air Separation, % of coal HHV	3%
H_2 HHV, % of coal HHV	3%
Gas Turbines Net, % of coal HHV	-0.2%
Steam Turbines Net, % of coal HHV	-2%
CO_2 Compression, % of coal HHV	2%
Auxiliary Losses, % of coal HHV	0%
Net H_2 and Electricity Efficiency Difference	**6%**

Potential advantages of the UFP-based plant over the IGCC-based system include:

1. No Air Separation Unit (ASU)
2. No CO_2 separation unit (UFP inherently separates CO_2)

3. Use of the higher-efficiency Bryton-Rankine cycle (IGCC uses the less-efficient Rankine cycle as well as the Bryton-Rankine cycle)

Gatecycle Modeling

Gatecycle software was selected to evaluate the potential power recovery from the combined cycle system due to its robust thermodynamic calculation methodology. The availability of real GE product performance maps and the ability to alter turbomachinery performance settings are added benefits. Unfortunately, Gatecycle is not well-suited to simulate the UFP block because it was not designed for reforming operations or composition changes other than direct combustion. Thus, the UFP unit is modeled as a "black box" in Gatecycle, with transfer functions defining the outlet material streams to be used for power recovery. The transfer function for the UFP block was based on the Aspen model.

The first stage of model development was to incorporate one UFP design point into the Gatecycle model. Included in this model is a turbo expander to draw power from the hot, nitrogen-rich stream, an HRSG block to recover the heat, and a series of steam turbines to utilize the heat generated in the HRSG as well as the steam from the UFP block. The real steam turbine for this process is artificially modeled as a series of several turbines to ensure proper thermodynamic calculations for all pressure levels. These steam turbines are assumed to expand the high-pressure steam down to 1 bar, but not condense it.

The next steps in the analysis were to further refine and enable the Gatecycle model. The HRSG block was separated into three pressure levels. This separation provides an improved heat recovery estimate, but is not expected to change the calculations significantly. Macros were written to run multiple design points in the Gatecycle model without manual input of stream conditions, facilitating process optimization. More detailed heat integration may be considered in future versions.

The turboexpander requires further refinement, as a performance map is not available in Gatecycle for that component alone. The low exhaust temperature from R3 of the UFP must be addressed either by confirming acceptable turboexpander performance at that temperature or by introducing supplemental firing of an alternative fuel (i.e., hydrogen) to achieve the necessary temperature. After completing these steps the efficiency of the UFP system combined with the combined cycle plant will be estimated and compared with the IGCC process with CO_2 sequestration.

Future Work

The GE Global Research team will work closely with the GE Energy Gasification (formerly ChevronTexaco Gasification) team to verify ASPEN modeling results and make progress toward obtaining Gatecycle results. The research team will work to resolve outstanding process modeling issues identified by the GE Energy gasification team. Detailed combined cycle models will be developed based on the DOE-Parson's IGCC report using Gatecycle software. Some of the outstanding issues identified by the GE Energy gasification team and their implementation plans are shown in Table 4-3.

Future process modeling and analysis work will include the following:

- Optimization of UFP and IGCC process efficiency based on modeling and experimental results
- Comparison of the efficiency of the IGCC and UFP technologies at various H_2 to electricity co-production ratios to identify the optimum operating conditions
- Development of a robust CO_2 separation unit simulation using a chemical solvent
- Developing a dynamic model to analyze the start-up of the UFP technology to aid in development of an UFP technology control strategy

Table 4-3. Outstanding issues in UFP process modeling.

No.	Suggestions/Outstanding Issues	Implementation Plan
1	Account for NH_3 formation in gasifier	NH_3 formation being included based on kinetic modeling
2	Improve LM6000 simulation: cooling flows, tuning characteristics	Detailed GT simulation (MS 7001FA or LM 6000) is being developed using Gatecycle
3	Account for heat loss from the solid streams and the possible phase changes in the solids	Heat loss based on the experimental results will be accounted. Kinetic modeling will be used to account for any phase changes
4	Compare pressure & heat losses with the GE studies with air recycle	Currently using 13% pressure loss and no heat loss. Will be updated
5	Develop IGCC simulation based on DOE-Parson's study (MS 70001FA GT)	Current IGCC simulation was developed for apples-to-apples comparison with UFP. Will base both the IGCC and UFP analyses on DOE-Parson's study using Gatecycle
6	Move the CO_2 separation before the combustion in the IGCC case	Develop a case with DOE-Parson's study using Gatecycle as the base case and make changes to account for H_2 production and CO_2 separation

4.2 Kinetic Modeling

The behavior of bed materials as they circulate between reactors is strongly influenced by kinetic considerations. Thus, kinetic modeling can provide insight into how to manipulate variables such as solids circulation rate to achieve optimized performance. It is also important to consider kinetics when scaling up a process or planning for system integration. Kinetic models can be used to predict the selectivity and conversion of key UFP reactions at given operating conditions, setting the stage for optimization. A global kinetic process model was developed for the UFP technology using ASPEN Plus software.

Kinetic parameters for various reactions were obtained from the literature and by using Chemkin software for gas phase reactions. These kinetic parameters were validated using bench-scale UFP results. A semi-batch kinetic model was developed to represent the bench-scale experiments. The validated kinetic parameters were used in the integrated kinetic model of the UFP pilot scale reactors. The kinetic parameters used in the integrated model will be further validated using

pilot-scale experimental data as the program proceeds to the next stage. The kinetic model will also be used to optimize the operating conditions of the UFP technology and perform scale-up design.

4.2.1 Kinetic Model Setup

ASPEN Plus was used to model the UFP reactors using global kinetic equations. Major assumptions for UFP fluidized bed modeling include: steady state, completely mixed fluidized bed and adiabatic operation (heat loss will be added in a future version). The UFP reactions include both gas-solid reactions that are kinetically limited (e.g. steam gasification of coal) and equilibrium reactions (e.g. water gas shift reaction). The ASPEN kinetic model appropriately considers both kinetically limited and equilibrium reactions.

Table 4-4 lists the main UFP reactions in the three reactors. The type of the reaction (kinetic or equilibrium) was decided based on the information available in the literature as well as experimental results. Chemkin was used to estimate gas phase reaction rates.

Table 4-4. Main UFP reactions in the kinetic model.

Reactor	Reactions	Reference/Comments
R1	C(s) + H2O -> CO + H2	Kinetic, Van Heek et al., Journal of the Institute of Fuel, (1973) 249
	CO + H2O <--> CO2 + H2	Equilibrium, Mann et al., Fuel 83 (2004)1643
	S + 2H(fuel bound) -> H2S	Kinetic, reducing environment
	Cl + H(fuel bound) -> HCl	Equilibrium, Chemkin, reducing environment
	CO2 + CaO(s) <-> CaCO3(s)	Equilibrium
	NH (fuel bound) + 2H(fuel bound) -> NH3	Kinetic, reducing environment
R2	C(s) + H2O -> CO + H2	Kinetic, Van Heek et al., Journal of the Institute of Fuel, (1973) 249
	Fe2O3(s) + H2 <--> 2 FeO(s) + H2O	Kinetic, reversible, bench scale results
	Fe2O3(s) + CO --> 2 FeO(s) + CO2	Kinetic, bench scale results
	CaCO3(s) <--> CaO(s) + CO2	Equilibrium
R3	2FeO(s) + (1/2) O2 --> Fe2O3(s)	Equilibrium, bench scale results

The global kinetic rate equation used for each kinetic reaction shown in Table 4-4 is shown below:

$$r_n = k_{0n} (T/T_o)^m e^{-E_n/R(1/T-1/To)} \Pi C_i \alpha_I$$

Where

r_n = rate of n^{th} reaction
k_{0n} = pre-exponential factor
T_o = reference temperature, K
T = temperature, K
m = temperature exponent
E_n = activation energy for n^{th} reaction
C_i = concentration of i^{th} component
A_i = concentration exponent for i^{th} component

4.2.2 Modeling of bench-scale kinetic data

The bench-scale UFP experiments were carried out in a semi-batch mode, while the bed was filled with coal and bed materials: CAM and OTM. The reactor bed was fluidized with steam, air or syngas. Only the gaseous products were analyzed during these experiments. An ASPEN semi-batch model was developed to determine the kinetic parameters from the bench scale results.

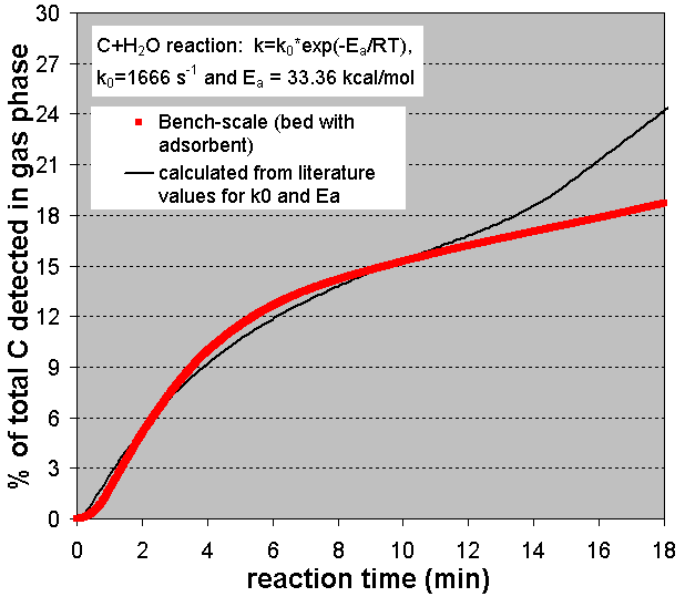

Figure 4-5. Comparison of coal gasification reaction model with bench-scale results.

Figure 4-5 shows a comparison of model predictions and the experimental data for the coal gasification reaction in R1. The percentage of total carbon detected in the gas phase is plotted as a function of time. The model predictions showed good agreement with experimental data. The kinetic parameters obtained from the experimental data were identical to kinetic parameters reported in the literature (Van Heek 1973).

Figure 4-6 shows a comparison of the kinetic model predictions and the bench-scale results for reduction of OTM by CO and H_2 in Reactor 2. The conversion of OTM is plotted as a function of reaction time. The OTM re-oxidation reaction by steam needs to be considered along with the reduction reaction of OTM by CO and H_2 in order to match the model predictions with the experimentally observed results.

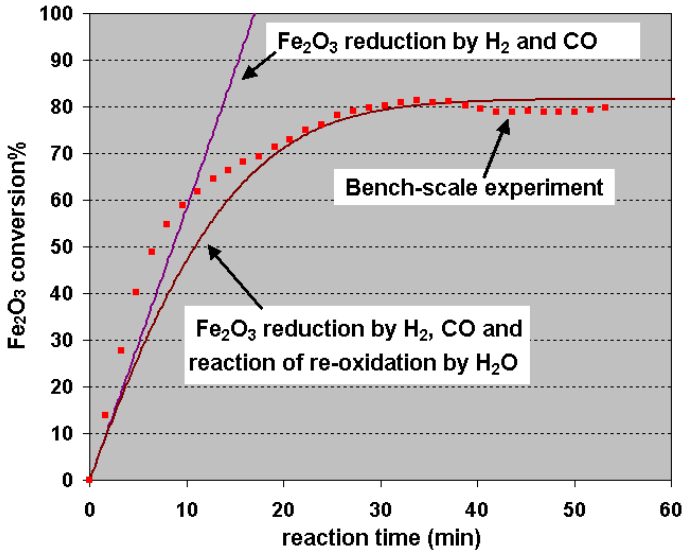

Figure 4-6. Comparison of OTM reduction model results with bench-scale results.

It was determined from the experiments carried out by GE and SIU that OTM oxidation in R3 is fast and the reaction approaches equilibrium. Table 4-5 shows the kinetic parameters obtained from the bench scale data for various reactions.

4.2.3 Integrated Three-Reactor Kinetic Model

The kinetic parameters obtained from the bench-scale results and from the literature were used in the integrated three-reactor model. The main difference between the bench-scale kinetic model and the integrated model is that the integrated model is a continuous three-reactor model while

the bench-scale model is a semi-batch model. The integrated kinetic model will be used to optimize the operating conditions for the UFP technology. Figure 4-7 shows an example of sensitivity analysis that can be carried out using the integrated kinetic model. The coal conversion in R1 is plotted as a function of two parameters: coal flow rate and % water in slurry. Under the given process conditions, coal conversion decreases as the coal flow rate and % water in slurry increase. Typically ~50% conversion of coal is obtained in the first reactor (gasifier). These results match the equilibrium-based model predictions used to estimate process efficiency.

Table 4-5. Kinetic parameters obtained from bench-scale data.

Reaction	k_o, s-1	E_a (kcal/mol)
C(s) + H_2O --> CO + H_2	1,666	33.3
OTM-O(s) + H_2 --> 2 OTM(s) + H_2O	1E5	30
OTM-O(s) + CO --> 2 OTM(s) + CO_2	5E4	30
2 OTM(s) + H_2O --> OTM-O(s) + H_2	90	30

Figure 4-8 shows the dry mole fraction of H_2 in R1 predicted by the kinetic model. Typically > 85% H_2 (dry basis) will be present in the R1 product stream.

Additional kinetic modeling is planned, particularly for validation of the kinetic parameters used in the integrated model using pilot plant test results from the next stage of this program. The kinetic parameters for the reactions of impurities present in coal (sulfur, ammonia and chlorine) will be evaluated carefully. This updated model will be used to identify operating conditions that will provide optimized performance.

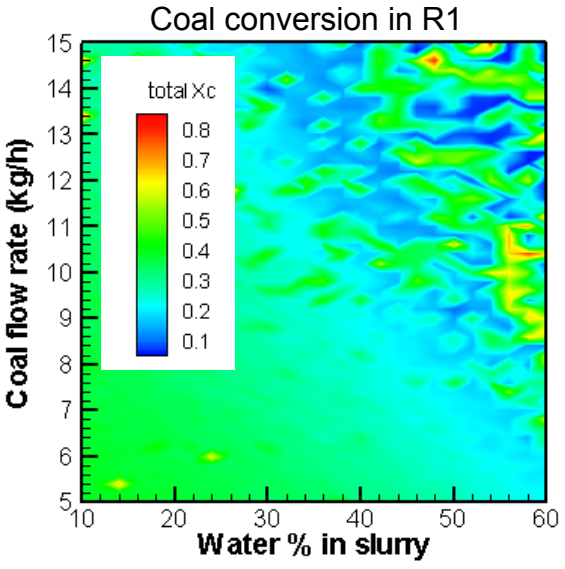

Figure 4-7. Coal conversion in R1 as a function of coal flow rate and % water in slurry.

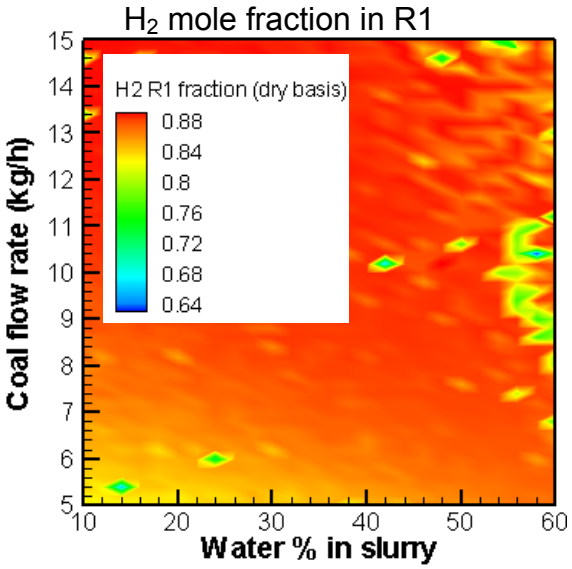

Figure 4-8. Hydrogen mole fraction in R1 as a function of coal flow rate and % water in slurry.

4.3 Opportunity Fuels Resource Assessment

The objective of the opportunity fuels resource assessment was to identify and select alternative "opportunity" fuels to be tested in conjunction with coal in experimental evaluations of the UFP process. This effort included development of an extensive bibliography as well as a compilation of information based on literature searches, previous opportunity fuel assessments and discussions with experts in the opportunity fuel industry such as fuel producers, fuel handlers, fuel users, and fuel recyclers.

Detailed results of the opportunity fuels resource assessment were described previously in Appendix F of the First Annual Report (October 2001) for this DOE program. The study provided estimates for:

- Total opportunity fuel production rates;
- Fuel availability, considering current handling practices, uses and fate of fuels, seasonality of generation, sustainability of production, etc.;
- Fuel costs, including purchasing / tipping and transportation; and
- Location of fuels by state.

This assessment will be used as a guide for identifying suitable opportunity fuels for use with coal in the UFP process. Current information with regard to the availability of opportunity fuels will aid in leveraging the fuel-flexibility of the UFP process to enhance its economic viability. Future UFP test programs will include testing of mixed biomass/coal fuels.

4.4 Economic Assessments

Although the development of the Unmixed Fuel Processor (UFP) technology is still at a relatively early stage, preliminary economic analyses were conducted based on results from the ASPEN modeling and energy balances described earlier. The objective of the economic assessment was to estimate costs associated with the UFP process to establish the economic feasibility of a full-scale UFP-based energy plant.

For benchmarking purposes, the economics of a UFP-based plant was estimated and compared to an IGCC plant. To conduct an "apples-to-apples" assessment, an ASPEN model was developed for an IGCC system producing both electricity and H_2, with conventional CO_2 separation. Major differences in the capital costs of IGCC and UFP systems are shown in Table 4-6, which lists the process units unique to each process. The IGCC system requires the use of an air separation unit and a CO_2 separation unit, while the UFP system requires the use of regeneration and oxidation reactors. (Both systems make use of a gasification reactor, and they are roughly comparable in cost). Other system components (coal handling, ash handling, turbines, electrical plant, etc.) are similar in cost.

Table 4-6. Contribution of process units to capital cost for IGCCC and UFP systems.

Unique Process Units	Capital Cost ($/kW)	
	IGCC w/CO_2 separation	UFP
Air separation unit	95*	0
CO_2 separation unit	400**	0
Regeneration reactor	0	160***
Oxidation reactor	0	160***
Total capital cost for units of interest	495	320

* (Parsons 2003)
** (EPRI 2002)
*** rough estimate

The preliminary economic analysis was conducted using standard guidelines for cost estimation such as those recommended by the DOE (U.S. DOE NETL 2003). Capital equipment costs were estimated (scaled) from "reference" costs that have been used in advanced coal power system studies (Parsons 1998, Simbeck 2001). Specifically, reference costs for similar equipment types were obtained from the previous studies for equipment sizes / processing rates that are as close as possible to those required by the UFP model plant. UFP costs are obtained from the reference equipment costs by scaling based on an industry-standard engineering relation:

$$C_{UFP} = C_{Ref} * (X_{UFP} / X_{Ref})^{0.67}$$

Where C_{UFP} and C_{Ref} are the equipment costs of the UFP and reference equipment, and where X_{UFP} and X_{Ref} are the "scale" of the UFP and reference equipment. The scale will depend on the equipment function; for example, tons of coal processed, amount of power generated, gas flow rate processed, etc.

Using these guidelines, a preliminary cost of electricity was generated for both the IGCC and UFP cases based on their ASPEN modeling results. These preliminary results did not reflect the optimized maximum efficiency attainable for either system, but were preliminary ASPEN model results and are used primarily for comparative cost analysis. Future modeling work is aimed at optimizing the efficiency of the UFP system as well as bringing the IGCC model closer to published estimates of IGCC costs with CO_2 separation.

The preliminary economic estimates show that the UFP system has comparable capital costs and electricity costs, with the UFP having slightly lower costs in both cases. However, since UFP technology is still at an early stage of development, the UFP cost estimates are preliminary and some operational issues that may impact costs have not yet been fully characterized. Many of these issues are of high priority in future testing efforts. Additional work is planned to increase the confidence level for the estimates of reactor costs, consumables costs, and HRSG costs.

The economic analysis conducted as part of this program has identified key aspects of the technology that may have a significant impact on system economics. The harsh UFP operating conditions may require more expensive construction materials and potentially more maintenance; it is important to design the reactors to minimize their size and improve their durability. The UFP system is designed to operate with near-zero emissions. The equipment associated with gas cleanup can add significantly to capital and operating costs, so it is important to understand the ultimate disposition of all potential pollutants and their concentrations in order to devise the most effective and efficient gas cleanup strategy and accurately gauge cleanup costs. The operating costs associated with consumable materials and fuel are also significant. Understanding how frequently bed materials must be replaced will allow more accurate consideration of these costs, while the flexibility to use low-cost fuels can also impact the overall economics. These are some of the technical issues impacting economics that will be more fully characterized as part of future development efforts.

The economics of the UFP process are critical to its eventual commercialization. Developing relationships between technical performance goals and economic targets will ensure that UFP development results in a viable commercial product. Continuing work will focus on characterizing aspects of the technology that could significantly impact process costs. These include environmental issues and integration issues. GE Global Research is planning to work with an experienced company, such as Bechtel, to develop detailed estimates of UFP plant costs to assess the commercialization potential of the technology as well as to guide future development efforts.

5.0 CONCLUSIONS

The first stage of the UFP technology development program has been successfully completed. The program objectives were met through extensive lab and bench-scale experimentation, successful design and assembly of a pilot-scale system, and limited pilot plant testing. Modeling efforts guided pilot plant design, and were used to assess overall plant efficiencies as well as the economic viability and commercialization potential of the UFP technology. Results have provided support for the UFP's high technical and commercial potential. Although many issues arose during testing, including some that negatively impacted the program schedule, no showstoppers were identified to date. Although additional experimental work is needed at the pilot scale to further characterize performance and resolve open issues such as bed effectiveness and lifetime that could impact process economics, the results obtained to date suggest that the UFP technology has the capability to meet the efficiency, environmental and economic goals of both the DOE and industrial customers.

Key accomplishments in each program task are briefly reviewed below.

Task 1 Lab-Scale Experiments – Fundamentals
A lab-scale high-temperature, high-pressure reactor and furnace were designed, built, and used for experimental analysis of coal gasification, CO_2 absorption, and OTM reduction. These tests provided kinetic data used in modeling efforts. Testing was also conducted in a fixed-bed reactor, as well as experiments using TGA to evaluate OTM reduction in the presence of CAM. Results of fundamental tests provided data on kinetics used to estimate residence times needed for optimization of key reactions. Additional tests provided insight into the behavior of bed materials at elevated temperatures. An investigation of alternate CAM preparation methods yielded materials with improved CAM performance. The lab-scale studies were conducted at Southern Illinois University at Carbondale (SIU-C).

Task 2 Bench-Scale Test Facility
Two bench-scale facilities were constructed, assembled, and subjected to shakedown testing: a bench-scale UFP system, and a cold-flow model of fluidization and solids transfer. The bench-scale UFP system was designed for high-temperature, high-pressure operation of a metal reactor inside an electric furnace. Methods for feeding coal, superheated steam, high-pressure air, and compressed gases were developed. The testing strategy included evaluation of key reactions/processes separately in order to indirectly measure the performance of reaction cycles that could not be measured directly. System instrumentation was specified to measure key variables, and a data acquisition system was developed to continuously monitor and record operating and performance data. This system was tested to ensure its safety and effectiveness at measuring the desired performance behavior.

The cold-flow model was designed to simulate bed fluidization and solids transfer via three clear plexiglass reactors that allowed direct observation of fluidization behavior. The cold flow model was designed with the flexibility to evaluate different transfer configurations. Pressure drop and flow rate meters were specified to provide the type of data that would be available in the pilot

plant, to facilitate correlations between observed and measured behavior that would be useful when the behavior was not visible.

Task 3 Bench-Scale Testing

The bench-scale UFP system was tested in gasification-CO_2 absorption/CO_2 desorption mode to establish the chemical feasibility of CO_2 absorption during coal gasification, and CO_2 desorption at elevated temperatures. The results confirmed the production of high-purity H_2 of up to 80% and the capture/release of the majority of CO_2. Parametric testing provided data for evaluation of the preferred temperature for coal gasification to optimize CO_2 absorption (750-800°C). The oxidation/reduction of OTM was tested extensively, both with coal and with simulated char oxidation products CO and H_2. A designed experimental matrix was developed to identify OTM reduction as a function of key variables. At projected pilot plant conditions, 20% OTM reduction was achieved by optimizing the test matrix results. The chemical feasibility of OTM oxidation and reduction was confirmed.

The cold-flow model was used to evaluate different distributor plate designs as well as different solids transfer mechanisms. An experimental matrix was designed to establish the key variables affecting solids transfer, and these were identified as the inlet and outlet duct diameters. Experiments also showed the importance of keeping the transport gas flow rate below the vortex level, to prevent a decrease in solids transfer rate with increasing transport flow. Initial values for the pilot plant transfer system were established based on cold-flow model data.

Task 4 Engineering and Modeling Studies

Engineering and modeling studies have been conducted in conjunction with the experimental programs. Process modeling provided early guidance for the design of the pilot plant. Lab- and bench-scale data were used to validate process models and derive kinetic parameters that could be used to predict behavior at larger scales and in complex systems where measurements of individual reactions are not possible. The complexity of the UFP system makes modeling a necessity, since models can take into account the complex interactions of variables in a more effective way than experiments since experimental data generally represents a blend of several processes that cannot be isolated. Economic studies were also conducted using process modeling results to establish the commercial feasibility of the process and identify aspects of the technology that are sensitive to cost.

Task 5 Pilot Plant Design and Engineering

The design of the pilot plant was centered on the design of the three reactors, and made use of cold flow modeling data in designing the solids transfer mechanism. Auxiliary systems were also designed for feeding coal, steam and air, as well as conditioning the product gas for analysis, and removing environmental pollutants from the exhaust gas. A detailed P&ID was developed to provide important operational and performance measurements, and a data acquisition and control system was developed to interface with instrumentation, providing control and monitoring online.

Task 6 Pilot Plant Assembly

The pilot plant was assembled at the Irvine Test Site, as shown in Figure 5-1. All parts, piping, equipment and instrumentation were specified, ordered, and organized for assembly. A detailed three-dimensional plan for system assembly was developed while awaiting permit approval from

the South Coast AQMD. This planning expedited the assembly and shakedown testing of the system, which took place in a few short weeks following the fourteen-month wait to receive permit approval "to construct and operate". System components were subjected to shakedown testing, including the validation of all instrumentation for control and monitoring. Operating procedures were developed, and safety reviews were completed.

Figure 5-1. UFP pilot-scale system and auxiliary systems.

Task 7 Pilot Plant Demonstration

Results of the pilot plant testing confirmed the feasibility of the UFP technology, both mechanically and chemically. The circulation of solids between three fluidized bed reactors was demonstrated in the pilot plant. The ability to maintain consistent bed levels was shown, as well as the ability to manipulate bed levels using reactor pressure. The key chemical processes were tested and demonstrated the production of high-purity H_2, the absorption and desorption of CO_2, and the oxidation and reduction of OTM. Time and budget constraints associated with the relocation of the test facilities required the deferral of additional testing at steady state and higher pressures to the next stage of this program.

Task 8 Vision 21 Plant Systems Analysis

The integration of UFP models with a complete combined-cycle energy plant confirmed the promise of the technology. The comparison of UFP with IGCC-based combined cycle plants showed that UFP has the potential for higher process efficiencies than IGCC with conventional CO_2 separation. Gatecycle modeling has addressed potential integration issues early, and will guide the direction of future technology development efforts. Economic analysis has identified key technology areas with a significant impact on cost, which will be investigated further.

Task 9 Project Management and Technology Transfer

Despite delays in obtaining operating permits and an unexpected relocation of the testing facilities, the project has consistently provided results, generated meaningful data, and been managed toward validation of the essential aspects of the UFP technology. The results of work conducted to date were presented at every stage of the program in over a dozen technical conferences throughout the course of this 3+ year program. The technical presentations have been well received, and have resulted in numerous inquiries from industry and academia. In addition, the management team has been very active in communicating with DOE representatives, including hosting status reviews and traveling to DOE offices to present intermediate results. Quarterly reports were submitted consistently, and this draft final report represents the culmination of project management efforts, and is the final milestone for the first stage of this program.

6.0 FUTURE WORK

Future work planned for the UFP technology is aimed at reducing the technical and economic risks associated with a commercial full-scale UFP-based energy plant. Although developments efforts have thus far focused on the fundamental reactions and processes of the UFP, continuing development will also consider and assess issues such as combined cycle plant integration, environmental impact, and long-term control and operability; issues that directly impact the economic and commercialization potential of the proposed process. The process design will be updated and serve as the basis for an assessment of the economic viability of a full-scale UFP-based system.

The economics of the UFP process are an important aspect of development efforts. GE Global Research will work with an experienced company, such as Bechtel, to develop detailed estimates of UFP plant costs to assess the commercialization potential of the technology as well as to guide future development efforts.

Additional pilot-scale testing is the next stage of UFP development. A two-year testing program will allow the testing of the pilot plant in a steady state mode with three circulating fluidized bed reactors and continuous coal feeding. Operation at high pressure will reduce several system integration risks. The focus of testing will be on performance optimization and risk reduction.

Team meetings with GE Energy and DOE personnel have identified specific technical risks that could impact the performance and cost of a full-scale UFP energy plant. The UFP team has also worked to identify, assess and categorize UFP technical risks. Some risks have been addressed through the experimental evaluation of chemical and mechanical feasibility that are the subject of this final report, but others remain. Major risk categories include environmental issues, integration issues, and robustness/durability. Environmental issues include contaminant levels in wastewater and exhaust gas, as well as identification of the final disposition of pollutants such as sulfur and mercury present in coal. Compatibility of the Reactor 3 product stream with gas turbines is one of the system integration issues identified; others include materials of construction for the turbine piping and potential modifications to the gas turbine. Robustness/durability issues are related to the behavior and performance of bed materials during circulation, such as deactivation and the need for continuous bed replacement/ash removal. All of these risks can be resolved, but some mitigation techniques may result in prohibitively high costs. Thus, economic assessment is an important aspect of all future work, and will be used to assess risk mitigation alternatives.

A preliminary test matrix has been developed for additional pilot plant tests of the three-reactor system. The tests have been organized into a sequence of baseline, parametric, optimization and long-term experiments. Each identified risk was assigned to a specific set of experiments. Detailed experimental plans will be guided by the CTQs of characterizing and mitigating the identified risks before proceeding to the next set of tests. Risks associated with some integration and scalability issues will be deferred to testing of a more integrated prototype facility. The experiments and risk reduction activities of the next stage of pilot plant testing are designed to ensure the success of the future prototype experimental evaluation.

7.0 PUBLICATIONS AND PRESENTATIONS

Team members have presented the UFP concept and progress on UFP and other gasification technologies development at several conferences. These presentations and their subsequent publication in conference proceedings have generated interest in the UFP technology and helped in raising awareness of the DOE's technology development program. Educating the technical sector and industry about this emerging technology will continue to be a priority as the program progresses. The presentations are listed below.

- A. Frydman, G. Rizeq, J. West, R. Subia, P. Kulkarni, and V. Zamansky, "Modeling of Unmixed Fuel Processor for Production of Hydrogen from Coal," *National Hydrogen Association 15th Annual U.S. Hydrogen Conference*, Los Angeles, CA, April 26-29, 2004.

- George Rizeq, Arnaldo Frydman, Raul Subia, Janice West, Vladimir Zamansky and Kamalendu Das, "Unmixed Fuel Processor: Pilot-Scale System Design and Initial Experimental Results," *The 29th International Technical Conference on Coal Utilization & Fuel Systems (Clearwater 2004*), Clearwater, FL, April 18-22, 2004

- George Rizeq, Raul Subia, Arnaldo Frydman, Janice West, Vladimir Zamansky, and Kamalendu Das, "Unmixed Fuel Processor for Production of H_2, Power, and Sequestration-Ready CO_2," *Twelfth International Conference on Coal Science (ICCS)*, Cairns, Queensland, Australia, November 2-6, 2003.

- George Rizeq, Arnaldo Frydman, Janice West, Raul Subia, Vladimir Zamansky, and Kamalendu Das, "Advanced Gasification-Combustion Technology for Production of Hydrogen, Power and Sequestration-Ready CO_2", *Gasification Technologies 2003*, San Francisco, CA, October 12-15, 2003.

- George Rizeq, Raul Subia, Arnaldo Frydman, Janice West, Vladimir Zamansky, and Kamalendo Das, "Development of Unmixed Fuel Processor for Production of H_2, Electricity, and Sequestration-Ready CO_2," *Twentieth Annual International Pittsburgh Coal Conference*, Pittsburgh, PA, September 15-19, 2003.

- George Rizeq, Raul Subia, Janice West, Arnaldo Frydman, Vladimir Zamansky, and Kamalendu Das, "Advanced Gasification-Combustion: Bench-Scale Parametric Study." *19th Annual International Pittsburgh Coal Conference*, Pittsburgh, PA, Sept 23-27, 2002.

- George Rizeq, Vladimir Zamansky, Vitali Lissianski, Loc Ho, Bruce Springsteen, Lucky Benedict, Thomas Miles, Valentino Tiangco, and Rajesh Kapoor, "Gasification-Combustion Technology for Utilization of Waste Renewable Fuels," *Bioenergy 2002: Bioenergy for the Environment*, Boise, Idaho, September 22- 26, 2002.

- Zamansky, V.M., Advanced Gasification-Combustion Technology for Production of H_2, Power and Sequestration-Ready CO_2, Invited Lecture at the Advanced Clean Coal Technology Workshop, Tokyo, Japan, September 2002.

- Lissianski, V., Zamansky, V., and Rizeq, G. "Integration of Direct Combustion with Gasification for Reduction of NO_x Emissions," presented and published in the proceedings of the *29th Symposium (International) on Combustion*, Hokkaido University, Sapporo, Japan, July 21-26, 2002.

- George Rizeq, Janice West, Arnaldo Frydman, Raul Subia, and Vladimir Zamansky, Poster entitled: "Advanced Gasification-Combustion Technology for Utilization of Coal Energy with Zero Pollution." *29th International Symposium on Combustion*, Sapporo, Japan, July 22-26, 2002.

- George Rizeq, Janice West, Raul Subia, Arnaldo Frydman, Vladimir Zamansky, and Kamalendu Das, "Advanced-Gasification Combustion: Bench-Scale System Design and Experimental Results," *27th International Technical Conference on Coal Utilization & Fuel Systems (Clearwater 2002)*, Clearwater, FL, March 4-7, 2002.

- R. George Rizeq, Ravi Kumar, Janice West, Vladimir Zamansky, and Kamalendu Das, "Advanced Gasification-Combustion Technology for Production of H_2, Power, and Sequestration," *18th Annual International Pittsburgh Coal Conference*, Newcastle, New South Wales, Australia, December 4-7, 2001.

- George Rizeq, Janice West, Arnaldo Frydman, Raul Subia, Ravi Kumar, Vladimir Zamansky and Kamalendu Das, "Fuel-Flexible Gasification-Combustion Technology for Production of Hydrogen and Sequestration-Ready Carbon Dioxide," *Vision 21 Program Review Meeting,* NETL, Morgantown, WV, November 6-7, 2001.

- R. George Rizeq, Richard K. Lyon, Janice West, Vladimir M. Zamansky and Kamalendu Das, "AGC Technology for Converting Coal to Pure H_2 and Sequestration-Ready CO_2," *11th International Conference on Coal Science* (ICCS), San Francisco, CA (Sept 30-Oct 5, 2001). NOTE: This conference was cancelled, but a proceedings volume was published.

- R. George Rizeq, Richard K. Lyon, Vladimir M. Zamansky, and Kamalendu Das, "Fuel-Flexible AGC Technology for Production of H_2, Power, and Sequestration-Ready CO_2," *26th International Technical Conference on Coal Utilization & Fuel Systems* (Clearwater Conference 2001), Clearwater, FL, March 5-8, 2001.

8.0 REFERENCES

EPRI (Holt), "Updated Cost and Performance Estimates for Fossil Fuel Power Plants with CO2 Removal", 1004483 Interim Report, December 2002.

Parsons, "Market-Based Advanced Coal Power Systems, Final Report," Prepared for the U.S. Department of Energy, Office of Fossil Energy, Contract No. DE-AC01-94FE62747, December 1998.

Parsons (Munson & Adams), "Cost Allocation Targets for Vision 21 Plant Modules," 2003 Pittsburgh Coal Conference.

Simbeck, D.R., "CO_2 Mitigation Economics of Existing Coal-Fired Power Plants," Presented at the U.S. DOE First National Conference on Carbon Sequestration, Washington, DC, May 14-17, 2001.

U.S. DOE NETL Office of Systems and Policy Support, "Quality Guidelines for Energy System Studies" July 2003 draft.

Van Heek, K.H., Juntgen, H., Peters, W., "Fundamental studies on coal gasification in the utilization of thermal energy from nuclear high temperature reactors" Journal of the Institute of Fuel, 46 (1973) 249.

9.0 LIST OF ACRONYMS AND ABBREVIATIONS

AQMD	Air Quality Management District
ASME	American Society of Mechanical Engineers
ASU	Air Separation Unit
CAM	CO_2 Absorber Material
CAM-NS	CAM prepared with no surfactant
CEC	California Energy Commission
CEMS	Continuous Emissions Monitoring System
CTQ	Critical to Quality
DFSS	Design for Six Sigma
GC	Gas Chromatograph
GEGR	General Electric Global Research
GHSV	Gas Hourly Space Velocity
HRSG	Heat Recovery Steam Generator
IGCC	Integrated Gasification Combined Cycle
NETL	National Energy Technology Laboratory
NTI	New Technology Introduction
OTM	Oxygen Transfer Material
OTM-O	Oxidized OTM
OTM-R	Reduced OTM
PSA	Pressure Swing Adsorber
P&ID	Process and Instrumentation Diagram
PID	Proportional Integral Derivative (controller)
R1	Reactor 1
R2	Reactor 2
R3	Reactor 3
SIU-C	Southern Illinois University – Carbondale
TGA	ThermoGravimetric Analyzer
UFP	Unmixed Fuel Processor
U.S. DOE	United States Department of Energy